Molecular Mechanism of Asi-Mediated Protein Quality Control



Nivedita Natarajan

Sir William Dunn School of Pathology
Lincoln College
University of Oxford

A thesis submitted to the University of Oxford
for the degree of Doctor of Philosophy

Trinity Term 2019

Table of Contents

Acknowledgments 1

Abstract 5

1 Introduction 7

1.1 Nuclear Envelope Overview 7

1.2 Inner Nuclear membrane proteome 9

1.3 En route to the INM 12

1.4 Inner nuclear membrane proteins and diseases 13

1.5 Protein quality control mechanisms in the ER 14

1.6 ER-Associated Degradation (ERAD) 17

1.7 Ubiquitination cascade 18

1.8 E3 ubiquitin ligases 20

1.9 ERAD substrates 24

1.10 Protein quality control at the INM 28

1.11 Discovery of *ASI* genes 28

1.12 Asi Complex 29

2 Materials and Methods 34

2.1 Molecular biology methods 34

2.1.2 Restriction digestion 40

2.1.3 Agarose gel purification 40

2.1.4 DNA assembly 41
2.1.5 Site-directed mutagenesis 41
2.1.6 Bacterial transformation 42
2.1.7 Preparation of plasmid and sequencing 42
2.2 Yeast cell biology methods 43
2.2.1 Yeast strains, growth conditions and storage 43
2.2.3 Mating, sporulation and dissection 47
2.2.4 Plasmid, PCR transformation and verification of genotypes 48
2.3 Biochemical methods 50
2.3.1 Yeast culture 50
2.3.2 Whole cell extract preparation 50
2.3.3 SDS-PAGE and western blotting 50
2.3.4 Cycloheximide shut off chases 51
2.3.5 Auxin dependent depletion of proteins 52
2.3.6 Sucrose gradient centrifugation 52
2.3.7 Native Immunoprecipitation (IP) 53
2.3.8 *In vivo* cross-linking 54
2.3.9 Growth assays 55
2.4 Expression and purification of proteins 56
2.4.1 Asi complex 56
2.4.2 Recombinant protein expression and purification 58

2.5 *In vitro* reconstitution 60

2.5.1 Preparation of liposomes 60

2.5.2 Reconstitution into proteoliposomes 61

2.5.3 *In vitro* ubiquitination assay with Proteoliposomes 62

2.5.4 *In vitro* ubiquitination assay in Detergent 63

2.5.5 Floatation assay 65

2.5.5 Protease protection assay 65

2.5.7 BMB *in vitro* cross-linking 65

3 Assembly and organization of the Asi complex 68

3.1 Introduction 68

3.2 Stability of Asi3 is dependent on Asi1 70

3.3 Asi3 is a short-lived protein 71

3.4 Asi1 mediates the interaction between Asi2 and Asi3 72

3.5 Mapping the region of interaction on Asi1 with Asi3 75

3.6 Asi proteins form a high molecular weight complex 78

3.7 Discussion 81

4 Asi complex recognizes orphan subunits of ER protein complexes at the Inner Nuclear Membrane 85

4.1 Introduction 85

4.2 Asi complex recognizes unassembled protein subunits for degradation 87

4.3 Asi complex recognizes Vph1 as an orphan subunit for degradation 98

4.4 Asi complex recognizes the transmembrane domain of Erg11 99

4.5 Voa1 is a substrate of Asi complex 104

4.6 TMDs are the degradation signal for Asi-mediated ERAD 107

4.7 TM56 directly crosslinks to Asi complex components 111

4.8 Discussion 114

5 Purification and in vitro reconstitution of the Asi complex 118

5.1 Introduction 118

5.2 Construct design and small scale expression 120

5.3 Large scale purification of the Asi complex on SBP-TEV-Asi1 125

5.4 Purification of the substrate for Asi complex 127

5.5 *In vitro* ubiquitination assay 129

5.6 Large scale purification of the Asi complex using SBP-Asi2 and reconstitution into proteoliposomes 131

5.7 *In vitro* ubiquitination of TM68-MBP with SBP-Asi2 affinity-purified Asi complex 135

5.8 Role of ubiquitin-conjugating enzymes 139

5.9 Asi2 recognizes transmembrane segment on substrates 140

5.10 Discussion 148

6 Conclusions and future directions 152

6.1 Characterization of the Asi complex 152

6.2 Role of Asi complex in the quality control of unassembled subunits of ER membrane complexes 153

6.3 Role of Asi2 in recognition of orphan substrates 156

6.4 Role of E2 conjugating enzymes Ubc4 and Ubc7 157

Appendix 160

References 162

Acknowledgments

Firstly, I want to thank the Almighty for offering me with this fantastic chance, exciting turns in life and all the beautiful individuals I've encountered in my daily life to help me reach here.

My heartfelt gratitude and immense thankfulness goes to my supervisor Prof. Pedro Carvalho, for providing this fantastic opportunity to be a part of this amazing lab. With his enthusiasm, support, motivation, I have been able to reach the goal. I am tremendously grateful for his guidance for making my journey in science from Barcelona to Oxford with an incredible learning experience.

I am incredibly grateful to Dr. Alexander Stein at Max Planck Institute for Biophysical Chemistry, Göttingen, for allowing me to spend time in his lab, teaching all about protein purification, being incredibly supportive, patient, encouraging and inspiring me during the tough times with purifications.

I want to thank my previous lab members in CRG, Barcelona, who helped me establish a new home there. My immense gratitude to Ombretta Foresti, who walked me through everything about yeast with all her support, encouragement, guidance and for her precious time for proofreading all my pieces of writing including this thesis. My sincere gratitude to Gabriel Mora who had immense patience in explaining all kinds of topics including science and fiction in-depth, Annamaria Ruggiano for teaching me cloning, supporting and encouraging me in science and personal life. My thankfulness to Alexandra Grippa for her uplifting

spirit always. My flatmates in Barcelona- Paula and Anu for sailing in the same boat during my masters and Ph.D. for all the support, encouragement and weekend outings making my time in Barcelona just amazing. I thank Paula's parents, Anu and Shekar for having looked after me as their daughter in Barcelona. My co-workers in the MPI Goettingen- Vedran, Claudia, Nupur and Iris for all the support and help to teach new techniques and for making the time spent in the lab- very memorable one. Garima for being so supportive, encouraging and allowing me to stay with her during my time in Goettingen and providing me yummy meals.

My previous and present lab members in Oxford- Kim, Loges, Daniel, Mike V, Mike R, Joana F, Lilli, Yoel, Sabrina, Jake, Alexis, Giorgia and Vitor for being supportive and encouraging and this would not have been possible without your contributions in many different ways. I would like to specially acknowledge Kim for working along on the same project and contributing to its success. An exceptional thanks to Loges for his time and efforts to proofread my thesis and discussions. Daniel for all the wonderful fun, discussions, arguments, fights we have had and finally for your precious time spent to proofread the thesis and uplifting my spirit when I am down.

I am grateful and thank my friends from Dunn School- Saroj, Sonia, Nandita, Arun, Satyan, Deeksha, Shree, Lucrezia, Ulrike who have been continuously supporting and providing an amiable atmosphere. Frank, and Jackie for being such caring

friends, for the cooking sessions and outings which made my first few months extremely enjoyable in Oxford.

All my graduate advisors, thesis committee members, administrative, stores, kitchen personnel at CRG, UPF, Dunn School and Lincoln College for being extremely helpful and making things work smoothly. All my daily colleagues who add to the stimulating atmosphere at the Dunn School. My colleagues at Innovation Forum, friends at the meditation class, especially Shalini Di for being there for me at the most challenging and stressful times of life.

I want to thank all my teachers from school and MSRIT for their encouragement, inspiration and help over the years. I am incredibly grateful to Dr. Kannan and Dr. Sravanti for offering me with several reference letters to finally land on this Ph.D. position.

I want to thank all my school friends - Ramya, Sharon, Arpitha, Jomit, Rashmi, Lorraine for their continuous encouragement from miles away in the most challenging times. My engineering best friends- Adi, Upasana, Vignesh, Veena, Manoj, Ashok, Karthik, Phani, and Padma who continuously send me their support from miles apart.

I would like to end by thanking my family back in India for believing in me and sending me miles away from them to a new city and offering me all their support, encouragement and made me feel at home with their everyday calls, pampering me with the best when I go back home.

Thanks a ton to Avva, Minna, Uncle, Maama, Atta, Roopa, Sunny, Kannan uncle, Revathy aunty, Radhika, Senthil, Priya, Ram and Harinee for all your love, encouragement, support and care continuously and when I was in Sweden and Chennai. Little baby Reyansh for your mesmerizing smiles and laughter that uplifts my spirit whenever I see any of your videos or call.

Ma (Sukanya) and Dad (Natarajan C) I cannot thank you enough for providing me the best things throughout my life, making sure I am alright at every moment and by supporting all my decisions. I am incredibly blessed to be all yours, without you I would not have been at this position today. Nammu (Namrutha) and Chintu (Niranjan Kumar) for being there all the time, to help me, make me forget all my troubles and just enjoy the time we spend and for creating troubles as well☺. Prathap for coming at the right time into our family not only changed my life but made my parents' lives better. Thanks a ton for being with me in every moment of happiness, stress as well as pain. I am eternally grateful to you to stand by me at all times, providing the best food, lifting me when I am down and celebrating every minute’s success of mine. Thank you very much for being there for me.

Abstract

Misfolded proteins in the membrane and lumen of the endoplasmic reticulum (ER) are eliminated by a quality control system called ER-associated protein degradation (ERAD). ERAD comprises several branches, each dependent on a different ubiquitin ligase complex with a preference for a particular type of misfolded protein. A third ERAD branch in *Saccharomyces cerevisiae* acting specifically at the inner nuclear membrane (INM) was uncovered. The core component of this branch is the Asi complex, consisting of the ubiquitin ligases Asi1 and Asi3 and the accessory protein Asi2. Asi complex promotes the degradation of ER proteins that mistarget to the INM and misfolded proteins thereby contributing to the quality control at the INM. However, how these proteins are unnoticed by ER ubiquitin ligases and selectively recognised by the Asi complex at the INM is unclear. We found that unassembled subunits of membrane complexes are prone to mislocalize to the INM and targeted by Asi complex for degradation. Using *in vivo* and *in vitro* studies, we show that recognition of the unassembled proteins is by direct binding of the transmembrane domain of the substrate to Asi2, subsequent ubiquitination by Asi1/3, extraction by the Cdc48 ATPase and finally degradation. Thus, our data suggest that protein complex assembly in the ER is facilitated by spatially restricting quality control of unassembled subunits to the INM. This INM quality control contributes to maintaining of the INM proteome identity and overall ER homeostasis.

Chapter 1

Introduction

1 Introduction

1.1 Nuclear envelope overview

A distinctive feature of eukaryotic cells is their nucleus. The nucleus contains the chromosomal DNA and physically segregates processes such as synthesis and processing of RNA, assembly of ribosomes from all cytoplasmic events, such as protein synthesis. Surrounding the core of the nucleus lays the nuclear envelope (NE), which forms a physical barrier separating nucleoplasm from the cytoplasm. Additionally, NE plays an essential role in gene regulation, cell signalling and chromatin organization (Buchwalter et al., 2019; Mekhail and Moazed, 2010).

NE comprises of two lipid bilayers- inner and outer nuclear membranes (INM and ONM). INM and ONM are connected at many junctions, where the nuclear pore complex (NPC) is placed. Over 500 different proteins, nucleoporins are assembled into NPCs which prevent the free diffusion of large molecules and controls the traffic of proteins between the nucleoplasm and the cytoplasm (De Magistris and Antonin, 2018). In between the ONM and INM is the periplasmic space, which is continuous with the endoplasmic reticulum (ER) lumen. The ONM, facing the cytoplasm, is also continuous with the ER membrane and contains similar protein and lipid composition with certain specific proteins (Buchwalter et al., 2019; Hetzer, 2010; Starr and Fischer, 2005) (Figure- 1.1)

Due to the NE organization and topology, the INM forms a specialized subdomain of the ER with a distinct set of proteome essential for nuclear functions. Many of

these proteins interact with chromosomes and/or nuclear lamina (Antonin et al., 2011; Schirmer and Gerace, 2005). In higher eukaryotes, the nucleoplasmic face of the INM is lined by nuclear lamina – a meshwork of intermediate filaments and associated proteins that are essential to maintain nuclear integrity and its rigid structure (Dittmer and Misteli, 2011). In contrast, nuclear lamins are absent in budding yeast *Saccharomyces cerevisiae* (Cohen et al., 2001; Meseroll and Cohen-Fix, 2016).

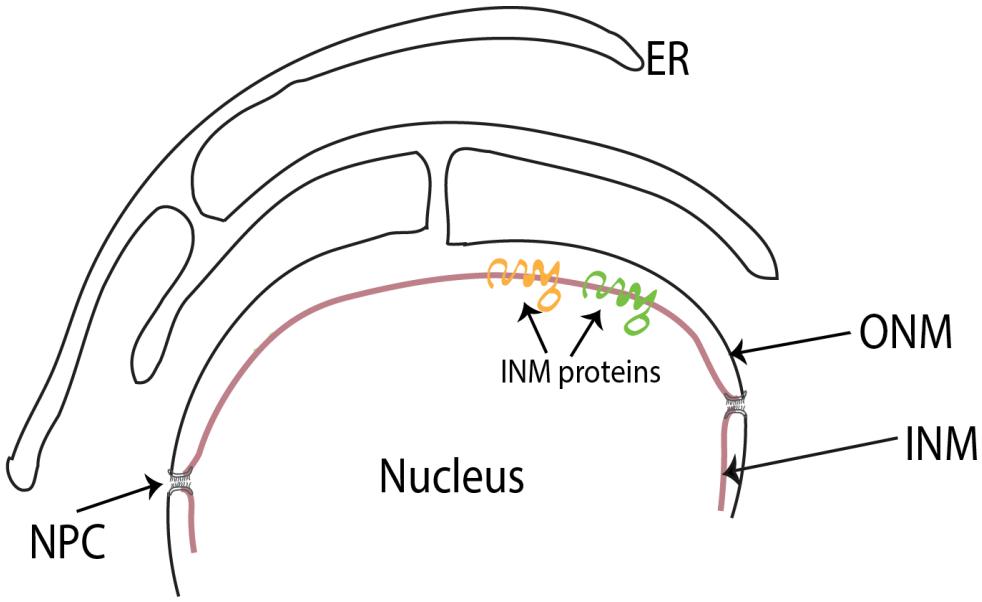


Figure 1.1- Schematic representation of the periphery of the nucleus

Endoplasmic reticulum (ER), outer and inner nuclear membrane (ONM and INM), nuclear pore complex (NPC)

In higher eukaryotes, nuclear envelope integrity is challenged during cell division. Metazoan cell nuclei are subjected to "open" mitosis during which nuclear lamina

and NPCs disassemble reversibly; nuclear membranes merge into the ER and nuclear proteins release into the cytoplasm (Meseroll and Cohen-Fix, 2016; Ungricht and Kutay, 2017; Yang et al., 1997). This process is reversed at the end of mitosis: nuclear membranes reassociate with chromatin, NPCs re-assemble and nuclear proteins return to the nucleus (Ungricht and Kutay, 2017). On the other hand*, S. Cerevisiae* undergoes "closed" mitosis where the NE remains intact and does not include reassembly of NE at the end of mitosis (Boettcher and Barral, 2013).

1.2 Inner nuclear membrane proteome

Proteins of the INM and its interactions with DNA play a crucial role in various processes including genome organization, transcription regulation in the nucleus and nuclear reassembly after mitosis (Katta et al., 2014). Proteomic approaches have identified around 80 NE transmembrane protein (Schirmer et al., 2003). Interestingly, many of these proteins were encoded by genes associated with various muscular dystrophies and laminopathies emphasising the significance of nuclear proteome in cellular and organismal function.

It is inherently challenging to study the composition of the INM due to the continuity between bulk ER, ONM and INM. While some proteins localise exclusively to the INM, for other proteins their INM localisation appears more dynamic, and only a small pool is detected at the INM. In addition to the

complexity, a mammalian study estimates at least 40% of proteins are shared between organelles (Foster et al., 2006). A genome-wide study in yeast showed that about 35% of all predicted transmembrane proteins had shared access to the INM and the ER (Smoyer et al., 2016). How specific proteins are targeted to the INM and how the unique INM proteome is maintained is a concern that the field begins to uncover. Hence, there are only a few well-characterised INM proteins.

In metazoans, a group of INM proteins share the LEM domain. This 40 amino acid sequence consists of two helices separated by a short turn and is named after Lap2, Emerin and Man1 proteins (Gruenbaum et al., 2005). LEM domain proteins bind A and/or B-type lamins and also mediate the interaction with a conserved DNA binding protein called barrier-to-autointegration factor (BAF). In both interphase and mitosis, LEM proteins and BAF are suggested to play essential roles in chromatin organisation (Haraguchi et al., 2008; Margalit et al., 2007). The major lamin-binding proteins at the INM are the lamina-associated polypeptides LAP1, LAP2 and lamin B receptor (LBR). The SUN proteins (Sad1 and UNC-84), constitute another class of INM proteins. They interact with the KASH-domain (Klarsicht, ANC-1, and Syne/Nesprin homology) containing proteins that localise to the ONM. SUN and KASH domain proteins together form the linker of nucleoskeleton and cytoskeleton (LINC) complexes which are vital for transmission of forces across the NE and maintaining nuclear morphology (Sosa et al., 2012, 2013; Ungricht and Kutay, 2015).

In yeast, there are few proteins identified as exclusive INM proteins. The membrane ring of the NPC is associated with three integral membrane proteins-Ndc1, Pom152 and Pom34 essential for nucleocytoplasmic transport and biogenesis of NPCs (Rout et al., 2000). Two INM proteins, Heh1 (helix-extension-helix-1/Src1) and Heh2 share homology with mammalian LEM domain-containing proteins. Heh1 was shown to be the most upstream element of the NPC surveillance pathway (Webster et al., 2016).

Mps3 (SUN protein) similar to the mammalian SUN protein is located at the INM, binds to Mps2 (KASH protein) in the ONM and are essential for the insertion of the newly supplicated spindle body into the NE (Chen et al., 2019; Jaspersen et al., 2006). Mps3 also interacts with Ndj1, a telomere adaptor protein that mediates tethering of telomeres during meiosis (Bupp et al., 2007; Conrad et al., 2008). An INM protein called Prm3 plays an essential role in the fusion of NE during the process of mating in yeast (Beilharz et al., 2003). In addition to these, E3 ubiquitin ligases, Doa10 and Asi complex localises to the INM. Doa10 is an E3 ubiquitin ligase localised to both ER and INM, targets both ER and nuclear proteins for degradation (Deng and Hochstrasser, 2006). Asi complex which is composed of Asi1, Asi2 and Asi3 subunits, were initially shown to be essential regulators of the amino-acid uptake signalling pathway (Foresti et al., 2014; Ljungdahl and Daignan-Fornier, 2012)

1.3 En route to the INM

Majority of membrane proteins, including INM proteins, are synthesised in the ER and then the INM resident proteins must be trafficked to the INM. Many studies have been performed on the transport of soluble proteins into the nucleus, but there is still a very limited understanding of the transport of transmembrane protein into the INM. Currently, two major INM transport pathways- transport factor-mediated translocation and diffusion-retention mechanisms have been described (Katta et al., 2014).

Transport factor-mediated translocation is a sequence-based targeting process that requires sequence motifs or nuclear localisation signal (NLS) on the INM cargo's extraluminal region. Karyopherins recognise these sequence motifs and mediate the cargo into the INM through the central channel of the NPC. Once at the INM, interaction between importins and RanGTP results in the dissociation of the cargo molecule. In yeast, transportation of LEM domain-containing proteins Heh1 and Heh2, have shown to follow such a mechanism mediated by the transport factor and pass through the central channel of the NPC (King et al., 2006; Meinema et al., 2011).

In the case of diffusion- retention mechanism, it is for INM proteins with their cytoplasmic domain with <90kDa (Popken et al., 2015). As the INM proteins are synthesised in the ER, they diffuse through the ER to the ONM and finally reach the INM through the lateral channel of the NPC. Once in the INM, they are

retained thereby binding to lamins, chromatin or nuclear proteins and non-INM proteins may diffuse back to the ER (Boni et al., 2015; Ungricht and Kutay, 2015). A recent genome-wide study of INM proteins in yeast primarily supports the diffusion retention model as there was no sequence dependence on the enrichment of proteins but rather a robust increase in proteins based on domain size at the INM (Smoyer et al., 2016). This concept that proteins below a certain size can easily diffuse through the NPCs suggests that any small membrane protein from the ER can be found at the INM transiently or at low levels. This is consistent with the recent study that 35% of transmembrane proteins had shared access to the ER and INM (Smoyer et al., 2016). It indicates that a feasible way to control the free diffusion of membrane proteins is to establish strict quality control mechanisms that monitor foreign proteins at the INM.

1.4 Inner nuclear membrane proteins and diseases

Disturbance of NE integrity and homeostasis has been linked to more than two dozen diseases, including dystrophies, premature ageing syndromes and cancers. However, the majority of laminopathies have been associated with mutations in lamin A, studies show that mistargeting or mutations of INM proteins are also involved in disease phenotypes such as Hutchinson-Gilford Progeria syndrome, Emery-Dreifuss muscular dystrophy or digestive tract cancer (Chen et al., 2012; Schirmer et al., 2003; Starr, 2012; Worman, 2016).

Regarding the role of the NE in many biological processes and the numerous diseases associated with loss of NE integrity, the question arises on how cells protect their INM proteome. Quality control (QC) mechanisms acting within the INM must firstly be able to recognise and remove proteins which mistarget to the INM, and secondly, it must be able to distinguish between resident INM proteins and misfolded proteins. One of the major QC mechanisms found in organelles is the ubiquitin-proteasome system. As the NE is continuous with the ER, components of the endoplasmic reticulum-associated protein degradation (ERAD) pathway play a significant role in maintaining NE protein homeostasis. Below I will first discuss details about ERAD quality control mechanisms and then focus on the quality control at the INM.

1.5 Protein quality control mechanisms in the ER

Protein synthesis is a very delicate process, and protein function depends on proper folding and appropriate post-translational modifications. In eukaryotic cells, roughly a third of the genes encode for secreted and membrane-embedded proteins, many of which are primarily involved in exchanging information with neighbouring cells and the extracellular environment (Chen et al., 2005; Uhlén et al., 2015). The biogenesis of these proteins occurs in the endoplasmic reticulum (Jan et al., 2014) where the newly synthesised polypeptides undergo folding with the help of chaperones and enzymes to attain the native structures. In many

instances, folding is facilitated with glycosylation and formation of disulphide bonds (Braakman and Bulleid, 2011; Braakman and Hebert, 2013; Hebert et al., 2005). At this point, subunits of multiprotein complexes also assemble into the complex with the defined stoichiometries. Despite the high fidelity of the folding factors in the ER, a sizeable portion of the secretory and membrane proteome fail to acquire the native conformation (Hartl and Hayer-Hartl, 2009). Several events impair the efficiency of protein folding including mutations in the primary sequence and unbalanced subunit synthesis due to unavailability of the binding partner (Juszkiewicz and Hegde, 2018; Schubert et al., 2000) (Figure-1.2).

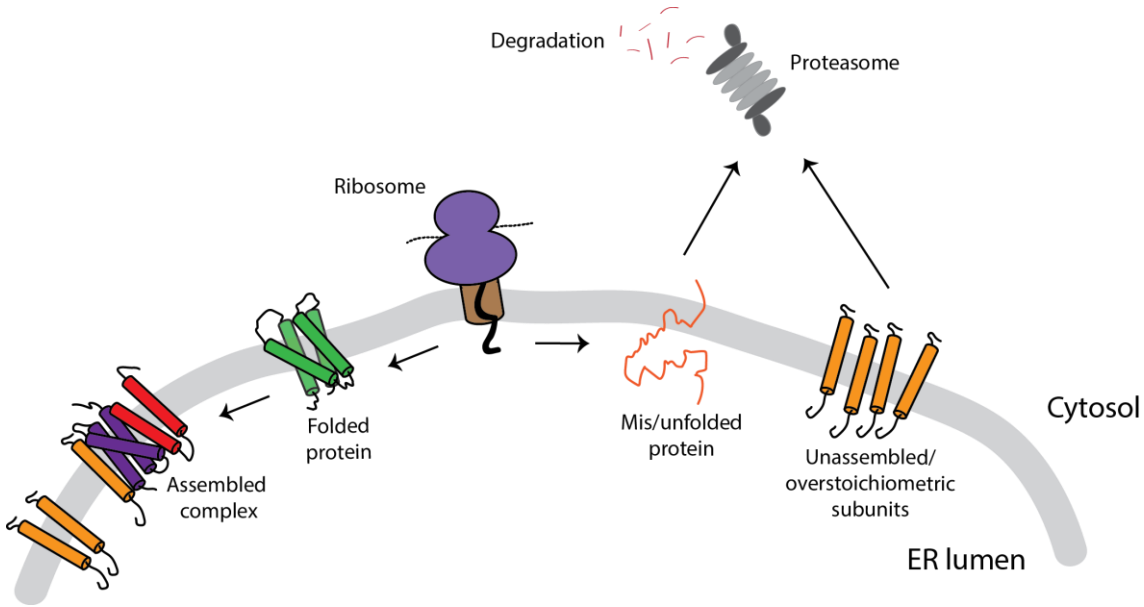


Figure 1.2– Protein Quality Control

Newly synthesised protein that enters the ER lumen from the ribosome is being folded with the help of chaperones to attain its native conformation. Many times proteins are also assembled into multi-protein complex and reach its final destination and perform functions. There are high

chances of proteins being misfolded or unassembled into complexes. Under these circumstances, they need to detected and removed from the ER through protein quality control pathways.

Moreover, circumstances such as enhanced protein synthesis or increase in the number of aberrant protein species that challenge the organelle's folding ability, exposure to elevated temperature, oxidative stress, alterations in the redox balance in the ER lumen, pharmacological agents can lead to ER stress (Ron and Walter, 2007). ER stress leads to activation of intracellular signalling pathways collectively called as unfolded protein response (UPR). UPR manages stress owing to the excess amount of misfolded proteins by increasing biosynthesis of membrane lipids, chaperones and ERAD factors (Gardner et al., 2013). Ultimately, prolonged or irreversible ER stress can result in apoptotic cell death (Sano and Reed, 2013; Tabas and Ron, 2011). Importantly, the accumulation of misfolded or aberrant proteins is harmful to the cell and are linked with human illnesses such as Alzheimer's and Parkinson's diseases.

Therefore, cells have evolved a set of quality control mechanisms to ensure that aberrant and toxic species are detected and eliminated from the ER. One of the best-characterised pathways is called ER-associated protein degradation (ERAD) (Braakman and Bulleid, 2011; Ruggiano et al., 2014).

1.6 ER-Associated Degradation (ERAD)

In the endoplasmic reticulum, protein quality control is ensured by the ER-Associated Protein Degradation (ERAD) pathway (Hirsch et al., 2009). The removal of aberrant proteins from the ER is a multi-step process that requires the coordination of many proteins in both the ER and the cytoplasm. The preliminary evidence for an ER quality control was the lysosome-independent degradation of unassembled subunits of T-Cell receptor in a pre-golgi compartment (Lippincott-Schwartz et al., 1988). Later the ubiquitin-proteasome system was shown to be implicated in ER quality control (Chen et al., 1993a; Hiller et al., 1996; Sommer and Jentsch, 1993). Afterwhich, numerous studies have collected evidence of ubiquitin and proteasomal degradation of ER proteins including both ER membrane substrates (e.g. mutant cystic fibrosis transmembrane conductance regulator, CFTR ΔF508 mutant) and luminal substrates (e.g. mutant CPY*) both *in vivo* and *in vitro* (Hiller et al., 1996; Jensen et al., 1995; Ward et al., 1995; Werner et al., 1996)

ERAD is a multi-step process and it starts with the recognition of a substrate. Once selected, the substrate is transported across the ER membrane (or retrotranslocation). Once on the cytoplasmic side of the ER membrane, the substrate is ubiquitinated through a cascade of reactions catalysed by specific, membrane-bound ubiquitin E3 ligases. After several rounds, a poly-ubiquitin chain is built on the substrate which is recognised by a cytosolic ATPase complex, called Cdc48p in yeast, and its cofactors Ufd1p and Npl4p (Bodnar and Rapoport,

2017b). Finally, hydrolysis of ATP drives the retrotranslocation of the polypeptide into the cytosol and followed by degradation in the proteasome (Ruggiano et al., 2014) (Figure-1.3).

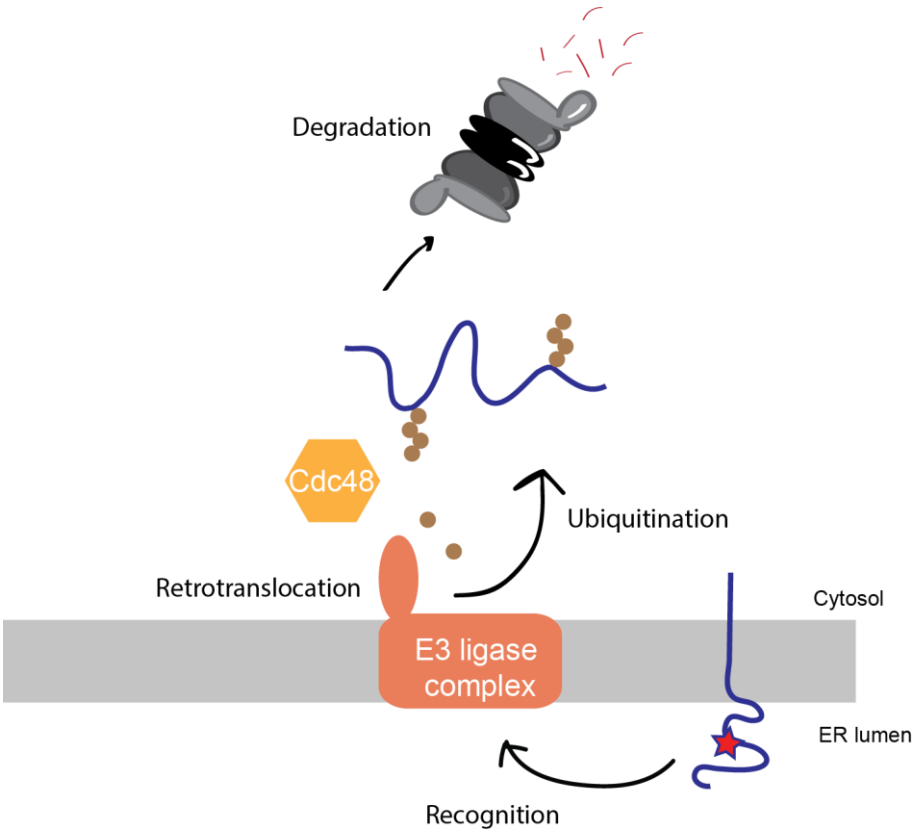


Figure 1.3– Schematic representation of ERAD

The canonical steps of Recognition, Retrotranslocation, Ubiquitination and Degradation in the proteasome are depicted. Red star indicates a misfolded lesion in a protein. Adapted from (Ruggiano et al., 2014)

1.7 Ubiquitination cascade

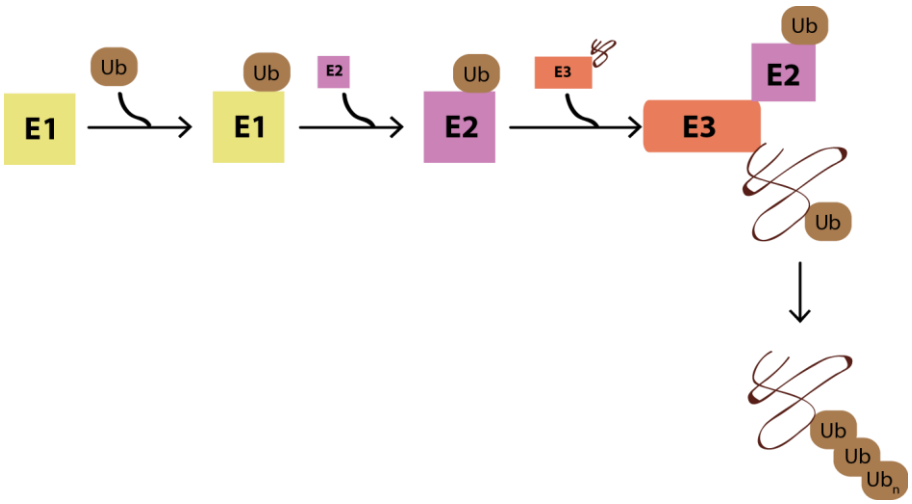
A key commitment step in ERAD is the modification of the substrate by the covalent attachment of a ubiquitin molecule. Ubiquitin (Ub) is a highly conserved

protein comprising of 76 amino acids encoded by a family of multiple genes. Yeast and human ubiquitin share 96% of sequence identity demonstrating the functional significance of this molecule (Komander and Rape, 2012). Moreover, specific areas on the surface of ubiquitin serve as platforms for interaction with proteins containing ubiquitin-binding domains.

Ubiquitination is catalysed by a cascade of enzymatic reactions which involves three main steps. In the first step, the ubiquitin-activating enzyme (E1) called Uba1 in yeast forms a reactive thioester bond with the C-terminus of ubiquitin, forming the activated E1 enzyme (Schulman and Harper, 2009). Next, the activated E1 enzyme transfers the ubiquitin molecule to the cysteine active site of E2 ubiquitin-conjugating enzymes (Ubc's) (Ye and Rape, 2009). In the last step, an E3 ubiquitin-ligase recruits the activated E2-ubiquitin conjugates and mediated the transfer of ubiquitin from the E2 to acceptor sites within the substrates (Metzger et al., 2014) (Figure-1.4). Generally, ubiquitin forms a peptide linkage with the ε-NH2 group on substrate lysyl residues. Also, ligation of ubiquitin to the N-terminal α-NH2 group, or to serines, threonines and cysteines on substrates is shown (Callis, 2014).

Followed by the addition of the first ubiquitin on the substrate, seven lysines on this ubiquitin can then serve as acceptor sites for covalent attachment of more ubiquitin molecules that ultimately extend the ubiquitin chain on the substrate (Callis, 2014; Pickart, 2001). Importantly, ubiquitin can be conjugated in several

ways to other ubiquitin molecules to form complex code of poly-ubiquitin chains on the target substrate (Dikic et al., 2009).


Ub
E1
Ub
E1
E2
Ub
E2
E3
Ub
E2
E3
Ub
Ub
Ub

recognition of the protein substrate to be degraded and brings the activated E2 in close proximity of the substrates to be ubiquitinated. There are three types of E3 ligases: HECT (Homologous to the E6-AP carboxy terminus), RING (Really Interesting New Gene) and U-box types. In yeast, there are only five members of the HECT ligases, and the majority of them belong to the RING-type ligases (Budhidarmo et al., 2012; Hicke et al., 2005; Rotin and Kumar, 2009).

The main characteristic feature of the HECT ligases is a conserved Cysteine residue which forms an intermediate thioester bond with C-terminus of the ubiquitin before the transfer of ubiquitin to the substrate. On the other hand, RING E3s behave as scaffolds and brings the E2 in close proximity to the substrate. RING ligases contain a consensus sequence of cysteine and histidine residues in the RING domain that adopts a conserved cross brace arrangements which are further stabilised by two zinc ions (Berndsen and Wolberger, 2014). This serves as a docking site for E2 enzymes carrying ubiquitin and stimulates its transfer to the substrates (Lorick et al., 1999).

ERAD pathways are best studied in the yeast *Saccharomyces cerevisiae* with two well-characterised E3 ligases including the Hrd1 and Doa10.

The Hrd1/Der3 ligase was the first E3 enzymes identified in the ERAD pathway in yeast (Bordallo et al., 1998; Hampton et al., 1996; Knop et al., 1996). It was identified in a genetic screen designed to isolate mutants that were impaired for the degradation of HMG-CoA reductase (Hampton et al., 1996). HMG-CoA

reductase is a membrane protein and a rate-limiting enzyme of the sterol biosynthetic pathway (Goldstein and Brown, 1990). The Hrd1 is a RING E3 ligase that localises exclusively to the ER and recognises lesions on both luminal (ERAD-L) and membrane (ERAD-M) domains of substrates (Carvalho et al., 2006; Nakatsukasa and Brodsky, 2008; Vashist and Ng, 2004).

Next, in a genetic screen that was designed to isolate genes that were defective for the degradation of Deg1- reporter fusion α2 identified Doa10 (Chen et al., 1993b; Swanson et al., 2001). Doa10 is also a RING E3 ligase that localised both to the ER and INM (Deng and Hochstrasser, 2006) and was initially shown to act on substrates with lesions on the cytosolic domain (ERAD-C) (Carvalho et al., 2006; Vashist and Ng, 2004). However, a later study showed that Doa10 could also degrade some ERAD-M substrates such as Sbh2 (Habeck et al., 2015). The initial division of ERAD-M, ERAD-L, ERAD-C was based on a small number of substrates (Figure- 1.5). However, now multiple ligases act and there seems to be an overlap between the pathways for the degradation of various substrates.

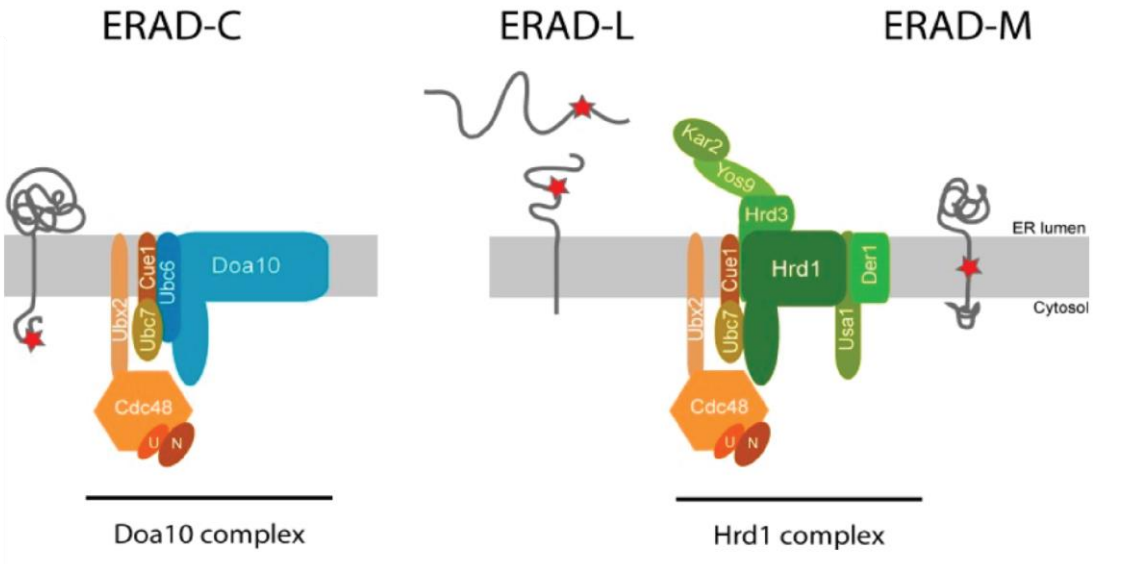


Figure 1.5- Schematic representation of the ERAD branches and its substrate specificities. Adapted from (Ruggiano et al., 2014)

The third ERAD E3 ligase complex –Asi complex which localises exclusively to the INM was uncovered. It was shown to degrade mislocalized and misfolded substrates at the INM (Foresti et al., 2014; Khmelinskii et al., 2014). It will be discussed in detail in a later section.

E2 enzymes play an essential role along with the E3s in determining whether the final product is mono or poly-ubiquitinated, as well as in dictating the specificity of lysine linkages and affecting the length of the ubiquitin chains formed (Chen and Pickart, 1990; Rape et al., 2006). Hrd1 and Doa10 E3 ligases exhibit varied preferences for E2 conjugating enzymes. Hrd1 is dependent on Ubc7 (Bays et al., 2001), whereas Doa10 primarily uses Ubc6 and Ubc7. Ubc7 is a cytosolic protein and requires an adaptor protein called Cue1 (Coupling of ubiquitin conjugation to ER degradation protein 1) (Biederer et al., 1997) to be recruited to the ER membrane, whereas Ubc6 associates with the ER through its transmembrane domain (TMD). While mammalian orthologues of Hrd1 and Doa10 have been reported, the spectrum of E3s and E2s involved in ERAD in the mammalian proteome is significantly greater and remains less characterised (Christianson and Ye, 2014; Ruggiano et al., 2014).

Regardless of the E3 complex involved, ubiquitinated substrates require the ATPase Cdc48 complex (p97 in mammals) along with its co-factors Ufd1-Npl4 for extraction from the ER membrane (Bodnar and Rapoport, 2017a; Ye et al., 2001, 2003). However, in some cases the ubiquitin chain assembly factor (Ufd2 in yeast) an E4 enzyme provides optimal ubiquitination by elongating the pre-existing ubiquitin chains under stress conditions (Koegl et al., 1999).

In mammalian cells, the increase in complexity in ERAD components has made it challenging to identify and define distinct pathways. HRD1 and gp78 in mammalian cells are the orthologs for Hrd1 in yeast. Ube2g2 and Ube2g1 in mammals resemble the Ubc7 E2 enzyme in yeast and Ube2j1 and Ube2j2 in mammals resemble Ubc6 E2 enzyme (Kostova et al., 2007). In the case of Doa10, it is broadly conserved in higher eukaryotes. TEB4 (MARCH 6) is its mammalian orthologs (Hassink et al., 2005; Kreft et al., 2006). Doa10 orthologs in plants called SUD1/CER9 were also identified in Arabidopsis thaliana (Doblas et al., 2013; Lü et al., 2012).

1.9 ERAD substrates

Misfolded proteins

Recognition of misfolded protein species presents a significant challenge for cells because it is based on the capacity of the quality control system to discriminate terminally misfolded proteins from folding intermediates. One of the best-

characterised misfolded substrates in yeast is the carboxypeptidase-Y (CPY*), a soluble glycoprotein in the ER lumen which is a substrate of the Hrd1 pathway (Benyair et al., 2015; Hiller et al., 1996). As a protein translocates into the ER, N-linked glycan moiety ($Gly_3Man_9GlcNAc_2$) is attached to the protein by the Oligosaccharyl transferase complex. These moieties undergo trimming by ER glycosidases to generate chains that promote folding and maturation. Early acting enzymes remove glucose so to allow the binding of lectins which initiate folding of the proteins. Alternatively, if the protein is retained in the ER lumen for a longer time, then late acting enzymes such as the mannosidase Htm1 in yeast or EDEMs in mammals, and protein disulphide isomerase recognises these misfolded proteins and processes them to $Man_7GlcNAc_2$. This trimming reveals α1,6-linked mannose which is recognised by the lectin Yos9 and an unstructured peptide segment recognised by Kar2, Hrd3 in the Hrd1 complex. Finally, it is ubiquitinated by Hrd1 and processed for degradation (Clerc et al., 2009; Gauss et al., 2011; Quan et al., 2008). Although the general mechanism of glycoprotein recognition in mammals is not fully understood the available data indicates that it is similar to yeast (Benyair et al., 2011).

Orphan subunits of protein complexes

The vast majority of newly synthesised proteins in the ER assemble with their partners to form multi-protein complexes prior to engaging the secretory

pathway. However, the efficiency of the complex assembly process is error-prone and imposes major challenges. Firstly, the components must be synthesised in the required stoichiometric ratios. Second, unassembled subunits must avoid incorrect interactions in the crowded environment of the ER. Finally, during diffusion through the ER they need to find the right binding partners (Juszkiewicz and Hegde, 2018). Thus, the resulting unassembled subunits of the complex are retained in the ER and are recognised by the ERAD machinery. Well-characterised examples are the mammalian octameric T cell receptor complex (TCR) subunits-TCRα and CD3δ (Bonifacino and Lippincott-Schwartz, 1991; Bonifacino et al., 1991). These subunits contain a single TMD that when unassembled are recognised through their TMDs for degradation through the E3 ligase Hrd1 (Kikkert et al., 2004). Interestingly, it was also shown that cells can infer the status of assembly based on the TMD. As less hydrophobic orphan TMDs from multimeric membrane complexes were shown to enter the ER lumen and recognised by the chaperone BiP which would further initiate the degradation process (Feige and Hendershot, 2013).

It was also shown that unassembled Sec61 β-subunit homolog 2 (Sbh2), a subunit of the trimeric Ssh1 complex, is a substrate of the E3 ligase Doa10 when its binding partner Ssh1 is unavailable. Interestingly, the degradation signal of Sbh2 was mapped to the membrane region of the tail-anchored sequence of Sbh2 (Habeck et al., 2015).

Regulated substrates

ERAD is not only for misfolded proteins but also controls the abundance of some folded proteins. The best-characterised example is the ER membrane protein 3-hydroxy-3-methylglutaryl-coenzymeA reductase (HMGR), a rate-limiting enzyme during the synthesis of sterols in the mevalonate pathway. Interestingly, ERAD of HMGR is regulated by sterol levels. Studies showed that when sufficient amount of sterols are present, cells turn off the transcription of HMGR (Brown and Goldstein, 2009) and trigger the degradation of HMGR via ERAD as a critical feedback mechanism to control the overall production of sterols (Ravid et al., 2000). Similarly in yeast, regulation of Hmg2 (HMGR homologue) activity also involves the negative feedback mechanism and requires the E3 ligase Hrd1 for degradation (Gardner et al., 2001).

Interestingly, degradation of another enzyme of the sterol pathway called Squalene monooxygenase is also regulated by ERAD in yeast and mammals based on the sterol levels in the cell. It requires the E3 ligase Doa10 in yeast and its homologue Teb4 in mammals (Foresti et al., 2013; Zelcer et al., 2014). Two different E3 ligases control distinct steps of the sterol biosynthetic pathway, exemplifying essential functions of ERAD beyond protein quality control.

1.10 Protein quality control at the INM

Since the nuclear envelope is continuous with the ER, it is possible that ERAD likely surveys the nuclear envelope membrane. Indeed, an ERAD E3 ligase Doa10 is shown to localise to the INM and degrades the transcription factor MAT α2 and some membrane proteins in yeast (Deng and Hochstrasser, 2006; Habeck et al., 2015). A specialised branch of ERAD defined by the Asi complex that localises exclusively to the INM was identified. Asi complex recognises mislocalised and misfolded protein at the INM and mediates their ubiquitination and degradation in the nucleus thereby contributing to INM homeostasis (Foresti et al., 2014; Khmelinskii et al., 2014). However, the molecular mechanisms involved in substrate recognition and degradation is still very limited.

1.11 Discovery of *ASI* genes

The ASI genes were initially identified while studying the SPS sensor pathway. Yeast cells utilise the (Ssy1-Ptr3-Ssy5) SPS sensor pathway to monitor amino acid uptake from the surroundings. Downstream effectors of the SPS pathway include transcription factors Stp1 and Stp2. In the presence of amino acids in the medium, Stp1 and Stp2 undergo cleavage and enter the nucleus to regulate the expression of amino acid permeases that allow the uptake of amino acids. In the absence of amino acids, the unprocessed forms of Stp1 and Stp2 remain in the cytoplasm. However, cytoplasmic retention of the unprocessed forms is not efficient and

low-levels of Stp1 and Stp2 leak into the nucleus and activate the expression of amino acid permeases even in the absence of amino acids. To identify downstream components of the SPS sensor pathway a genetic screen was designed to look for mutations that would restore the uptake of amino acids in SPS sensor deficient cells identified *ASI1, ASI2* and *ASI3* genes along with SSN6 and TUP1 genes (Forsberg et al., 2001). Further studies showed that *ASI* genes are required to maintain the latency of Stp1 and Stp2 transcription factors that escape cytoplasm retention by preventing their access to the amino acid permeases gene expression promoters (Boban et al., 2006; Forsberg et al., 2001; Zargari et al., 2007).

1.12 Asi Complex

Asi complex is made up of three transmembrane proteins- Asi1, Asi2 and Asi3 and localise exclusively to the INM (Foresti et al., 2014). Asi1 and Asi3 and are paralogous proteins, likely originating from a genome duplication event, containing the 5 predicted TMDs and approximately 40% similarity at the amino acid sequence. They contain RING domains at the extreme C-terminus which renders the ubiquitin ligase activity. Furthermore, Asi1 and Asi3 were shown to be glycosylated (Zargari et al., 2007).

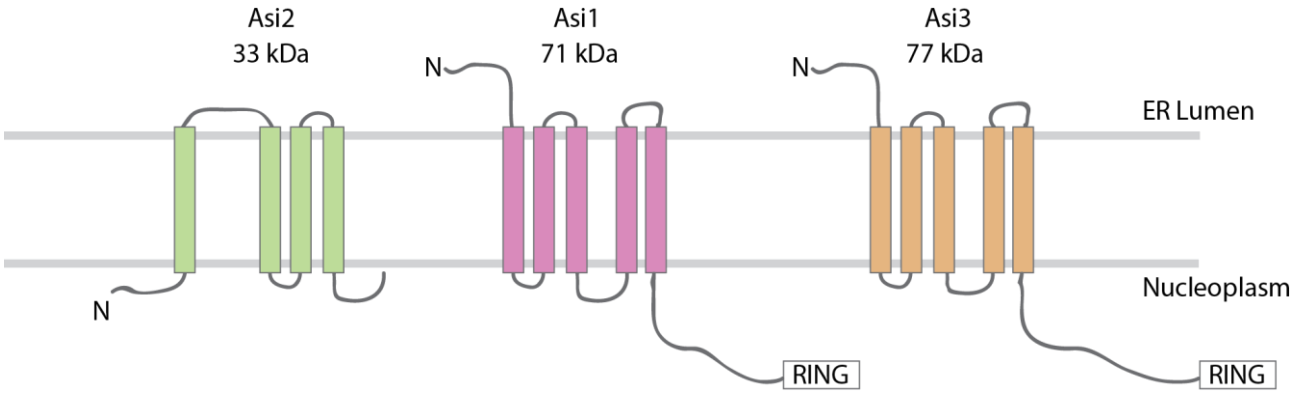


Figure 1.6- Schematic representation of the Asi complex

N and C terminus of Asi2 face the nucleoplasm and contains two transmembrane domains. Asi1 and Asi3 have five transmembrane domains with C-terminal RING domains in the nucleoplasm (Foresti et al., 2014; Zargari et al., 2007)

Immunoprecipitation experiments showed that Asi1/Asi3 form the core of the Asi complex, while Asi2 is a smaller protein with 4 predicted transmembrane domains and is a more peripherally associated component of the complex (Foresti et al., 2014; Zargari et al., 2007) (Figure-1.6). The entire protein sequence of Asi proteins is included in the appendix. It was also shown that the degradation of Asi2 was dependent on the E3 ligase Doa10 that also localises to the INM and required E2 conjugating enzymes Ubc6 and Ubc7 (Boban et al., 2014).

In order to identify a broader spectrum of the ERAD substrates, (Foresti et al., 2014) used SILAC (Stable Isotope Labeling by amino acids in Culture) (de Godoy et al., 2008) labelling followed by quantitative proteomics. This approach

uncovered an interesting class of substrates requiring the well-established ERAD components Ubc7 and the cytosolic Cdc48 ATPase complex but whose degradation was independent of the canonical ERAD ubiquitin ligases Hrd1 and Doa10. A candidate approach revealed Asi complex as the ubiquitin ligase involved in the degradation of these Hrd1- and Doa10-independent substrates.

Further characterisation of Asi complex showed that it could promote the degradation of proteins such as Erg11 and Nsg1 that mislocalizes to the INM. Asi complex was also shown to be important for the degradation of misfolded proteins such as *sec61-2*. These functions of the Asi complex were essential to maintain the identity of the inner nuclear membrane and contribute to ER homeostasis (Foresti et al., 2014). At the same time using tandem fluorescent timer approach in a genome-wide screen (Khmelinskii et al., 2014) identified vacuolar proteins Vcx1, Vtc1 and a range of other ER proteins as mislocalized substrates for Asi complex at the INM. Asi complex was also shown to promote the degradation of soluble transcription factor Stp1/2 explaining its requirement to the response of amino acid availability (Omnus and Ljungdahl, 2014). All known Asi complex substrates require both intact RING domains of Asi1 and Asi3 despite their similarity. However, Asi2 is dispensable for the degradation of some Asi substrates (Foresti et al., 2014; Khmelinskii et al., 2014). It was shown that Asi complex requires two E2 conjugating enzymes- Ubc4 and Ubc7 for the attachment of ubiquitin on the substrates. Like the other ERAD E3 ligases, Asi complex substrates also depend on Cdc48 for extraction and finally undergo

degradation in the nuclear proteasomes (Foresti et al., 2014). Thus, Asi complex in yeast plays an essential role by degrading mislocalized and misfolded proteins at the INM, thereby contributing to maintaining INM identity and ER homeostasis.

Towards understanding the underlying functions of the Asi complex, a combination of *in vivo* and *in vitro* approaches will be used in the thesis to elucidate the following aims:

1- Characterize the assembly and organisation of the Asi complex

2- Dissect the mechanistic basis of recognition of mislocalized substrates at the INM and how this pathway contributes to the overall homeostasis in the ER

3- Establish an *in vitro* functional assay to understand whether Asi complex defines the minimal unit required for recognition, ubiquitination and retrotranslocation of substrates.

Chapter 2

Materials and Methods

2 Materials and Methods

2.1 Molecular biology methods

2.1.1 Polymerase chain reaction

DNA fragments for cloning were amplified either by Phusion polymerase (New England Biolabs) or Q5 High-Fidelity 2X master mix (New England Biolabs) as indicated in Table 2.1a and 2.1b. PCR program used is described in Table 2.1c. Annealing temperatures were changed as per the primer requirements.

Table 2.1a- Phusion protocol

Component	Volume (µl)
Water	36
5x Phusion buffer	10
dNTP mix (10mM)	2
Forward primer	0.25
Reverse primer	0.25
Phusion polymerase	0.5
Template DNA (20ng)	1

Table 2.1b- Q5 protocol

Component	Volume (µl)
Water	22
2x Q5 master m	25
Forward primer	0.25
Reverse primer	0.25
Template DNA	2.5

Table 2.1c- Thermocycler program

Temperature	Time	Cycles
95˚C	3 min	1 x
95˚C	30 s	29 x
56˚C	30 s	
72˚C	1 min/kb	
72˚C	5 min	1 x
4˚C		hold

Table 2.2- List of primers

Number	Name	Sequence
2014	Erg11-(56-521)	CTATATTCTTTGAGAAAGGACCGTCCAGAAAAGAGAAATCCAGAACAAAAG
2015	Erg11-(68-521)	CTGGATTCCATGGGTCGGTAGTGCTGAAAAGAGAAATCCAGAACAAAAG
2302	FRB-F-SmaI	TACAAACCCGGGTCTGGTGGAATCCTCTGGCATGAGATGTGG
2304	FRB-R-BamHI	ACCTGCTCCGGATCCCTTTGAGATTCGTCGGAACACATGATA
2035	F39 tag	CTCTTTGATCATAATAATTCCTTAGATTTACAATATTGTATGGCAATTAC
2036	F22 tag	CGTAAACATTGGTTTAAGTCATTAGTTGGCTTTACCATTGGCCCAAAG
2478	L27TAG_F	GTTTAAGTCATTTCTTGGCTTTACCATAGGCCCAAAGAATCT
2479	L27TAG_R	AGATTCTTTGGGCCTATGGTAAAGCCAAGAAATGACTTAAAC
2480	I31TAG_F	ATTTCTTGGCTTTACCATTGGCCCAAAGATAGTCTTTGATCATAATAATTCCTTTCA
2481	I31TAG_R	TGAAAGGAATTATTATGATCAAAGACTATCTTTGGGCCAATGGTAAAGCCAAGAAAT
2482	I36TAG_F	TACCATTGGCCCAAAGAATCTCTTTGATCATATAGATTCCTTTCATTTACAATATTGTATGG
2483	I36TAG_R	CCATACAATATTGTAAATGAAAGGAATCTATATGATCAAAGAGATTCTTTGGGCCAATGGTA
2484	I43TAG_F	CTCTTTGATCATAATAATTCCTTTCATTTACAATTAGGTATGGCAATTACTATATTCTTTGAGAAAGGA
2485	I43TAG_R	TCCTTTCTCAAAGAATATAGTAATTGCCATACCTAATTGTAAATGAAAGGAATTATTATGATCAAAGAG
2486	L47TAG_F	ATAATAATTCCTTTCATTTACAATATTGTATGGCAATAGCTATATTCTTTGAGAAAGGAC
2487	L47TAG_R	GTCCTTTCTCAAAGAATATAGCTATTGCCATACAATATTGTAAATGAAAGGAATTATTAT
2488	L51TAG_F	ACAATATTGTATGGCAATTACTATATTCTTAGAGAAAGGACCGTCCA
2489	L51TAG_R	TGGACGGTCCTTTCTCTAAGAATATAGTAATTGCCATACAATATTGT
2367	Asi1-SmaI-F	gatatgtatCCCGGGATGAACTCTTCCACTTCTTCAGAAAATGTG
2368	Asi1-XhoI-R	gatatgtatCTCGAGTTATTTACTATCTGAAACAGGATGAAC
2371	Asi3-SmaI-F-1403	gatatgtatCCCGGGATGTCCACCAACATATTGCAACACGTC
2372	Asi3-XhoI-R-1403	gatatgtatCTCGAGTTAGACAATGTTCAACTTGGAGTAACC
2367	Asi1-SmaI-F	gatatgtatCCCGGGATGAACTCTTCCACTTCTTCAGAAAATGTG
2759	Asi1-XhoI-RingDR	gatatgtatCTCGAGTTAACTTTCTGTACCAAAAGTCTCATC
2371	Asi3-SmaI-F-1403	gatatgtatCCCGGGATGTCCACCAACATATTGCAACACGTC
2760	Asi3-XhoI-RingD R-1403	gatatgtatCTCGAGTTAGACTTCGTCACAAGAATCGAAGGC
947	Asi2_f-sbp-tev	gagaaaacttgtacttccaatcgATGGCGAGGCCTCAAAATC
948	Asi2_r-sbp-tev	gaattcctgcagcccgggctTCAGAATACGCCTGGCCC
2599	f-3X flag on Asi3-3	agaactagtggatcccccgggATGGACTACAAAGACCATGACGGTGATTATAAAGATCATGACATCGACTACAAGGATGACGATGACAAGATGTCCACCAACATATTG
2600	r-3X flag on Asi3-3	CAATATGTTGGTGGACATCTTGTCATCGTCATCCTTGTAGTCGATGTCATGATCTTTATAATCACCGTCATGGTCTTTGTAGTCCATcccgggggatccactagttct
2744	MBP_fwd	aacgtaacccggaacagaaaATGAAAATCGAAGAAGGTAAACTGGTAATCTG
2746	H14-sfGFP_rev-a	TTTCTGTTCCGGGTTACG
2747	H14-sfGFP_fwd-a	CTACCAGAAACAGGAGGCTAATAAGC

Number	Name	Sequence
2748	MBP_rev	tagcctcctgtttctggtagCTGCGCGTCTTTCAGGGC
2770	h14-erg11cys-MBP_rev	GTGAGACAGACCGATGTTAACGTATTC
2771	h14-erg11cys-MBP_fwd	TGGGTTGGTTCTGCTGAAAAACGTAAC
2765	Opt-Erg11-68- I36C	TTCCTGGCTCTGCCGCTGGCTCAGCGTATCTCTCTGATCATCTGCATCCCGTTCATC TACAACATCGTTTGGCAGCTGCTGTACTCTCTGCGTAAAGACCGTCCGCCGCTGG TTTTCTACTGGATCCCG
1560	Asi1NcoI2	ACGCGGGTCCATGGGCTTCAGAGATAACAAGGACG
2055	Asi1R1 Xho I	GTGGTGCTCGAGCTTACAGTACCCATGAAC
1942	Forward Primer Asi2F2 NcoI	CGACAAGGCCATGGAGAATGATTTTATAATC
1943	Reverse primer Asi2R2 Xho I	GTGGTGCTCGAGGTTGGGTTCATTGCCATC
1563	Asi3NcoI2	ACGCGGGTCCATGGATTCATCAAAAGACTACTTTCC
2056	Asi3R1 Xho I	GTGGTGCTCGAGGACTATATTCAACTTACTGTAACC
3334	ubc4_fwd	acagagaacagattggtggcATGTCTTCTTCTAAACGTATTG
3335	ubc4_rev	ttactagtaccggtaccggcTTATACAGCGTATTTCTTTGTC
3323	crispr oligo1 Asi2	GATCCAATACGAAGAAAAACCCAGGTTTTAGAGCTAG
3324	crispr oligo2 Asi2	CTAGCTCTAAAACCTGGGTTTTTCTTCGTATTG
3325	Asi2 temp amplify_FP	TACATGGTTACtGCTGGcTTcTTCTTtGTATT
3326	gRNA_1_Asi2_oligo1	GATCTTTAGTGAGAAAAAATGGCGGTTTTAGAGCTAG
3327	gRNA_1_Asi2_oligo2	CTAGCTCTAAAACCGCCATTTTTTCTCACTAAA
3328	gRNA_1_Hrd1_oligo1	GATCAGAAAATAGAAGGAAACAGTGTTTTAGAGCTAG
3329	gRNA_1_Hrd1_oligo2	CTAGCTCTAAAACACTGTTTCCTTCTATTTTCT
3330	gRNA_1_Doa10_oligo1	GATCGTAACAGGCTAGTATACCATGTTTTAGAGCTAG
3331	gRNA_1_Doa10_oligo2	CTAGCTCTAAAACATGGTATACTAGCCTGTTAC
3043	f_gB_CC_SBP-TEV-Asi2	TTGATGATCTTTTATAACAATAGTGAG
3044	r_gB_CC_SBP-TEV-Asi2	CTCGGTTACAGGTGAAGG
3051	f_CRISPR_ΔHRD1	ACTGTCGACTTTCTACC
3052	r_CRISPR_ΔHRD1	TCCGCTGATGTATAATATATATATATG
3363	RP to open H14-MBP-Mps3	CGGAGTCTGCGCGTCTTTCAG
3364	FP to open H14-MBP-Mps3	TAAGCGGCCGCACATCAC
3365	RP to open H14-Erg11-MBP	CTGTTCTCTGTGAGCCTC
3366	FP to open H14-Erg11-MBP	GAAGAAGGTAAACTGGTAATC
3042	gb_CRISPR_ΔDOA10	AGATTACGTTAAGAATAGTTCTTTGTTACTGATTTCAAAAACTGTTTTTTTAGCCA AGAGTACCACTAATTGAATCAAAGAGACTAGAAGTGTGAAAGTCAGGCGTTTTC TTCCTTACATTTAAAATGAATGCTAGCATATTTACATATATATATCTACATTAAGT TATATGTTTTTCCACTGTTTTATTTCTTATTGTT

Number	Name	Sequence
3034	gB_CC_SBP-TEV-Asi2	TTGATGATCTTTTATAACAATAGTGAGAGGAAACAACTCCCTCTACCTTCAAATA GGGTCGATTCGGGAATATGATTAAAGAGACACCGAATCAAACGCATACATCCTC ACAAGCATTTAGTGAGAAAAAATGACTGACGAGAGGACCACTGGTTGGCGAGG TGGACACGTTGTTGAAGGACTGGCTGGGGAACTTGAACAACTTCGTGCACGACT GGAGCATCACCCACAAGGTCAACGTGAACCAGGATCCTCCGGAGAAAACTTGTA CTTCCAATCGATGGCGAGGCCTCAAAATCATCGCCGCAGTAATTGGACAGAAAG AGACGATAATGATGATTATCTGTTTCAGCGATTTCTAGAAGAATCGGAAACGAG GCATAGTAGAGAGCCTTCACCTGTAACCGAG
3038	gb_CRISPR_ΔHRD1	ACTGTCGACTTTCTACCGATTTGTTGGTTCCTTTTTATAACCAGAAAATCATCTATC AATTGCAATTTGTAAGAGAAGGGGAGAAAGACAAAATAATAATATTGCATGTTT TATATTATACATAGTTTTTTTTAAAGAAAAAAACTACTGGATGAAAAACACACAC ACACACACATATATATATATTATACATCAGCGGA

Table 2.3- List of plasmids

Name	Insert/Gene	Primers	Vector	Procedure	Source
pPC1230	TM68-3xHA	2015	pRS316 (CEN, URA, AmpR)	TM68 (with promoter of Erg11) was obtained by the deletion of amino acids 68-521 by QuickerChange mutagenesis using primer 2015 and pPC1082 was used as as template	This study
pPC1302	SP-3xHA-Gpi8 (TM)	2095, 2096	pRS415 (CEN, LEU, AmpR)	Insert was amplified from plasmid primers 2095, 2096. Fragment digested with SmaI/BamHI and cloned in pPC1287 digested with the same enzymes.	This study
pPC1313	SP-3xHA-Gpi16 (TM)	2182, 2183	pRS415 (CEN, LEU, AmpR)	Insert was amplified from plasmid primers 2182, 2183. Fragment digested with SmaI/BamHI and cloned in pPC1287 digested with the same enzymes.	This study
pPC1301	SP-3xHA-Wbp1 (TM)	2093, 2097	pRS415 (CEN, LEU, AmpR)	Insert was amplified from plasmid primers 2093, 2097. Fragment digested with SmaI/BamHI and cloned in pPC1287 digested with the same enzymes.	This study
pPC 1229	TM56-3xHA	2014	pRS316 (CEN, URA, AmpR)	TM68 (with promoter of Erg11) was obtained by the deletion of amino acids 56-521 by QuickerChange mutagenesis using primer 2014 and pPC1082 was used as template	This study
pESC-Bpa	TyrRS-tRNACUA				Chin et al., 2003
pPC1450	TM56-3xHA, F22 amber(TAG)	2036	pRS316 (CEN, URA, AmpR)	Obtained by QuickerChange mutagenesis using primer 2036 was replace F22 by TAG. pPC1229 was used as template	This study
pPC1451	TM56-3xHA, L27 amber(TAG)	2478, 2479	pRS316 (CEN, URA, AmpR)	Obtained by QuickerChange mutagenesis using primer 2478, 2479 to replace L27 by TAG. pPC1229 was used as template	This study
pPC1452	TM56-3xHA, I31 amber(TAG)	2480, 2481	pRS316 (CEN, URA, AmpR)	Obtained by QuickerChange mutagenesis using primer 2480, 2481 to replace I31 by TAG. pPC1229 was used as template	This study
pPC1453	TM56-3xHA, I36 amber(TAG)	2482, 2483	pRS316 (CEN, URA, AmpR)	Obtained by QuickerChange mutagenesis using primer 2482, 2483 to replace I36 by TAG. pPC1229 was used as template	This study
pPC1454	TM56-3xHA, F39 amber(TAG)	2035	pRS316 (CEN, URA, AmpR)	Obtained by QuickerChange mutagenesis using primer 2035 to replace F39 by TAG. pPC1229 was used as template	This study
pPC1455	TM56-3xHA, I43 amber(TAG)	2484, 2485	pRS316 (CEN, URA, AmpR)	Obtained by QuickerChange mutagenesis using primer 2484, 2485 to replace I43 by TAG. pPC1229 was used as template	This study
pPC1456	TM56-3xHA, L47 amber(TAG)	2486, 2487	pRS316 (CEN, URA, AmpR)	Obtained by QuickerChange mutagenesis using primer 2486, 2487 to replace L47 by TAG. pPC1229 was used as template	This study
pPC1457	TM56-3xHA, L51 amber(TAG)	2488, 2489	pRS316 (CEN, URA, AmpR)	Obtained by QuickerChange mutagenesis using primer 2488, 2489 to replace L51 by TAG. pPC1229 was used as template	This study
pPC1082	Erg11-HA	1557, 185	pRS316 (CEN, URA, AmpR)		Foresti et al., 2014
pPC1417	Asi1	2367, 2368	pRS423 (2μ, HIS, AmpR)	Asi1 full length amplified using 2367, 2368 primers and inserted into the vector using enzymes SmaI, XhoI	This study
pPC1581	Asi3	2371, 2372	pRS425 (2μ, LEU, AmpR)	Codon optimized Asi3 full length amplified using 2371, 2372 primers and inserted into the vector using enzymes SmaI, XhoI	This study
pPC1585	Asi1 (Δ562-624)	2367, 2759	pRS423 (2μ, HIS, AmpR)	Asi1 lacking the residues amplified using 2367, 2759 primers and inserted into the vector using enzymes SmaI, XhoI	This study

Name	Insert/Gene	Primers	Vector	Procedure	Source
pPC1586	Asi3-3 (618-676Δ)	2371, 2760	pRS425 (2µ, LEU, AmpR)	Asi3 lacking the residues amplified using 2371, 2760 primers and inserted into the vector using enzymes SmaI, XhoI	This study
pPC1583	SBP-TEV-Asi2	33,323,333	pRS426 (2µ, URA, AmpR)	Vector containing an N-terminal SBP-TEV was linearised using primers 3332,3333. Asi2 was amplified and inserted into linearised vector by Gibson assembly	This study
pPC1587	3xFlag-Asi3	2599 , 2600	pRS425 (2µ, LEU, AmpR)	Obtained by QuickerChange mutagenesis using primer 2599, 2600 to insert the 3xFlag tag. pPC1581 was used as template	This study
pPC1822	His14-sumo-TM68-MBP-LPTEGG	2746, 2747, 2744, 2748	K27 (KanR)	Vector containing an H14-Sumo-TM68 was linearised using primers 2746,2747. MBP was amplified using 2744,2748 and inserted into linearised vector by Gibson assembly	This study
pPC1823	His14-sumo-TM68(I36C)-MBP-LPTEGG	2770, 2771, 2765	K27 (KanR)	pPC1822 was linearised using primers 2770, 2771. Gene fragment 2765 containing I36C mutation was inserted by gibson assembly	This study
pPC 1260	Asi1(424-616)-6xHis	1560+2055	pET30-b (KanR)	Asi1 fragment was amplified using primers 1560, 2055 and inserted into the vector containing an C-terminal 6xHis tag using enzymes NcoI, XhoI.	This study
pPC1234	Asi2(153-271)-6xHis	1942, 1943	pET30-b (KanR)	Asi2 fragment was amplified using primers 1942, 1943 and inserted into the vector containing an C-terminal 6xHis tag using enzymes NcoI, XhoI.	This study
pPC 1262	Asi3(484-676)-6xHis	1563, 2056	pET30-b (KanR)	Asi3 fragment was amplified using primers 1563, 2056 and inserted into the vector containing an C-terminal 6xHis tag using enzymes NcoI, XhoI.	This study
pPC 1878	His-Sumo-Ubc4	3334, 3335	K27 (KanR)	Coding region of Ubc4 was amplfied using 3334, 3335 from cDNA of a wild type strain. Amplified product was inserted into the vector by gibson assembly	
pPC1661	Asi2-gRNA1		pML107 (2µ, LEU, AmpR)	Asi2 gRNA1 was inserted into the vector enzymes BclI and SmiI.	This study
pPC1695	Hrd1-gRNA1		pML107 (2µ, LEU, AmpR)	Hrd1 gRNA1 was inserted into the vector enzymes BclI and SmiI.	This study
pPC1705	Doa10-gRNA1		pML107 (2µ, LEU, AmpR)	Doa10 gRNA1 was inserted into the vector enzymes BclI and SmiI.	This study

2.1.2 Restriction digestion

Some plasmids were constructed using conventional cloning using restriction enzymes. In this case, plasmid DNA was incubated with the required FastDigest enzymes (Thermo) at 37°C for 2-3 hr as per Table 2.4

Table 2.4- Enzyme digestion

Component	Volume (µl)
Water	37
Fast figest buffer	5
Enzyme 1	1.5
Enzyme 2	1.5
Plasmid	5

2.1.3 Agarose gel purification

PCR fragments and endonuclease digested plasmids were analysed by electrophoresis using 1% agarose (Sigma) gel prepared with 1xTAE (Tris/acetate/EDTA) buffer supplemented with SYBR safe (1: 10,000; Invitrogen). Fragments of interest were retrieved from gels using a clean scalpel. Subsequently, DNA was purified using a gel extraction purification kit (Qiagen) according to manufacturers protocol and resuspended in 30-50µl water.

2.1.4 DNA assembly

Ligation

For standard ligations, 4.5µl of the gel-purified DNA fragment, 0.5µl linearized plasmid and 5µl of 2x ligation mix (Takara) were incubated at 17°C for 30 min. Finally, the entire ligation mixture was transformed into bacteria.

Gibson Assembly

Some of the plasmids were constructed using Gibson assembly (Gibson et al., 2009). In these cases, fragments to clone were amplified by PCR with 20-25 bp overhangs to the linearised vector. Gel-purified fragments were mixed with the vector in a ratio of 4:1 pmols/µl in a total volume of 2.5µl. 2.5µl 2x Gibson Assembly master mix (New England Labs) was added to this mixture and incubated at 50°C for 1 hr. The entire reaction was transformed into bacteria.

2.1.5 Site-directed mutagenesis

Site-directed mutagenesis was used to generate point mutations. Forward and reverse primers with 22-26 bp homology on either side of the desired point mutation were used in PCR reactions according to the protocol in Table 2.1a. Ultra high fidelity Pfu polymerase (Agilent) and 6-7 min of extension time were used in these reactions. Reactions were digested with 1µl of DpnI restriction enzyme (Thermo) for 1-2 hr at 37°C and 5-8µl of the digested mixture was transformed into bacteria.

2.1.6 Bacterial transformation

DNA ligation reactions were transformed into chemically competent *E. coli* (DH5α strain). 5-8µl of the assembled product was incubated on ice with 50µl of competent *E. coli* for 20 min. Subsequently, it was subjected to heat shock at 42°C for 40 s and incubated on ice for 2 min. Further 300µl of LB media was added and recovered by incubation at 37°C for 30 min. Bacteria were pelleted at max speed for 30 sec. Pellet was resuspended in 50µl of water and plated on LB agar with 100µg/ml ampicillin or 30µg/ml kanamycin. Plates were incubated at 37°C overnight.

2.1.7 Preparation of plasmid and sequencing

Bacterial colonies were inoculated into 5ml of LB with respective antibiotics and grown overnight at 37°C in a shaker incubator at 180 rpm. Bacterial pellets were harvested by centrifugation at 1500g, 8 min at 4°C. Plasmid DNA was isolated by Thermo Scientific mini prep kit following the manufacturers' protocol. Restriction digestion and Sanger sequencing (Source Bioscience) were used for plasmid DNA analysis.

2.2 Yeast cell biology methods

2.2.1 Yeast strains, growth conditions and storage

All strains used were isogenic to BY4741 (*Mata ura3Δ0 his3Δ1 leu2Δ0 met15Δ0*), BY4742 (*Matα his3Δ1 leu2Δ0 lys2Δ0 ura3Δ0*) or FY251 (*Mata ura3-52 his3Δ200 leu2Δ1 trp1Δ63*).

Deletions and tagging of proteins were performed by PCR- based homologous recombination technique or CRISPR based gene-editing techniques (Janke et al., 2004; Laughery et al., 2015; Longtine et al., 1998).

For Asi2Δ4, AA residues (261-264) were deleted by CRISPR. Single guide RNA sequence for the required region of Asi2 was designed using online software (http://wyrickbioinfo2.smb.wsu.edu). Oligos 3323, 3324 were annealed and cloned into a pML vector (Addgene) containing the Cas9 endonuclease from *Streptococcus pyogenes*. Cas9 plasmid along with a PCR amplified template containing the deletion of AA (261-264) was transformed using standard transformation protocol. Colonies were screened by PCR or by sequencing of genomic DNA. Positive colonies were grown in rich media (YPD) for 2-3 days to allow the loss of Cas9 plasmid. All strains and primers used are listed in Tables 2.5 and 2.2, respectively.

Table 2.5- List of strains

yPC	Genotype	Source
yPC1507	*Mat a ura3-52 his3Δ200 leu2Δ1 trp1Δ63*	FY251
yPC1506	*Mat α ura3Δ0 his3Δ1 leu2Δ0 lys2Δ0*	BY4742
yPC1505	*Mat a ura3Δ0 his3Δ1 leu2Δ0 met15Δ0*	BY4741
yPC2008	*Mat a ura3Δ0 his3Δ1 leu2Δ0 met15Δ0 asi1::KANR*	Foresti et al., 2014
yPC2009	*Mat a ura3Δ0 his3Δ1 leu2Δ0 met15Δ0 asi2::KANR*	Foresti et al., 2014
yPC2010	*Mat a ura3Δ0 his3Δ1 leu2Δ0 met15Δ0 asi3::KANR*	Foresti et al., 2014
yPC7650	*Mat a ura3Δ0 his3Δ1 leu2Δ0 met15Δ0 NATR-ADHp-3xFlag-Asi1*	Foresti et al., 2015
yPC9795	*Mat a ura3Δ0 his3Δ1 leu2Δ0 met15Δ0 NATR-ADHp-3xFlag-Asi1(Δ435-624)*	This study
yPC9796	*Mat a ura3Δ0 his3Δ1 leu2Δ0 met15Δ0 NATR-ADHp-3xFlag-Asi1(Δ313-624)*	This study
yPC11635	*Mat a ura3Δ0 his3Δ1 leu2Δ0 met15Δ0 <pPC1230>*	This study
yPC11650	*Mat a ura3Δ0 his3Δ1 leu2Δ0 met15Δ0 asi1::KANR <pPC1230>*	This study
yPC11636	*Mat a ura3Δ0 his3Δ1 leu2Δ0 met15Δ0 asi2::KANR <pPC1230>*	This study
yPC11651	*Mat a ura3Δ0 his3Δ1 leu2Δ0 met15Δ0 asi3::KANR <pPC1230>*	This study
yPC11652	*Mat α his3Δ1 leu2Δ0 lys2Δ0 ura3Δ0 doa10::His5 <pPC1230>*	This study
yPC11653	*Mat a ura3-52 his3Δ200 leu2Δ1 trp1Δ63 lys2Δ0 hrd1::HYGB <pPC1230>*	This study
yPC11712	*Mat α his3Δ1 leu2Δ0 lys2Δ0 ura3Δ0 ubc7::HYGB <pPC1230>*	This study
yPC11713	*Mat a his3Δ1 leu2Δ0 lys2Δ0 ura3Δ0 ubc4::KANR <pPC1230>*	This study
yPC11714	*Mat ? his3Δ1 leu2Δ0 lys2Δ0 ura3Δ0 ubc7::HYGB ubc4::KANR <pPC1230>*	This study
yPC11667	*Mat a ura3Δ0 his3Δ1 leu2Δ0 met15Δ0 <pPC1302>*	This study
yPC11668	*Mat a ura3Δ0 his3Δ1 leu2Δ0 met15Δ0 asi1::KANR <pPC1302>*	This study
yPC11669	*Mat a his3Δ1 leu2Δ0 met15Δ0 ura3Δ0 doa10::KANR <pPC1302>*	This study
yPC11670	*Mat a ura3-52 his3Δ200 leu2Δ1 trp1Δ63 lys2Δ0 hrd1::HYGB <pPC1302>*	This study
yPC11671	*Mat a ura3Δ0 his3Δ1 leu2Δ0 met15Δ0 <pPC1313>*	This study
yPC11672	*Mat a ura3Δ0 his3Δ1 leu2Δ0 met15Δ0 asi1::KANR <pPC1313>*	This study
yPC11673	*Mat a his3Δ1 leu2Δ0 met15Δ0 ura3Δ0 doa10::KANR <pPC1313>*	This study
yPC11674	*Mat a ura3-52 his3Δ200 leu2Δ1 trp1Δ63 lys2Δ0 hrd1::HYGB <pPC1313>*	This study
yPC11663	*Mat a ura3Δ0 his3Δ1 leu2Δ0 met15Δ0 <pPC1301>*	This study
yPC11664	*Mat a ura3Δ0 his3Δ1 leu2Δ0 met15Δ0 asi1::KANR <pPC1301>*	This study
yPC11665	*Mat a his3Δ1 leu2Δ0 met15Δ0 ura3Δ0 doa10::KANR <pPC1301>*	This study
yPC11666	*Mat a ura3-52 his3Δ200 leu2Δ1 trp1Δ63 lys2Δ0 hrd1::HYGB <pPC1301>*	This study
yPC10511	*Mat a ura3-52 his3Δ200 leu2Δ1 trp1Δ63 ubc7::HYGB NATR-ADHp-3xFlag-Asi1 <pPC1229+ pPC557>*	This study
yPC10512	*Mat a ura3-52 his3Δ200 leu2Δ1 trp1Δ63 ubc7::HYGB NATR-ADHp-3xFlag-Asi1 <pPC1450+ pPC557>*	This study
yPC10513	*Mat a ura3-52 his3Δ200 leu2Δ1 trp1Δ63 ubc7::HYGB NATR-ADHp-3xFlag-Asi1 <pPC1451+ pPC557>*	This study
yPC10514	*Mat a ura3-52 his3Δ200 leu2Δ1 trp1Δ63 ubc7::HYGB NATR-ADHp-3xFlag-Asi1 <pPC1452+ pPC557>*	This study

yPC	Genotype	Source
yPC10515	*Mat a ura3-52 his3Δ200 leu2Δ1 trp1Δ63 ubc7::HYGB NATR-ADHp-3xFlag-Asi1 <pPC1453+ pPC557>*	This study
yPC10516	*Mat a ura3-52 his3Δ200 leu2Δ1 trp1Δ63 ubc7::HYGB NATR-ADHp-3xFlag-Asi1 <pPC1454+ pPC557>*	This study
yPC10517	*Mat a ura3-52 his3Δ200 leu2Δ1 trp1Δ63 ubc7::HYGB NATR-ADHp-3xFlag-Asi1 <pPC1455+ pPC557>*	This study
yPC10518	*Mat a ura3-52 his3Δ200 leu2Δ1 trp1Δ63 ubc7::HYGB NATR-ADHp-3xFlag-Asi1 <pPC1456+ pPC557>*	This study
yPC10519	*Mat a ura3-52 his3Δ200 leu2Δ1 trp1Δ63 ubc7::HYGB NATR-ADHp-3xFlag-Asi1 <pPC1457+ pPC557>*	This study
yPC9012	*Mat a his3Δ1 leu2Δ0 met15Δ0 ura3Δ0 ubc4::KANR <pPC1274>*	This study
yPC9013	*Mat a his3Δ1 leu2Δ0 ura3Δ0 ubc6::KANR <pPC1274>*	This study
yPC9014	*Mat α his3Δ1 leu2Δ0 lys2Δ0 ura3Δ0 ubc7::HYGB <pPC1274>*	This study
yPC9015	*Mat ? his3Δ1 leu2Δ0 lys2Δ0 ura3Δ0 ubc7::HYGB ubc4::KANR <pPC1274>*	This study
yPC8964	*Mat a ura3Δ0 his3Δ1 leu2Δ0 met15Δ0 <pPC1274>*	This study
yPC8965	*Mat a ura3Δ0 his3Δ1 leu2Δ0 met15Δ0 asi1::KANR <pPC1274>*	This study
yPC8966	*Mat α his3Δ1 leu2Δ0 lys2Δ0 ura3Δ0 doa10::His5 <pPC1274>*	This study
yPC8967	*Mat a ura3-52 his3Δ200 leu2Δ1 trp1Δ63 lys2Δ0 hrd1::HYGB <pPC1274>*	This study
yPC11777	*Mat a ura3Δ0 leu2Δ0 met15Δ0 vma3::KANR Vph1-GFP-HIS2*	This study
yPC11778	*Mat a ura3Δ0 leu2Δ0 met15Δ1 vma3::KANR asi1::NATR Vph1-GFP-HIS2*	This study
yPC11779	*Mat a ura3Δ0 leu2Δ0 met15Δ2 vma16::KANR Vph1-GFP-HIS2*	This study
yPC11780	*Mat a ura3Δ0 leu2Δ0 met15Δ3 vma16::KANR asi1::NATR Vph1-GFP-HIS2*	This study
yPC11563	*Mat ? ura3Δ0 his3Δ1 leu2Δ0 asi1::NATR asi2::HYGB asi3::KANR doa10::crispr hrd1::crispr <pPC1585 + pPC1583 + pPC1586>*	This study
yPC11565	*Mat ? ura3Δ0 his3Δ1 leu2Δ0 asi1::NATR asi2::HYGB asi3::KANR doa10::crispr hrd1::crispr <pPC1417 + pPC1587*	This study
yPC11566	*Mat ? ura3Δ0 his3Δ1 leu2Δ0 asi1::NATR asi2::HYGB asi3::KANR doa10::crispr hrd1::crispr <pPC1417 + pPC1583 + pPC1587>*	This study
yPC11567	*Mat ? ura3Δ0 his3Δ1 leu2Δ0 asi1::NATR asi2::HYGB asi3::KANR doa10::crispr hrd1::crispr <pPC1417 + pPC1583 + pPC1581>*	This study
yPC8632	*Mat a ura3Δ0 his3Δ1 leu2Δ0 met15Δ0 <pPC1082>*	Foresti et al., 2014
yPC8634	*Mat a ura3Δ0 his3Δ1 leu2Δ0 met15Δ0 asi2::KANR <pPC1082>*	Foresti et al., 2014
yPC11654	*Mat a ura3-52 his3Δ200 leu2Δ1 trp1Δ63 Asi2(261-264Δ)::crispr <pPC1082>*	This study
yPC11655	*Mat a ura3Δ0 his3Δ1 leu2Δ0 met15Δ0 NATR-ADHp-3xFlag-Asi2 <pPC1082>*	This study
yPC11656	*Mat a ura3Δ0 his3Δ1 leu2Δ0 met15Δ0 NATR-ADHp-3xFlag-Asi2 (261-264Δ)::crispr <pPC1082>*	This study
yPC8032	*Mat a ura3Δ0 his3Δ1 leu2Δ0 met15Δ0 wbp1-2::KANR*	Li et al., 2011
yPC8169	*Mat ? ura3Δ0 his3Δ1 leu2Δ0 met15Δ0 wbp1-2::KANR asi1::NATR*	This study
yPC8370	*Mat ? ura3Δ0 his3Δ1 leu2Δ0 met15Δ0 wbp1-2::KANR asi2::NATR*	This study
yPC8372	*Mat ? ura3Δ0 his3Δ1 leu2Δ0 met15Δ0 wbp1-2::KANR asi3::NATR*	This study
yPC8230	*Mat ? ura3Δ0 his3Δ1 leu2Δ0 met15Δ0 wbp1-2::KANR doa10::HIS*	This study
yPC8233	*Mat ? ura3Δ0 his3Δ1 leu2Δ0 met15Δ0 wbp1-2::KANR hrd1::HygB*	This study
yPC8227	*Mat ? ura3Δ0 his3Δ1 leu2Δ0 met15Δ0 wbp1-2::KANR ubc7::HYGB*	This study

yPC	Genotype	Source
yPC11735	*Mat a ura3-52 his3Δ200 leu2Δ1 trp1Δ63 URA3-GPDp-AtTIR1-9Myc Swp1-4AID-3xFlag-HYGB*	This study
yPC11736	*Mat a ura3-52 his3Δ200 leu2Δ1 trp1Δ63 URA3-GPDp-AtTIR1-9Myc Swp1-4AID-3xFlag-HYGB asi1::NATR*	This study
yPC9391	*Mat a ura3Δ0 his3Δ1 leu2Δ0 met15Δ0 lys2Δ0 can1Δ::LEU2-MFA1pr::His3 ost2-ts::URA3*	This study
yPC11309	*Mat ? ura3Δ0 his3Δ1 leu2Δ0 met15Δ0 lys2Δ0 ost2-ts::URA3 asi1::NATR*	This study
yPC11259	*Mat a ura3Δ0 his3Δ1 leu2Δ0 met15Δ0 stt3-7::KANR*	Li et al., 2011
yPC11645	*Mat ? ura3Δ0 his3Δ1 leu2Δ0 met15Δ0 stt3-7::KANR asi1::NATR*	This study
yPC11308	*Mat a ura3Δ0 his3Δ1 leu2Δ0 met15Δ0 lys2Δ0 can1Δ::LEU2-MFA1pr::His3 ost2-ts::URA3 OST4-3xFlag-HYGB*	This study
yPC11310	*Mat ? ura3Δ0 his3Δ1 leu2Δ0 met15Δ0 lys2Δ0 ost2-ts::URA3 asi1::NATR OST4-3xFlag-HYGB*	This study
yPC11661	*Mat a ura3Δ0 his3Δ1 leu2Δ0 met15Δ0 OST4-3xFlag-HYGB*	This study
yPC11662	*Mat a ura3Δ0 his3Δ1 leu2Δ0 met15Δ0 asi1::KANR OST4-3xFlag-HYGB*	This study
yPC11630	*Mat a ura3Δ0 his3Δ1 leu2Δ0 met15Δ0 <pPC1229>*	This study
yPC11646	*Mat a ura3Δ0 his3Δ1 leu2Δ0 met15Δ0 asi1::KANR <pPC1229>*	This study
yPC11631	*Mat a ura3Δ0 his3Δ1 leu2Δ0 met15Δ0 asi2::KANR <pPC1229>*	This study
yPC11647	*Mat a ura3Δ0 his3Δ1 leu2Δ0 met15Δ0 asi3::KANR <pPC1229>*	This study
yPC11648	*Mat α his3Δ1 leu2Δ0 lys2Δ0 ura3Δ0 doa10::His5 <pPC1229>*	This study
yPC11649	*Mat a ura3-52 his3Δ200 leu2Δ1 trp1Δ63 lys2Δ0 hrd1::HYGB <pPC1229>*	This study
yPC11715	*Mat α his3Δ1 leu2Δ0 lys2Δ0 ura3Δ0 ubc7::HYGB <pPC1229>*	This study
yPC11716	*Mat a his3Δ1 leu2Δ0 lys2Δ0 ura3Δ0 ubc4::KANR <pPC1229>*	This study
yPC11717	*Mat ? his3Δ1 leu2Δ0 lys2Δ0 ura3Δ0 ubc7::HYGB ubc4::KANR <pPC1229>*	This study
yPC11756	*Mat a ura3Δ0 his3Δ1 leu2Δ0 met15Δ0 SBP-TEV-ASI2:Crispr <pPC1229>*	This study

Yeast cells were grown either in YPD (Yeast extract- Peptone- Dextrose; Table 2.6a) or synthetic defined amino acid drop-out (SD; Table 2.6b). For short-term storage, they were streaked on respective agar plates and stored at 4°C. For long-term, strains from agar plates were resuspended in 700µl YPD and 300µl of 50% glycerol in cryovials and stored at -80°C.

Table 2.6a- YPD media

Component from Stock	Amount (g) for 1L
Bactopeptone	20
Yeast extract	10
40% Glucose	50ml

Table 2.6b- Synthetic drop-out media

Stock concentration	Component from Stock	Volume (ml) for 1L
40%	Glucose	50
20mM	Uracil	10
40mM	Tryptophan	10
100mM	Histidine	3
100mM	Lysine	10
100mM	Leucine	16.8
13.5mM	Methionine	10
	YNB (wo AA, ammonium sulphate), Difco	1.7
	Ammonium sulphate	5

2.2.3 Mating, sporulation and dissection

For mating, freshly streaked yeast cells with opposite mating types – *MATa and MATα* were mixed on YPD plates and incubated 3-4 hr at 30°C. Diploids were selected by replica plating in the appropriate selective media. Alternatively, diploids were isolated at the zygote stage by micromanipulation. In both cases, diploids were allowed to grow for 24-36hr. For sporulation, diploids were resuspended in 3ml of sporulation media (Table 2.6c) and incubated at 25°C for 2-3 days.

For dissection, 150µl of sporulated cells were pelleted at 3000g in a table-top centrifuge. Pellet was resuspended in 40µl of water and 10µl of zymolase (10mg/ml). It was incubated for 5min at RT followed by addition of 1ml of YPD. Subsequently, 20µl was added on YPD plate and spores were dissected under a microscope equipped with a microdissector.

Table 2.6c- Sporulation media

Stock concentration	Component from Stock	Volume (ml) for 1L
2%	Potassium acetate	500
20mM	Uracil	2
40mM	Tryptophan	2
100mM	Leucine	3.4
100mM	Histidine	0.6

2.2.4 Plasmid, PCR transformation and verification of genotypes

Plasmid transformation- a small amount of cells (freshly streaked on a plate for 12-14 hr) were resuspended in 100µl of transformation mix (Table 2.7a). 500ng of plasmid DNA and 5µl of carrier salmon sperm DNA were added to the mix and incubated at RT for 4-6 hr. Subsequently, they were spread of synthetic defined drop-out agar plates and incubated at 30°C for 2 days.

Table 2.7a - Transformation mix

Stock concentration	Component from Stock	Volume (ml) for 10ml
50%	PEG	8
1M	Lithium acetate	1
10x (100mM)	TE	1

Table 2.7b – LT buffer

Stock concentration	Component from Stock	Volume (ml) for 50ml
1M	Lithium acetate	5
10x (100mM)	Tris-EDTA buffer (TE)	5
	MQ water	40

PCR transformation- yeast cells were inoculated in 5ml of YPD for 12-14 hr. Subsequently, cells were diluted to ~0.05-0.06 OD_{600} and grown for additional 3-4 hr until 0.3-0.4 OD_{600}. Cells were pelleted by centrifugation (1500g, 5 min, RT), washed with 5 ml of LT buffer (Table 2.7b) and pelleted again. Pellet was resuspended in 400µl LT buffer. 120µl of the cell suspension was combined with 20µl of PCR fragment and 20µl of carrier DNA in 50ml falcon tubes and incubated in a shaker incubator (30°C, 200 rpm, 30 min). It was followed by heat shock at 42°C in a water bath for 20 min, 15 ml of YPD media was added and incubated in a shaker incubator (30°C, 200 rpm, ~3 hr). Finally, cells were pelleted, supernatant was discarded and pellet was resuspended in 200µl of YPD. Cells were spread on YPD supplemented with drugs or synthetic defined drop-out agar plates and incubated at 30°C for 2-3 days.

Verification of genotypes- Yeast cells that were either epitope-tagged or deleted for a gene by insertion of PCR cassettes were verified by a colony PCR with gene-specific and cassette-specific pair of primers. Different colonies from plates were picked, resuspended in 20µl of 20mM sodium hydroxide and incubated at 95°C for 15 min. Subsequently, a standard PCR protocol as indicated in Table 2.1b was followed.

2.3 Biochemical methods

2.3.1 Yeast culture

Unless specified otherwise, yeast experiments were performed during exponential growth conditions. Preculture was inoculated from freshly streaked plates in 3ml of YPD or SD media as required and grown at 25°C or 30°C for at least 6 hr. Subsequently, cells were diluted in a larger volume of media (5ml to 150ml) as required to an OD_{600}~ (0.006-0.009) and grown for an additional ~12 hr to reach an OD_{600}~ 0.8-1.

2.3.2 Whole-cell extract preparation

Extracts were prepared as described in (Kushnirov, 2000). Briefly, 1 OD_{600} of cells were harvested by centrifugation for 2 min at 13000g. Pellet was resuspended in 250µl of 0.15M sodium hydroxide and incubated on ice for 10 min. Resuspended cells were pelleted by centrifugation (13000g, 2 min, 4°C) and 50-100µl of 1.5x SDS reducing buffer (Table 2.8) was added. It was denatured at 65°C for 10-15 min and 8-15µl was loaded on SDS-PAGE and analysed by immunoblotting.

2.3.3 SDS-PAGE and western blotting

For protein analysis by sodium dodecyl sulfate-polyacrylamide gel electrophoresis (SDS-PAGE), 4-20% Criterion TGX gels (Bio-Rad) and TGS running buffer (25mM Tris pH 8.3, 192mM glycine, 0.1%(w/v) SDS) were used. Gels were directly stained with colloidal coomassie stain (Instant blue, Expedeon) or

proteins were transferred to polyvinylidene difluoride (PVDF) membranes (Bio-Rad) using a Turbo Transblot system (Bio-Rad). A program optimized for the transfer of high molecular weight proteins was used (2.5A, 25V, 10min). Membranes were blocked with 5% milk or 5% BSA prepared in PBS (0.1% Tween 20) for approximately 40 min at RT and incubated with the required primary antibodies for a minimum of 4 hr (Table 2.8a). Subsequently, membranes were washed three times with PBS (0.1% Tween 20) and incubated with secondary antibody for 45 min and washed as before. Proteins were detected using enhanced chemiluminescence (ECL reagent, Perkin Elmer) and imaged with an Amersham Imager 600 (GE).

2.3.4 Cycloheximide shut off chases

Synthesis of proteins was blocked by the addition of 100µl of cycloheximide (CHX, Sigma) from a stock of 12.5mg/ml (prepared in MQ water) to 5ml of yeast cells which were grown as described above (2.3.1). Aliquots were collected at specific timepoints and whole-cell extracts were prepared as per section 2.3.2.

In the case of temperature-sensitive strains, cells were grown at 25°C to reach exponential phase. At an OD_{600}~ 0.6-0.7 they were shifted to 37°C for 1 hr and CHX chase was performed as above.

2.3.5 Auxin dependent depletion of proteins

Yeast cells were grown at 25°C in YPD media to an exponential phase as mentioned in section 2.3.1. At an OD_{600}~ 0.3-0.4, 0.8mM of Auxin (3-Indoleacetic acid, Sigma) from a stock of 0.5M prepared in DMSO was added and incubated for 1 hr at 25°C. Time points were collects at 0 min and 60 min. Subsequently, CHX chase was performed as mentioned in section 2.3.3.

2.3.6 Sucrose gradient centrifugation

Approximately 100 OD_{600} of cells grown in YPD were harvested by centrifuge (3150g, 5 min, 4°C). Cell pellets were washed with cold water and re-suspended in 1.2ml of LB buffer containing 50mM Tris-HCl pH 7.4, 200mM NaCl, 1mM EDTA, 1mM PMSF and 1 tablet of protease inhibitor cocktail (Roche). Cell suspension was transferred to 2ml lysis tubes and glass beads (Biospec) were added to fill the tube followed by cell lysis (30 s on/off, 6-8 times). Unlysed cells were removed by a low-speed spin (376g, 10 min, 4°C). Whole-cell lysates were subjected to ultracentrifugation (100000g, 20 min, 4°C) to obtain crude membrane fractions. Membranes were resuspended in 1ml of LB buffer supplemented with 1% digitonin and solubilised for 3 hr at 4°C. Unsolubilised membranes were removed by a centrifuge spin (13000g, 15 min, 4°C). 200µl of solubilised membrane lysates were applied on to a 4ml 10-60% linear sucrose gradient in an SW60Ti tube (Ultraclear tubes, Beckman). The gradient was made in a Biocomp Gradient

maker (10-60% sucrose program). It was followed by ultracentrifugation in SW60Ti rotor (100000g, 4 hr, 4°C). 200µl fractions were collected from the top of the gradient, mixed with 100ul of SDS buffer(3X) and analysed by SDS PAGE and immunoblotting.

2.3.7 Native Immunoprecipitation (IP)

Approximately 100OD_{600} of cells were harvested at an OD_{600}~ 1 by centrifugation (3150g, 5 min, 4°C). Cell pellets were washed with cold water, resuspended in 1.2ml of LB buffer (50mM Tris-HCl pH 7.4, 200mM NaCl, 1mM EDTA, 1mM PMSF) supplemented with protease inhibitor cocktail (Roche) and transferred to 2ml lysis tubes. Glass beads (Biospec) were added to fill the tube. Lysis was carried out by bead beating in a biospec bead beater (30 s on/off, 6-8 times). Non lysed cells were removed by a low-speed spin (376g, 10 min, 4°C). Membranes were pelleted by ultracentrifugation (100000g, 20 min, 4°C). Membrane pellets were resuspended in 1ml of LB buffer supplemented with 1% detergent (digitonin, Decyl Maltose Neopentyl Glycol (DMNG) or glyco-diosgenin (GDN)) and solubilised for 3 hr at 4°C. Non-solubilised material was removed by centrifugation (13000g, 15 min, 4°C). Detergent solubilised extracts were used for immunoprecipitation. Typically for FLAG-IP, 30µl FLAG M2-magnetic beads (Sigma) per 950µl of solubilised extract were incubated overnight at 4°C. For IPs with in-house raised antibodies, 20µl of Protein A Dynabeads (Invitrogen) per

sample were coupled with 0.5µl of the antibodies. Immunoprecipitated material was washed 3 times with LB buffer supplemented with respective detergent and eluted in 90µl of non-reducing SDS buffer (1.5X) for 15 min at 65°C. Finally, eluted proteins were reduced by the addition of beta-mercaptoethanol, analysed by SDS-PAGE and immunoblotting. Input loaded normally corresponds to 10% of the total extract.

2.3.8 *In vivo* cross-linking

Ubc7 deleted cells were transformed with two plasmids. One encoding both for a modified tRNA synthetase which is capable of charging the unnatural amino acid benzoyl phenylalanine (BPA) on a tRNA as well as amber stop codon suppressor tRNA. The second plasmid encoded for TM56-HA with individual amber codons on different positions. Cells carrying both plasmids were grown at 25°C in 100ml of SD- UT media (synthetic media without uracil and tryptophan). At an OD_{600}~ 0.3-0.4, 150ml of BPA (stock- 0.2M in 1M NaOH prepared fresh) was added and incubated for an additional 6 hr at 25°C. Cells were harvested as above and resuspended in 1 ml of cold water. 500µl of cells were transferred to a 12 well plate. The lid of a 12- well plate was filled with cold water and laid on top of the 12- well plate containing cell suspensions. The UV lamp was placed directly on top of the water-filled lid and exposed to long-range UV irradiation for 60 min at 4°C using a B-100AP lamp (UVP, CA). The rest of 500µl of cells served as a

negative control without UV irradiation. Both UV radiated and not radiated cells were harvested by centrifugation (3150g, 5 min, 4°C) followed by lysis in LB buffer and membrane extraction as mentioned in section 2.3.6. Membranes were solubilised in 150µl buffer containing 50mM Tris/HCl [pH7.4], 1mM EDTA, 1% SDS and 2M urea for 30-45 min at 65°C until the solution was clear. Non solubilised material was removed by centrifugation (13000g, 15 min, RT). extracts were diluted with 1400µl of LB buffer supplemented 1% Nonidet P-40. 50µl of the diluted solubilised membranes were stored as the input sample. To the rest, 15µl of anti-HA magnetic beads (Pierce) were added and incubated overnight at 4°C. Finally, beads were washed with 1ml of LB buffer supplemented with 1% Nonidet P-40 four times. Proteins bound to the beads were eluted and analysed by SDS-PAGE and immunoblotting.

2.3.9 Growth assays

Cells were grown in YPD overnight at 25°C. They were diluted to obtain an OD_{600}~ 1.8-2. From here, 1 in 10 serial dilutions were made in sterile water and 3.5µl was spotted on YPD plates. Plates were incubated at 25°C, 33°C for 2-3 days and imaged in an EPSON scanner.

Table 2.8 – List of antibodies

Antibody	Source	Dilution	Blocking buffer (PBST 0.1% Tween 20)
Primary antibodies			
anti-HA (clone 3F10)	Roche	1 to 2000	5% Milk
anti-Pgk1	Invitrogen	1 to 10000	5% Milk
anti-Dpm1 (clone 5C5)	Invitrogen	1 to 10000	5% Milk
ANTI-FLAG M2-Peroxidase	Sigma-Aldrich	1 to 4000	5% Milk
ANTI-FLAG M2	Sigma-Aldrich	1 to 2000	5% Milk
anti-SBP tag (clone 20)	Merck	1 to 1000	5% Milk
anti-MBP	New England BioLabs	1 to 2000	5% Milk
anti-Wbp1	Riezman lab	1 to 3000	5% Milk
anti-Gpi8	Conzelmann lab	1 to 1000	5% Milk
anti-Asi1	raised in rabbit	1 to 1000	5% BSA
anti-Asi2	raised in rabbit	1 to 3000	5% Milk
anti-Asi3	raised in rabbit	1 to 1000	5% Non fat milk (Biorad)
Secondary antibodies			
anti-rabbit HRP	Jackson	1 to 10000	5% Milk
anti-mouse HRP	Jackson	2 to 10000	5% Milk
anti-rat HRP	Jackson	3 to 10000	5% Milk

2.4 Expression and purification of proteins

2.4.1 Asi complex

All Asi proteins (Asi1, Asi2 and Asi3) were co-expressed and purified as described (Stein et al., 2014). Cells lacking *ASI1*, *ASI2*, *ASI3*, *HRD1* and *DOA10* were transformed with high copy plasmids from the pRS42X series (Mumberg et al., 1994) encoding untagged Asi1 or Asi1 fused to N-terminal SBP (Streptavidin peptide tag) followed by a TEV protease cleavage site (SBP-TEV-Asi1), Asi3 or

FLAG-Asi3 as well as untagged Asi2 or SBP-TEV-Asi2. Codon optimized version of ASI3 was used.

Preculture was inoculated in synthetic drop our media with 2% (w/v) glucose and grown for 24 hr at 30˚C. It was further diluted in the ratio of 1:40 in fresh medium for another 24 hr. This was followed by the induction with galactose 8% (w/v) to induce protein expression in 4x YEP broth for 12 hr Cell pellet (~90gm) was harvested, washed with water and resuspended in 140ml of buffer A (20mM HEPES, 2mM Magnesium acetate, 150mM potassium chloride) with 1mM PMSF and 1.5µM of pepstatin A. 150g Glass beads (0.5mM diameter from BioSpec) was added, followed by cell lysis in a bead beater (BioSpec) with an ice water jacket. It was lysed for 30 sec on/off for 40 cycles. Glass beads were removed by filtration and unlysed cells were removed by a low-speed spin at 2000xg for 18 min. The supernatant was transferred to a Ti45 tube and centrifuged at 40,000 rpm for 45 min to obtain crude membranes. Membranes were washed twice with buffer B (20mM HEPES, 2mM Magnesium acetate, 300mM sodium chloride, 200mM sucrose) and solubilised for 90 min with 1%(w/v) of DMNG (decyl maltose neopentyl glycol) in buffer B supplemented with 1mM PMSF and 1.5UM Pepstatin A, 200ul of beta-mercaptoethanol (14.3M). Non-soluble membranes were removed by ultracentrifugation in Ti45 tubes for 30 min at 40000 rpm. 3 ml of High Capacity Streptavidin Agarose resin (Pierce) was added to the solubilised membranes and incubated overnight. After incubation, material was to 20ml gravity columns and the resin was washed with 25 column volumes of buffer C

(20mM HEPES, 2mM Magnesium acetate, 300mM sodium chloride, 0.3mM DMNG). Finally, bound proteins were eluted with buffer C containing 2mM Biotin. Eluted material was pooled, concentrated with 50kDa cut off filters (Amicon Ultra, Merck) and snap frozen in liquid nitrogen until use.

2.4.2 Recombinant protein expression and purification

Codon-optimized TM68 followed by an MBP tag and sortase labelling peptide LPTEGG were inserted in a K27 vector that contained an N-terminal His14-Sumo tag. This plasmid was transformed into BL21 DE3 RIPL cells (Agilent). Preculture was grown in 120ml of LB supplemented with kanamycin. Overnight cultures were diluted in 3L of terrific broth with Kanamycin. Expression was induced by the addition of 0.5mM IPTG at 30˚C for 3 hours. Cell pellets were obtained by centrifugation at 4000g for 10 min, followed by resuspension in buffer 20mM Tris-HCl (pH 8), 500mM NaCl, 20mM imidazole, pH 8.0, 1mM PMSF. The cells were lysed by in a microfluidizer (5x, 10000 psi). Non lysed cells were removed by a low-speed spin at 3000g for 10 min. The supernatant was subjected to ultracentrifugation in a Ti45 rotor, 40,000 rpm for 30 min. Membrane pellet obtained was solubilised in buffer W (50mM Tris-HCl (pH 8.0), 500mM NaCl, 30mM imidazole,1mM PMSF) supplemented with 1% DDM and solubilised for 90 min at 4˚C. Insoluble material was removed by ultracentrifugation in a Ti45 rotor, 40,000 rpm for 30 min. Supernatant was incubated with 3ml of Ni-NTA beads

(Pierce) for 3 hours at 4˚C on a rolling incubator. Beads were washed with 20 column volume of Buffer W supplemented 1% DDM and 10 column volumes of cleavage buffer 20mM Tris-HCl (pH 8), 200mM NaCl, 10mM imidazole. Beads were then resuspended in cleavage buffer supplemented with 1µM of Ulp1 (Frey and Görlich, 2014). Elutions were concentrated and applied on a Superdex 200 10/300 column equilibrated with buffer 20mM HEPES, 200mM NaCl, 0.3mM DMNG. Peak fractions were collected, and sortase labelling was performed using Dy800 dye as in (Stein et al., 2014). This was followed by repurifying on a Superdex 200 10/300 column.

TM68(I36C) was purified as described above just that Buffer W was supplemented with 0.4mM TCEP.

Uba1, Ubc7, Cue1, Cdc48, Npl4-Ufd1 were purified as described in (Stein et al., 2014)

2.5 *In vitro* reconstitution

2.5.1 Preparation of liposomes

Synthetic lipids 1-palmitoyl-2-oleoyl-*sn*-glycero-3-phosphocholine (POPC), 1,2-dioleoyl-*sn*-glycero-3-phosphoethanolamine (DOPE), 1,2-dioleoyl-*sn*-glycero-3-phospho-L-serine (DOPS), cholesterol and 1,2-dioleoyl-sn-glycero-3-phosphoethanolamine-N-(lissamine rhodamine B sulfonyl) ammonium salt (18:1 Liss Rhod PE) were obtained from Avanti lipids (Table 12.13). The stocks were prepared as indicated in Table 2.9 and the required volume of each lipid was transferred to a round bottom flask using Hamilton syringes.

Table 2.9 - Liposome mix

% Lipid	Lipid	Stock conc (mg/ml)	Volume required (µL)
64.5	POPC	25	392.2116
20	DOPE	10	297.6
10	DOPS	25	64.8024
5	Cholesterol	25	15.4662
0.5	Rhd-PE	2	65.0858

Subsequently, chloroform was evaporated in a Rotavap (Butchi) at a pressure of 200 mbar for 30 min to obtain a uniform lipid film. 1ml of diethyl ether and 300µl of an aqueous buffer L (20mM HEPES/KOH (pH 7.4), 50mM potassium chloride, 5mM magnesium acetate) was added to resuspend the lipid film. This mixture was sonicated at 10% amplitude for 1 min. Sonicated mixture was subjected to a rotavap in order to evaporate diethyl ether at 500 mbar for 10 min and followed by the addition of 700µl of buffer L. It was again subjected to rotavap to

evaporate any remaining diethyl ether at 500 mbar for 1 hr, 300 mbar for 1 hr and 80 mbar for 2 hr. The final volume of the liposomes was adjusted to 1ml with MQ water and extruded through 400nm size filters (11x) and 100 nm filters (21x) and stored at 4°C for 2-3 weeks.

2.5.2 Reconstitution into proteoliposomes

The following components were added sequentially in a total volume of 100µl:

Freshly prepared liposomes - **40µl**

From 60mM DMNG - **3.4µl (Final conc- 2mM)**

Incubate on ice for 30 min

Asi complex - **40µl (Final conc- 2.3µM)**

TM68-MBP - **0.5µl (Final conc- 0.43µM)**

Buffer U- **16.1µl to make up the volume to 100µl**

Incubate on ice for 60 min

Detergent removal spin columns (Thermo, Table 12.13) were equilibrated with 400µl of Buffer U (20mM HEPES (pH 7.4), 2mM magnesium acetate, 150mM sodium chloride, 0.5mM TCEP) followed by a spin at 1150g on a tabletop centrifuge for 1 min at RT. This step was repeated 2 more times without letting the columns to dry. Followed by equilibration, liposome+protein mixture was

applied on the detergent removal spin columns. It was incubated on the column for 30min at RT. This was followed by centrifugation (1150g, 1min, RT). Eluate was collected and reapplied on another freshly equilibrated column. Proteoliposomes were applied on three different columns in total. Final elution from the third column was collected and used for *in vitro* ubiquitination.

2.5.3 *In vitro* ubiquitination assay with Proteoliposomes

A master ubiquitination reaction mix was prepared as described in Table 2.10.

Table 2.10 - Proteoliposome ubiquitination master mix

Component	Stock conc (µM)	Final conc (µM)	Volume rquired per reaction in 25µl
E1- Uba1	22.7	0.23	0.25
E2- Ubc4	142	2.1	0.37
E2- Ubc7	311	2.3	0.18
Cue1	250	2.2	0.22
BSA	10 mg/ml	0.2mg/ml	0.50
His-Ubiquitin	250	50	5.00
Buffer U			10.35
ATP	100	2.5	
Master mixture			16.87

To the above master mix, reconstituted proteoliposomes and ATP were added as described in Table 2.11.

Table 2.11

Reactions	ATP+	ATP-
From master mix	16.87	16.87
Proteoliposomes	7.50	7.50
ATP	0.625	0
Buffer U	0	0.625

Buffer U- 20mM HEPES (pH 7.4), 2mM magnesium acetate, 150mM sodium chloride, 0.5mM TCEP

Reactions were incubated at 30°C for 1 hr on a 96-well thermal cycler block. 10µl of the reactions were mixed with 10µl of SDS buffer(3X), resolved by SDS-PAGE and directly analysed by scanning the gel in an imager or by immunoblotting. In some experiments, reactions were subjected to Ni-NTA affinity purification to enrich for His-Ubiquitin conjugates. In this case, the reaction mixture containing ubiquitin conjugates were solubilised with 500µl of buffer (20mM HEPES (pH 7.4), 2mM magnesium acetate, 150mM sodium chloride, 6M urea, 10mM imidazole, 1% Triton X-100) for 15min at 4°C. 30µl of was stored as Input. To the remaining, 20µl of Ni-NTA agarose beads (Pierce) was added and incubated for 3 hr or overnight at 4°C. Unbound was collected and beads were washed five times with 1ml of buffer (20mM HEPES (pH 7.4), 2mM magnesium acetate, 150mM sodium chloride, 6M urea, 20mM imidazole, 1% Triton X-100). Finally, bound proteins were eluted with 50µl of 1xSDS buffer supplemented with 500mM Imidazole.

2.5.4 *In vitro* ubiquitination assay in Detergent

Reaction mixture containing the below components with specific concentrations were prepared as indicated in Table2.12 in 200µl PCR tubes.

Table 2.12- Detergent ubiquitination master mix

Component	Stock conc (µM)	Final conc (µM)	Volume rquired per reaction in 25µl
E1- Uba1	22.7	0.23	0.25
E2- Ubc4	142	2.1	0.37
E2- Ubc7	311	2.3	0.18
Cue1	250	2.2	0.22
BSA	10 mg/ml	0.2mg/ml	0.50
His-Ubiquitin	250	50	5.00
TM68-MBP	87	0.35	0.10
SBP purified Asi complex	5.7	2.5	11.27
ATP	100	2.5	0.625
Buffer C			6.48

Buffer C (20mM HEPES (pH 7.4), 2mM magnesium acetate, 300mM sodium chloride, 0.3mM DMNG)

In case some components needed to be omitted for certain experiments, specific component volume was replaced by Buffer C**.** ATP was always the last component to be added and the mixture was incubated at 30°C for 1 hr on a 96-well thermal cycler block. Subsequently, 10µl reaction was mixed with 10µl of SDS buffer(3X) and analysed by SDS-PAGE. It was followed by directly scanning the gel using Li-Cor imager or analysed by immunoblotting. In some experiments, reaction mixture was followed by a Ni-NTA affinity purification as explained above in section 2.6.3.

2.5.5 Floatation assay

80%, 30%, 15% glycerol stocks solutions were prepared in buffer U. 50µl of 80% glycerol solution was mixed with 50µl of proteoliposomes. It was overlayed with 50µl of 30% glycerol solution, 50µl of 15% glycerol solution and 50µl of buffer U in TLS55 ultracentrifuge tubes. It was followed by centrifugation at 100000g for 1 hr at 4°C in TLS55 rotor. Followed by, 38µl fractions were collected from the top and mixed with 19µl of 3x SDS buffer. 5µl was loaded on an SDS PAGE and analysed either by direct gel scanning using Li-Cor imager or analysed by immunoblotting.

2.5.5 Protease protection assay

Asi complex containing – SBP-TEV-Asi2, untagged Asi1/3 were reconstituted into liposomes. To check the topology, 5µl of reconstituted proteoliposomes were mixed with 15µl of buffer U or 15µl of Buffer U supplemented with 2mM DMNG or 15µl of buffer U supplemented with 0.5µg of TEV protease. Reaction mixture was incubated for 1 hr at RT and analysed by SDS-PAGE and immunoblotting.

2.5.7 BMB *in vitro* cross-linking

6mM of 1,4-bismaleimidobutane (BMB stock – 20mM in DMSO) (Thermo) was added to 30µl of reconstituted proteoliposomes and incubated for 1 hr at RT.

Reactions were stopped by addition of 30µl of 3x SDS buffer and analysed by SDS-PAGE followed by immunoblotting.

Table 2.13- List of Chemicals and commercial kits

Chemicals/Kits	Indentifier	Source
Cycloheximide	C7698	Sigma
3-Indolacetic acid (Auxin)	I2886	Sigma
Rapamycin	37094	Sigma
H-p-Bz-Phe-OH (BPA)	F2800.0005	Bachem
Phenylmethylsulfonyl fluoride (PMSF)	32610822	Roche
Protease inhibitor cocktail tablets	37378900	Roche
2-mercaptoethanol	M6250	Sigma
Adenosine 5' triphosphate (ATP)	10127531001	Roche
Biotin	B4501	Sigma
Imidazole	56750	Sigma
Isopropyl β-D-1-thiogalactopyranoside (IPTG)	I6758	Sigma
Cholesterol	700000	Avanti
1-palmitoyl-2-oleoyl-*sn*-glycero-3-phosphocholine (POPC)	850457	Avanti
1,2-dioleoyl-*sn*-glycero-3-phosphoethanolamine (DOPE)	850725	Avanti
1,2-dioleoyl-*sn*-glycero-3-phospho-L-serine (DOPS)	840035	Avanti
1,2-dioleoyl-sn-glycero-3-phosphoethanolamine-N-(lissamine rhodamine B sulfonyl) ammonium salt (18:1 Liss Rhod PE)	810150	Avanti
Chloroform	1.02445.2500	Merck
Diethyl ether	1.00921.1000	Merck
Decyl Maltose Neopentyl Glycol (DMNG)	NG322	Anatrace
IGEPAL CA-630 (NP40)	I8896	Sigma
Glyco-diosgenin (GDN)	GDN101	Anatrace
n-Dodecyl-β-D-Maltopyranoside (DDM)	D310	Anatrace
3x FLAG peptide	Sigma	F4799
His-ubiquitin	U530	Boston Biochem
DyLight™ 800 Maleimide	46621	Thermo Scientific
Peptide: Gly-Gly-Gly-Cys, counter ion -chloride	This study	Thermo Scientific
anti-HA magnetic beads	88837	Thermo Scientific
anti-FLAG M2 affinity gel	A2220	Sigma
anti-FLAG M2 magnetic beads	M8823	Sigma
Dynabeads Protein A	10002D	Thermo Fisher
High capacity streptavidin agarose resin	20361	Thermo Scientific
Streptavidin magnetic beads	88817	Thermo Scientific
NiNTA Agarose Beads	88222	Thermo Scientific
BL21-CodonPlus (DE3)-RIPL cells	230280	Agilent Technologies
Mini extruder kit	610000	Avanti
400nm size filters	800282	Avanti
100 nm filters	800309	Avanti
Detergent removal spin columns	87777	Thermo scientific

Chapter 3

Assembly and organization of the Asi complex

3 Assembly and organization of the Asi complex

3.1 Introduction

The functional roles of ERAD ubiquitin ligases have been well-characterized in budding yeast *S.cerevisiae*, in which two ubiquitin ligases, Hrd1 and Doa10, had been implicated in the degradation of ER proteins with lesions in cytosolic, luminal or membrane domains (Carvalho et al., 2006; Huyer et al., 2004; Vashist and Ng, 2004; Zattas and Hochstrasser, 2015).

Our lab and others uncovered a novel quality control pathway, which is defined by the Asi complex that exclusively localizes to the Inner Nuclear Membrane (INM). The INM is a specialized sub-domain of the ER comprising of a unique proteome necessary for nuclear functions. Asi complex was shown to degrade mislocalized and misfolded ER proteins thereby maintaining the INM proteome and its homeostasis (Foresti et al., 2014; Khmelinskii et al., 2014). Importantly, mutations or loss of INM proteins has been associated with a wide range of abnormalities including neurodegenerative diseases such as muscular dystrophies and cancer (Burke and Stewart, 2014; Woulfe, 2008), emphasizing the importance of quality control mechanisms at the INM.

Asi complex is made up of three integral membrane proteins which include the RING domain-containing proteins Asi1 and Asi3, along with the accessory protein Asi2. Asi1 and Asi3 are paralogous proteins, likely originating from a genome duplication event, containing 5-6 membrane-spanning domains and a RING-

finger domain at the C-terminus with approximately 40% similarity at the amino acid sequence (Boban et al., 2006; Forsberg et al., 2001; Zargari et al., 2007). Despite their similarity, Asi1 and Asi3 are non-redundant and the degradation of all known Asi substrates requires intact RING domains of the two proteins (Foresti et al., 2014). On the contrary, Asi2 is dispensable for the degradation of some these substrates (Foresti et al., 2014).

While genetic dissection of Asi complex has uncovered its general functions, molecular details of how Asi complex executes its functions is still elusive. Before deciphering its molecular roles, it is crucial to biochemically characterize the complex which will facilitate a better understanding of its functions and its mechanism of action.

It was also shown that subunits of the Asi complex undergo rapid turnover, a screen to identify factors for degradation of Asi1 revealed the requirement of nuclear 26S proteasomes, Ubc7, Cue1, AAA ATPase Cdc48 its co-factor Ubx1 and an unknown E3 ligase (Pantazopoulou et al., 2016). However, they suggest that Asi1 was not autoubiquitinated rather an unknown pathway is responsible for the degradation of Asi1 (Pantazopoulou et al., 2016). Furthermore, degradation of Asi2 depends on Doa10 (Boban et al., 2014; Pantazopoulou et al., 2016). These studies show that Asi subunits are short-lived proteins.

In this chapter, I took a biochemical approach in order to get insights about the assembly and organization of the Asi complex.

3.2 Stability of Asi3 is dependent on Asi1

Epitope tags at the C-terminus of Asi1, Asi2 and Asi3 affect their function (Foresti et al., 2014). In order to avoid problems associated with epitope tagging, antibodies were raised against each of the proteins. Antibodies against Asi2 and Asi3 worked well both for immunoprecipitation and western blotting. In contrast, anti-Asi1 antibodies did not specifically recognize and it was possible to use the antibodies only in immunoprecipitation and were not suitable for whole-cell lysates. Hence the experiments in the below section are focussed on the analysis of Asi2 and Asi3.

To get insight into the interdependence between the Asi complex subunits, I analysed the levels of the individual Asi proteins in the absence of their partners. Using antibodies targeted at endogenous proteins, I analysed the steady-state levels of Asi2 and Asi3 by immunoblotting. In Asi1 and Asi3 deletion mutants, levels of Asi2 were comparable to the WT condition. In contrast, in Asi1 deletion mutant, Asi3 levels were reduced by 50 %. However, Asi3 level was not affected in Asi2 deletion mutant (Figure- 3.1). These results indicated that Asi1 is required for Asi3 stability.

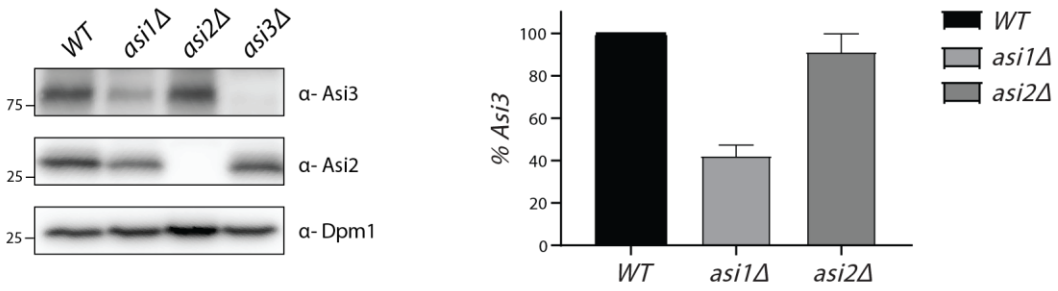


Figure 3.1 – Steady-state levels of Asi3 and Asi2

Levels of Asi3 and Asi2 were analysed in the specified genotypes. Whole-cell lysates were prepared from exponentially growing cells and analysed by SDS-PAGE followed by immunoblotting for endogenous Asi3 and Asi2 with anti-Asi3 and anti-Asi2 antibodies, respectively. Dolichol phosphate mannose synthase (Dpm1) was detected with anti-Dpm1 antibody and was used as a loading control.

3.3 Asi3 is a short-lived protein

To gain further insights into the turnover of Asi3 subunit, I analysed the degradation rate of Asi3 after the addition of the translation inhibitor cycloheximide (CHX). Cells growing in exponential phase were treated with CHX and endogenous levels of Asi3 was monitored by immunoblotting. In *WT* cells, the degradation of Asi3 was evident within 2 hours, suggesting a short half-life. Similarly, in cells lacking other E3 ligases Hrd1, Doa10, Asi1 or the indicated double mutants, the turnover of Asi3 was similar to *WT* cells (Figure- 3.2). This data suggests that Asi3 has a fast degradation rate and appeared to be a short-lived protein like Asi2 and Asi1 (Boban et al., 2014; Pantazopoulou et al., 2016)

and its degradation relies on either autoubiquitination or through an unknown mechanism yet to be discovered.

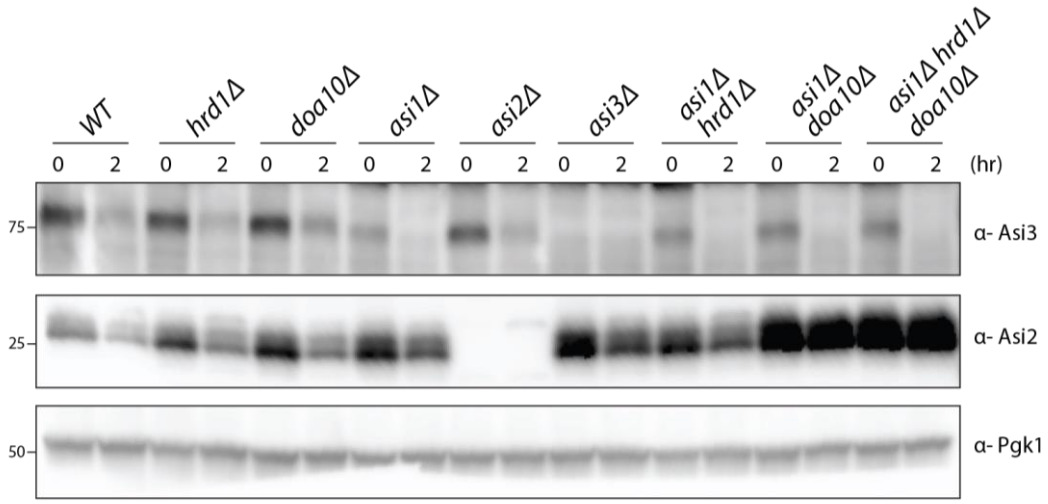


Figure 3.2 – Asi3 and Asi2 are turned over

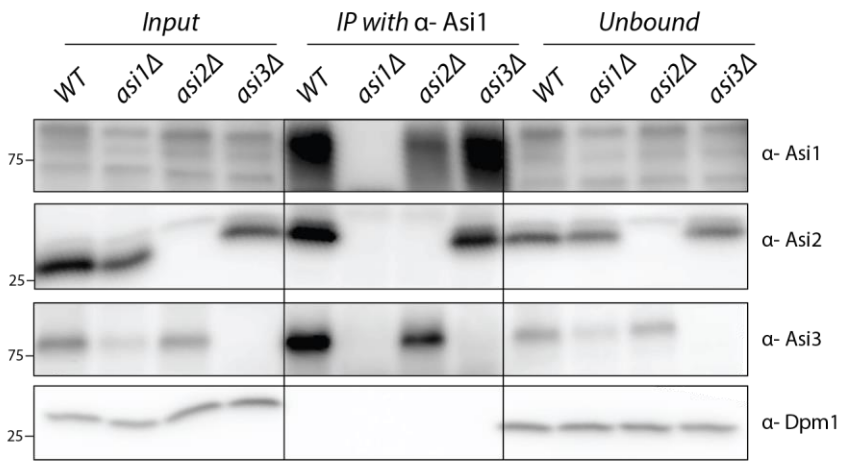
Degradation of Asi3 and Asi2 were analysed in the specified genotypes. Turnover rates were monitored upon addition of CHX to exponentially growing cells. Whole-cell lysates were prepared and analysed by SDS-PAGE followed by immunoblotting for endogenous Asi3 and Asi2 with anti-Asi3 and anti-Asi2 antibodies respectively. Phosphoglycerate kinase (Pgk1) detected with anti- Pgk1 was used as a loading control.

3.4 Asi1 mediates the interaction between Asi2 and Asi3

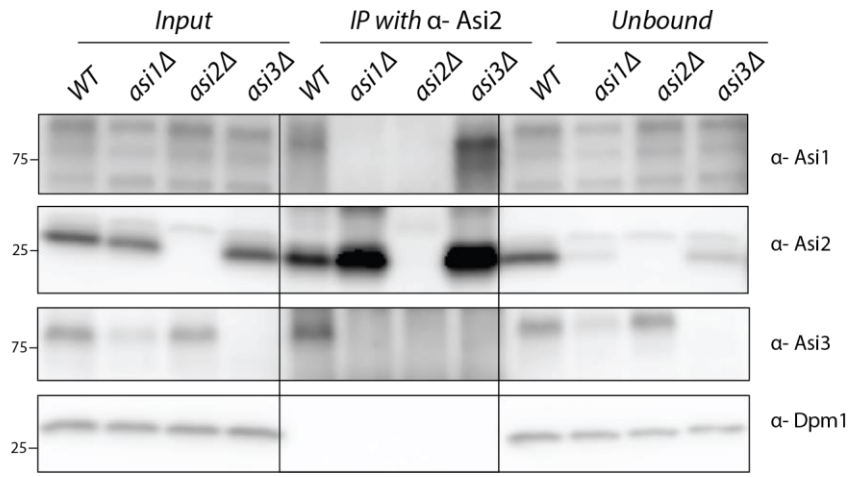
To get insights into the assembly of Asi1, Asi2 and Asi3 into the Asi complex, I performed immunoprecipitations (IP) on each of its subunits. As previously shown with tagged proteins (Foresti et al., 2014), I found that immunoprecipitation of endogenous Asi1 resulted in co-precipitation of Asi2 and Asi3. Asi1 also interacted with Asi2 in *asi3Δ* cells and with Asi3 in *asi2Δ* cells

(Figure- 3.3A). Immunoprecipitations with anti-Asi2 also precipitated Asi1 and Asi3, as expected. The interaction between Asi2 and Asi1 was unaffected by loss of Asi3 in *asi3Δ* cells. In contrast, immunoprecipitation of Asi2 in *asi1Δ* cells failed to precipitate Asi3. These results suggested the possibility of Asi1 mediated the interaction between Asi2 and Asi3 (Figure- 3.3B). To further explore this possibility, reciprocal IP was performed using anti- Asi3 antibody. In *asi1Δ* cells, Asi3 was not able to interact with Asi2. In contrast, Asi3 could still interact with Asi1 in *asi2Δ* cells (Figure- 3.3C). Thus, these data strongly indicate that Asi1 mediates the interaction between Asi2 and Asi3.

A


Input
IP with α- Asi1
Unbound
WT
asi1Δ
asi2Δ
asi3Δ
75
25
α- Asi1
α- Asi2
α- Asi3
α- Dpm1

B


Input
IP with α- Asi2
Unbound
WT
asi1Δ
asi2Δ
asi3Δ
75
25
α- Asi1
α- Asi2
α- Asi3
α- Dpm1

C

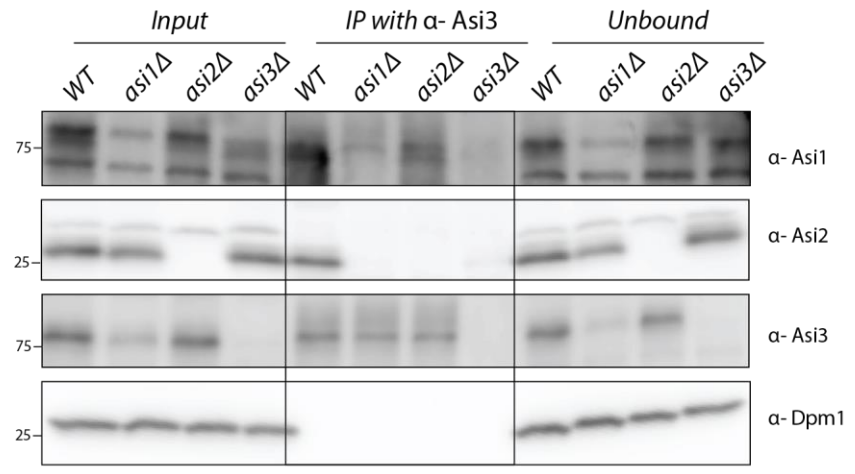

Input
IP with α- Asi3
Unbound
WT
asi1Δ
asi2Δ
asi3Δ
75
25
α- Asi1
α- Asi2
α- Asi3
α- Dpm1

Figure 3.3 – Asi1 bridges the interaction between Asi2 and Asi3

(A) Immunoprecipitation with anti- Asi1 antibody. Membrane fractions were prepared from cells with the indicated genotypes. Membrane pellets were solubilised with 1% Digitonin and incubated with protein A magnetic beads coupled with anti-Asi1 antibody overnight. Proteins bound to the beads were eluted using SDS buffer and analysed by SDS-PAGE followed by immunoblotting for Asi1, Asi2 and Asi3 with anti- Asi1, anti- Asi2 and anti-Asi3 antibodies respectively. Dpm1 was used as a negative control. 10% of the total extract corresponds to Input.

(B) Immunoprecipitation with anti- Asi2 antibody and analysed as in (A)

(C) Immunoprecipitation with anti- Asi3 antibody and analysed as in (A)

3.5 Mapping the region of interaction on Asi1 with Asi3

Asi1 is a membrane protein with five or six predicted TMDs with its Zn^{2+} binding RING domain at the C-terminus facing the nucleoplasm. In the previous section, it was shown that Asi1 is required to stabilise Asi3 and also to bridge the interaction between Asi2 and Asi3 (Figures 3.1 and 3.3). Now, to map the Asi1 region required for its interaction with Asi3 two C-terminal truncations were generated. Like the full-length control, the Asi1 derivatives, FLAG-Asi1 (Δ434-624) and FLAG-Asi1(Δ312-624) were expressed from the ADH1 promoter at the endogenous Asi1 locus and contained a FLAG-epitope tag at the N-terminus (Figure 3.4A). All FLAG-tagged proteins were detected by western blot with anti-FLAG antibodies. Both Asi1 truncations were present at higher levels when compared to FLAG-Asi1^{WT}. Given that all Asi-derivatives are expressed from the

same promoter; this suggests that Asi1 C terminus which contains the RING domain is necessary for controlling Asi1 levels.

For the immunoprecipitation, cells were harvested in the exponential phase, and total membrane was collected and solubilised with 1% digitonin. FLAG-beads were added to solubilised membranes, bound proteins were eluted and analysed. Immunoprecipitation of FLAG-Asi1 resulted in the co-precipitation of Asi2 and Asi3 indicating that the N-terminal FLAG tag does not interfere with Asi complex assembly. Similarly, immunoprecipitation of FLAG-Asi1$^{434\text{-}624\Delta}$ resulted in the co-precipitation of Asi2 and Asi3. In contrast, FLAG-Asi1$^{312\text{-}624\Delta}$ interacted only weekly with Asi2 and no more interacted with Asi3 (Figure 3.4B). Untagged cells were used as a control in the immunoprecipitation experiments. This demonstrates that Asi1 region adjacent to the predicted TMDs between amino acids 312-434, is required for the interaction with Asi3.

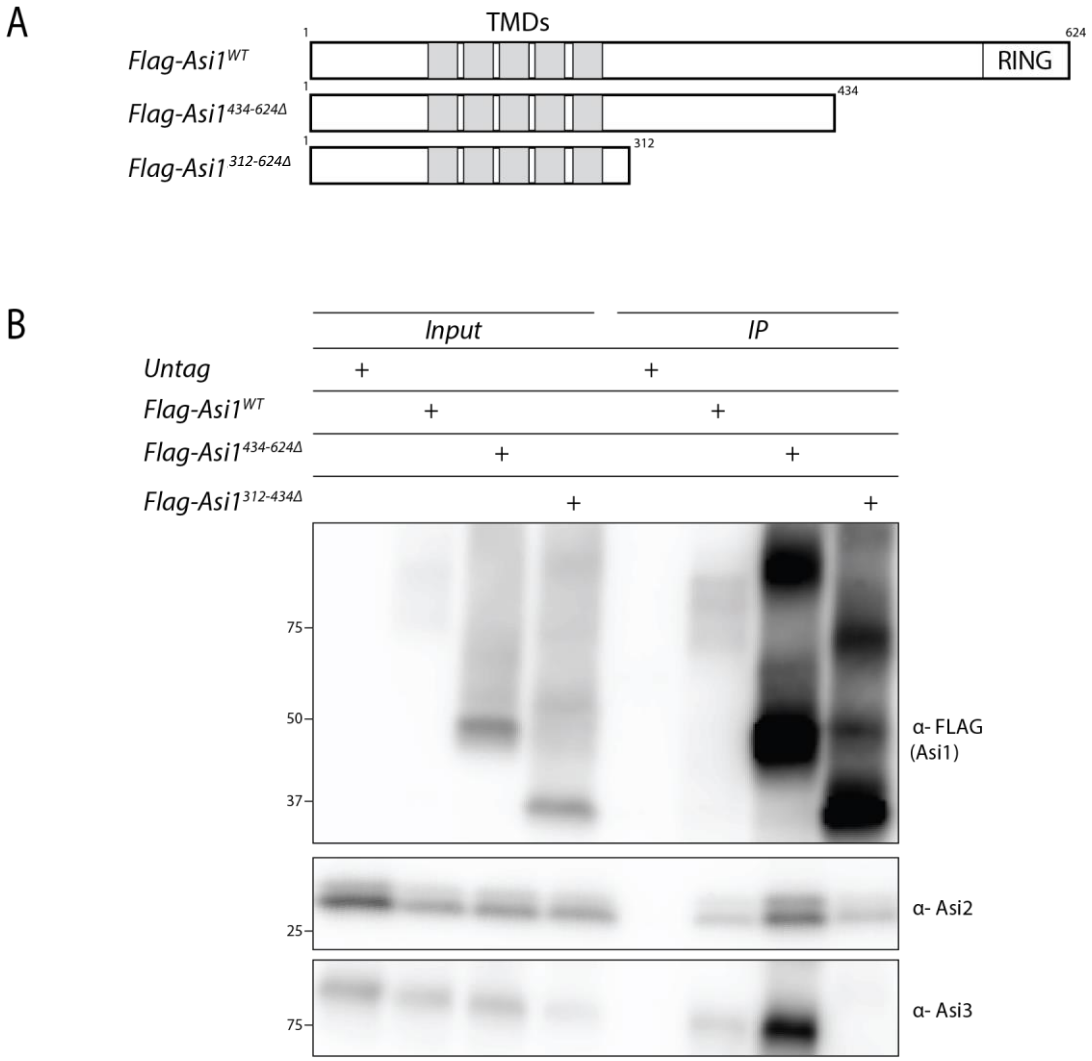


Figure 3.4 – Asi1 interacts with Asi3 at the cytoplasmic tail region

(A) Schematic representation of the truncations that were generated on N-terminal FLAG-tagged Asi1

(B) Immunoprecipitation on FLAG-Asi1 constructs. Membrane fractions were prepared from cells with the indicated genotypes. Membrane pellets were solubilised with 1% Digitonin and incubated with FLAG-M2 magnetic beads overnight. Proteins bound to the beads were eluted using SDS buffer and analysed by SDS-PAGE followed by immunoblotting for Asi1, Asi2 and Asi3 with anti- FLAG, anti- Asi2 and anti-Asi3 antibodies respectively.

3.6 Asi proteins form a high molecular weight complex

Immunoprecipitation experiments indicated that Asi1, Asi2, and Asi3 are present in a protein complex (Foresti et al., 2014). To gain further insight into the size of the Asi complex, sucrose gradient centrifugation of digitonin solubilised extracts were performed (Figure- 3.5). Solubilised membrane lysates were layered on top of a 10-60% sucrose gradient and subjected to ultracentrifuge spin and analysed. It was observed that Asi2 and Asi3 co-fractionate (Figure- 3.5, panel A and B) confirming they are part of the same complex and as expected from the immunoprecipitation experiments. Protein denaturation with 1% SDS induced the proteins to migrate at the top of the gradient (Figure- 3.5, panel C and D) further reassuring that Asi complex was denatured in the presence of SDS and individual subunits migrate to lower percent of the gradient. To get an estimate of the molecular weight of the Asi complex, the samples were analysed for Hrd1. Previous experiments showed that Hrd1 is part of a complex with a molecular weight of approximately 600kDa (Carvalho et al., 2006). Thus, we analysed the size of Asi complex in relation to the Hrd1 complex (Figure- 3.5, panel E). Asi appears to be slightly larger than Hrd1. Hrd1 has its main peaks between fractions (10-12) when compared to Asi whose main peaks are in fractions (14-16) suggesting it to be higher than 600kDa. Immunoprecipitation followed by mass spectrometry analysis did not identify any additional new potential binding partners for Asi complex (data not shown). Hence, there is a possibility of

individual components being subjected to oligomerisation, or multiple copies of Asi complex are present in the high molecular weight complex.

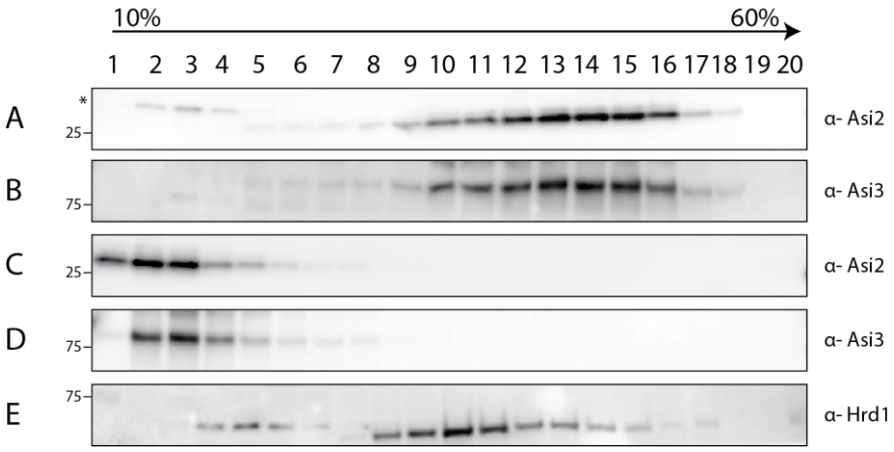


Figure 3.5 – Asi2 and Asi3 co-fractionate in sucrose gradients forming a large complex

Membrane pellets from *WT* cells were prepared and solubilised in 1% digitonin. Solubilised membrane lysates were layered on top of a sucrose gradient of 10-60% and subjected to an ultracentrifuge spin for 4 hr. Subsequently, fractions were collected from top of the gradient and analysed by SDS-PAGE and immunoblotting for Asi2, Asi3 and Hrd1 using anti-Asi2, anti-Asi3 and anti-Hrd1 antibodies. (Asterisk (*) indicates unspecific band detected by the Asi2 antibody).

To further investigate how deletion of Asi subunits would affect the formation of this high molecular weight complex, sucrose gradients centrifugation was performed for solubilised membranes from WT, *asi1Δ, asi2Δ* and *asi3Δ* cells. Fractions were analysed by immunoblotting for Asi2 and Asi3. High molecular weight complex of Asi2 that was detected in *WT* cells by anti-Asi2 antibody was entirely disrupted in *asi1Δ* cells and partially in *asi3Δ* cells (Figure- 3.6A). However, Asi3-containing complex detected with anti-Asi3 antibody was only partially disrupted in *asi2Δ* when compared to *asi1Δ* cells (Figure- 3.6B). Partial

disruption of the Asi3- containing complex suggests a possibility of multiple copies of Asi1/3 which is not affected by the absence of Asi2. These results reinforce the idea of Asi1 being vital to hold the Asi complex together and bridging the interactions between Asi2 and Asi3.

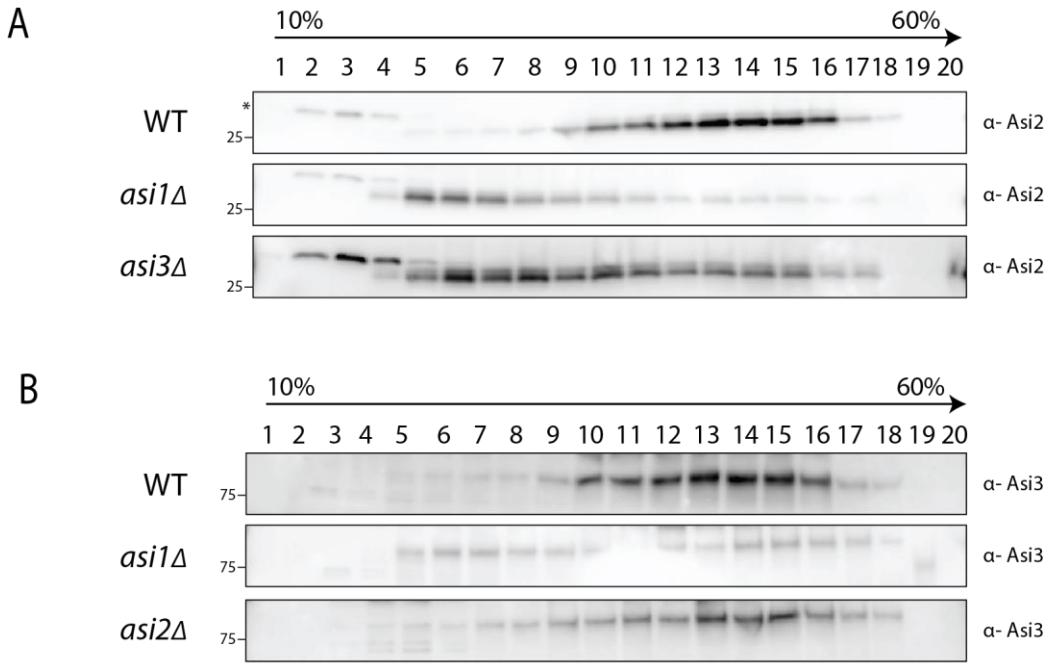


Figure 3.6 – Deletion of subunits disrupts the high molecular weight complex

Membrane pellets from the indicated genotypes were prepared and solubilised in 1% digitonin. Solubilised membrane lysates were layered on top of a sucrose gradient of 10-60% and subjected to an ultracentrifuge spin for 4 hr. Subsequently, fractions were collected from top of the gradient and analysed by SDS-PAGE and immunoblotting for Asi2 and Asi3. They were detected using anti-Asi2 and anti-Asi3 antibodies, respectively. (Asterisk (*) indicates unspecific band detected by the Asi2 antibody).

3.7 Discussion

As Asi complex is essential to maintain overall homeostasis, we set out to biochemically characterise the complex to allow a better understanding of its functions and its mechanism of action that will be discussed in the following chapters.

In this chapter, I investigated the interactions between the subunits of the Asi complex. I show that there is a tight regulation between the subunits of the complex and both endogenous Asi2 and Asi3 have short half-lives. Experiments revealed two novel critical roles for Asi1 – in maintaining the levels of Asi3 and the recruitment of Asi2 by bridging the interaction between Asi2 and Asi3. Immunoprecipitation experiments showed that Asi1/Asi3 form the core of the Asi complex, while Asi2 is a more peripherally associated component of the complex. In fact, without Asi1, Asi2 cannot interact with Asi3. Consistent with this organisation, Asi2 is dispensable for the degradation of some Asi substrates such as Sec61-2 (Foresti et al., 2014). These findings suggest that Asi2 may act as a receptor for selecting specific substrates for degradation. Based on *in vivo* analysis, Asi2 dependence does not correlate with the substrate being misfolded or mistargeted, indicating that the Asi2 requirement involves a different determinant. Additionally, on blots, Asi2 always has double bands indicating that some post-translational modifications might be involved to regulate its function, which needs to be studied in the future.

Furthermore, we identified a region on Asi1 that is important for interaction with Asi3. A stretch of 122 amino acids in the C-terminus after the predicted TMDs seems to be required. Based on structure prediction algorithms (Phyre2), the region presents a largely disordered loop on the C-terminus where some amino acids might potentially play crucial roles in the specificity of the interaction. Mapping of the corresponding Asi1-interacting region on Asi3 can be addressed in the future. Asi1 interaction with Asi2 is likely mediated by the transmembrane region as an Asi1 mutant lacking the whole cytoplasmic tail still interacts with Asi2.

We also determined that Asi complex forms a high molecular weight complex which is slightly higher than 600kDa by performing sucrose gradient centrifugation. Our search to identify proteins within Asi high molecular weight complex by IP followed by mass spectrometry analysis did not yield any validated candidate. Like Hrd1 which forms oligomers (Carvalho et al., 2006; Schoebel et al., 2017; Stein et al., 2014), we speculate that Asi proteins might also be forming oligomers that make up the large complex. Interestingly, this size is greater than the sum of the molecular weights of the individual components. This suggests that there could be at least three copies of the complex containing (Asi1/2/3) or multiple copies of the individual subunits forming the high molecular weight complex. As discussed earlier, Asi1 seems to be the core component of the complex mediating interaction between Asi2 and Asi3, and we could speculate

that Asi1 could potentially behave as a scaffold for the oligomerisation. Future experiments should be able to address the hypothesis.

Chapter 4

Asi complex recognises orphan subunits of ER protein complexes at the Inner Nuclear Membrane

4 Asi complex recognizes orphan subunits of ER protein complexes at the Inner Nuclear Membrane

4.1 Introduction

Newly synthesized membrane and secretory proteins enter the ER as nascent, unfolded polypeptide chains. In the ER, they undergo folding and the majority of the proteins assemble with their partners to form multi-protein complexes. Hence, ER hosts a diverse set of molecular chaperones and enzymes to help the nascent chains to fold and assemble into stable complexes (Braakman and Bulleid, 2011). Despite the dedicated role of these factors, a significant proportion of the newly synthesized proteins undergo misfolding or remain unassembled in the ER (Hartl and Hayer-Hartl, 2009). These aberrant species if unnoticed, have the potential to exhibit toxic effects to the cells (Schwartz and Ciechanover, 2009). Thus, to ensure that only properly-folded and correctly-assembled proteins traffic through the secretory pathway, quality control mechanism like endoplasmic reticulum-associated degradation (ERAD) are in place to identify species that fail to mature. (Christianson and Ye, 2014; Ruggiano et al., 2014; Zattas and Hochstrasser, 2015). ERAD involves three essential steps- (1) recognition of the aberrant substrate to be degraded, (2) retrotranslocation towards the cytoplasmic side of the ER membrane and (3) ubiquitination of the substrate for proteasomal degradation. ER membrane-embedded E3 ligases co-ordinate all the above steps.

Mechanisms of ERAD is conserved throughout eukaryotes and are very well-studied in budding yeast *S.Cerevisiae.* Until recently, there were two well-known ERAD branches lead by the Hrd1 and Doa10 complexes, which degrade most of the misfolded substrates in the ER (Ruggiano et al., 2014). The third arm of quality control machinery governed by the E3 ligase – Asi complex was uncovered. The Asi complex localizes specifically to the INM and was implicated in the degradation of a variety of substrates, including, mislocalized ER proteins and soluble nuclear factors (Foresti et al., 2014; Khmelinskii et al., 2014; Omnus and Ljungdahl, 2014). In the previous chapter, I characterized the Asi complex biochemically. Here, I focus on understanding how the Asi complex recognizes mislocalized substrates at the INM and how this pathway contributes to the overall homeostasis in the ER.

4.2 Asi complex recognizes unassembled protein subunits for degradation

Our lab previously showed that the ER membrane protein Nsg1 was degraded by Asi complex only when its binding partner Hmg2 was absent (Foresti et al., 2014). Another ER protein, Erg11- an enzyme of the sterol biosynthetic pathway, was also shown to be an Asi substrate. However, Erg11 appeared to be constitutively degraded. Interestingly, Erg11 does not appear to form stable complexes (Debose-Boyd, 2007; Hughes et al., 2007). These observations led to the hypothesis that Asi complex could potentially degrade unassembled/orphan subunits that diffuse to the INM.

To test this hypothesis, we took advantage of a well understood ER multiprotein complex, the Oligosaccharyl transferase (OST) complex (Figure- 4.1A), which is essential for asparagine-linked (N-) glycosylation of newly synthesized proteins in the ER lumen (te Heesen et al., 1993; Kelleher and Gilmore, 1994). The OST complex is made up of three subcomplexes that assemble independently (Figure-4.1A each subcomplex is colour-coded) and sequential assembly of the subcomplexes results in a functional OST complex. As OST complex is required for the viability of yeast cells, temperature-sensitive (ts) alleles were used in the experiments. The advantage of proteins encoded by *ts* alleles is - at the permissive temperature they remain mostly functional, but at a higher restrictive temperature renders them non-functional often because they undergo rapid degradation.

I focussed on one of the subunits Wbp1 that is part of the Swp1-Wbp1-Ost2 subcomplex and tested the turnover rate of *wbp1-2* ts allele using a CHX chase experiment. At the restrictive temperature of 37˚C, Wbp1 was degraded quickly (Figure- 4.1B). Interestingly, in Asi complex deletion mutants, degradation was delayed suggesting that under conditions of improper complex assembly, full-length Wbp1 was a substrate of the Asi complex. In Asi complex deletion mutants, Wbp1 accumulated at the NE when observed by light microscopy (data not shown). However, under WT conditions, Wbp1 was a very stable protein (Figure-4.1C).

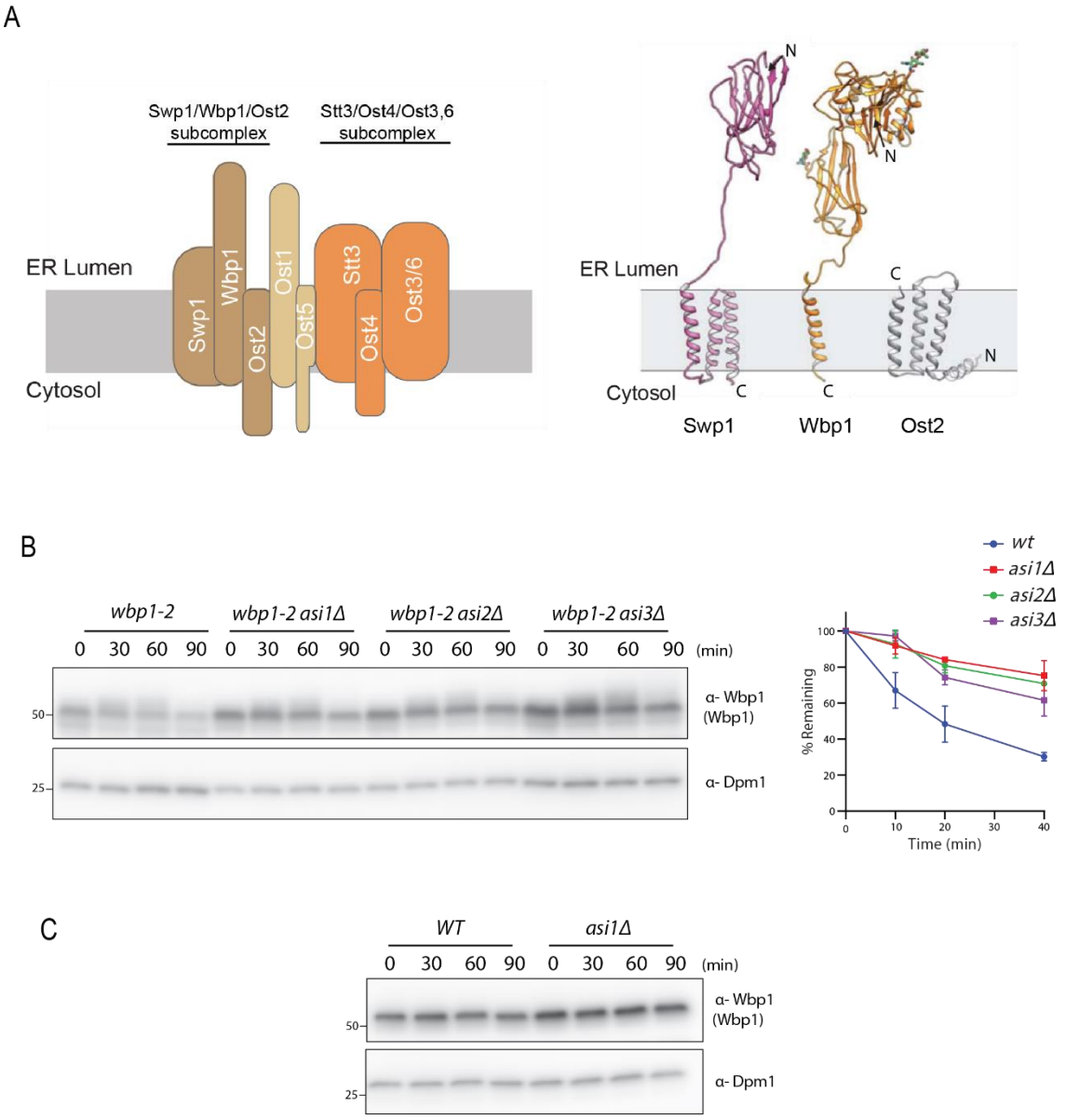


Figure 4.1 – Degradation of Wbp1 requires Asi complex

(A) Schematic representation of the OST complex. Each colour represents a different subcomplex. On the right is the Swp1/Wbp1/Ost2 subcomplex adapted from (Wild et al., 2018)

(B) Turnover of temperature-sensitive allele *wbp1-2* was analysed in the indicated genotypes. Exponentially growing cells were shifted to 37˚C for 60 min. Subsequently, cycloheximide (CHX) was added and the degradation rate was monitored. Whole-cell lysates were prepared and analysed by SDS-PAGE followed by immunoblotting for Wbp1

with anti-Wbp1 antibody. Dpm1 detected with anti- Dpm1 antibody was used as a loading control.

(C) Turnover of Wbp1 was analysed in the indicated genotypes. Degradation was monitored upon addition of cycloheximide (CHX) to exponentially growing cells. Whole-cell lysates were prepared and analysed by immunoblotting for Wbp1 with anti-Wbp1 antibody. Dpm1 detected with anti- Dpm1 antibody was used as a loading control.

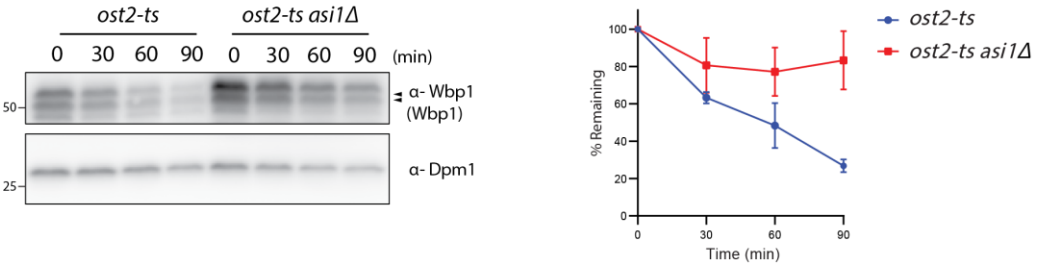
Previous work from the Aebi group analysed the assembly of the OST complex and its subcomplexes. It was shown that the stability of subunits within each subcomplex are interdependent. For each of the subcomplex to be formed accurately, their binding partners bind and stabilise each other (Mueller et al., 2015). Thus, OST complex served as an ideal model complex to understand the degradation of unassembled subunits by the Asi complex.

To understand the degradation of Wbp1 under improper assembly, I triggered destabilization of the complex using an *ost2*-ts allele and performed a CHX shut off experiment at the restrictive temperature. In *ost2*-ts cells, Wbp1 was degraded quickly and in Asi complex deleted mutant cells its degradation was delayed (Figure 4.2A). This result suggests that upon destabilization of Wbp1-Ost2-Swp1 subcomplex, Wbp1 accesses the INM where it is targeted for degradation by the Asi complex. To confirm that *ost2*-ts mutations trigger disassembly of the OST complex I performed immunoprecipitation experiments to examine the interaction between Wbp1 and Ost4, a subunit of a different OST

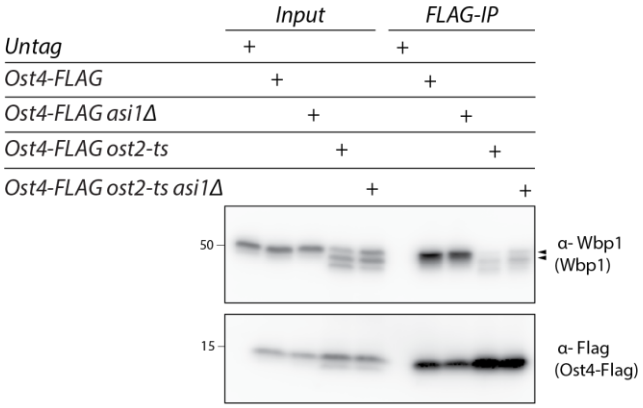
subcomplex. In both WT and *ost2*-ts cells, endogenous Ost4 was tagged with a FLAG tag (Ost4-FLAG) resulting in a functional fusion protein. Membrane extracts were obtained and solubilised membranes were incubated with FLAG beads, proteins bound to the beads were eluted and analysed. We observed that in WT cells Ost4 and Wbp1 interact robustly. In contrast, in cells with o*st2*-ts allele, only a very minor fraction of Wbp1 co-IPs with Ost4. This demonstrates that Ost2-ts triggers OST complex disassembly (Figure- 4.2B).

Furthermore, to assess the specificity of Wbp1 degradation in *ost2*-ts, I analysed the turnover of Wbp1 upon destabilization of another Ost subcomplex in cells with the *stt3-7* ts allele. Stt3 is a subunit of another subcomplex of the OST complex that does not directly bind to Wbp1 and that should not interfere with its stability. In this scenario, the destabilization of Stt3 should not have any effect on the degradation of Wbp1. Hence, I performed a CHX chase to evaluate the turnover of Wbp1 in *stt3-7* cells at the restrictive temperature. Indeed, Wbp1 degradation is unaffected in *stt3-7* cells nor in *stt3-7* cells lacking Asi components (Figure- 4.2C). Altogether, these results indicate that Asi complex degrades unassembled/orphan subunits.

A


ost2-ts
ost2-ts asi1Δ
0 30 60 90 0 30 60 90 (min)
50
25
α- Wbp1
(Wbp1)
α- Dpm1
% Remaining
Time (min)
ost2-ts
ost2-ts asi1Δ

B


Input
FLAG-IP
Untag
Ost4-FLAG
Ost4-FLAG asi1Δ
Ost4-FLAG ost2-ts
Ost4-FLAG ost2-ts asi1Δ
50
15
α- Wbp1
(Wbp1)
α- Flag
(Ost4-Flag)

C

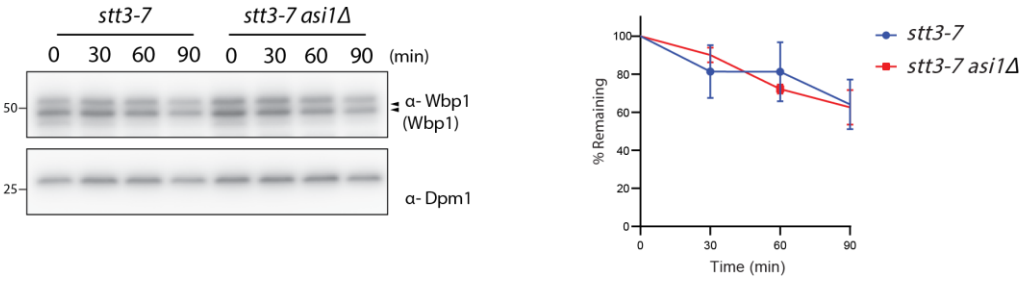

stt3-7
stt3-7 asi1Δ
0 30 60 90 0 30 60 90 (min)
50
25
α- Wbp1
(Wbp1)
α- Dpm1
% Remaining
Time (min)
stt3-7
stt3-7 asi1Δ

Figure 4.2 – Asi complex degrades Wbp1 under defective complex assembly

(A) Turnover of Wbp1 was analysed in the indicated genotypes. Exponentially growing cells were shifted to 37˚C for 60 min. Subsequently, cycloheximide (CHX) was added and the degradation rate was monitored. Whole-cell lysates were analysed by SDS-PAGE followed by immunoblotting for Wbp1 with anti-Wbp1 antibody. Arrowheads indicate hypoglycosylated forms of Wbp1. Dpm1 detected with anti- Dpm1 antibody was used as a loading control. Quantification of at least three independent replicates is represented in the graph on the right panel.

(B) Immunoprecipitation with anti- FLAG antibody. Membrane fractions were prepared from cells with the indicated genotypes. Membrane pellets were solubilised with 1% GDN and incubated with FLAG magnetic beads overnight. Bound proteins to the beads were eluted using SDS buffer and analysed by SDS-PAGE followed by immunoblotting for Wbp1 and Ost4 with anti- Wbp1 and anti-FLAG antibodies, respectively. Arrowheads indicate hypoglycosylated forms of Wbp1.

(C) Turnover of Wbp1 was analysed in the indicated genotypes as in (A)

To exclude the possibility of artefacts introduced by the use of temperature-sensitive alleles, I decided to induce OST disassembly using an alternative strategy. Towards this goal, I took advantage of the auxin-induced acute degradation of proteins (Morawska and Ulrich, 2013; Nishimura et al., 2009). Here, cells contain a Tir1 adaptor protein that recognizes AID tag as a degradation signal in the presence of a plant hormone auxin. AID tag is the degron for SCF E3 ligase which induces its acute degradation. In this case, the AID tag was added to Swp1, another subunit of the Wbp1/Ost2/Swp1 subcomplex. Swp1-AID was

functional and in the absence of auxin a relatively stable protein. Then we added auxin to the cell for 1 hr and observed that Swp1 was depleted from the cells (Figure- 4.3A). Subsequently, CHX was added and a chase was performed to assess the turnover of Wbp1. In WT cells, with the presence of auxin, Wbp1 levels were reduced in 4 hr and its degradation was inhibited or reduced in cells lacking Asi complex components (Figure- 4.3B). On the other hand, in control cells without auxin, there were no significant changes, although the minor changes in degradation in WT cells were attributed to the tag on Swp1 (Figure- 4.3C). Thus, these results confirm that unassembled or orphan subunits from the ER that diffuse to the INM are targeted by Asi complex for degradation.

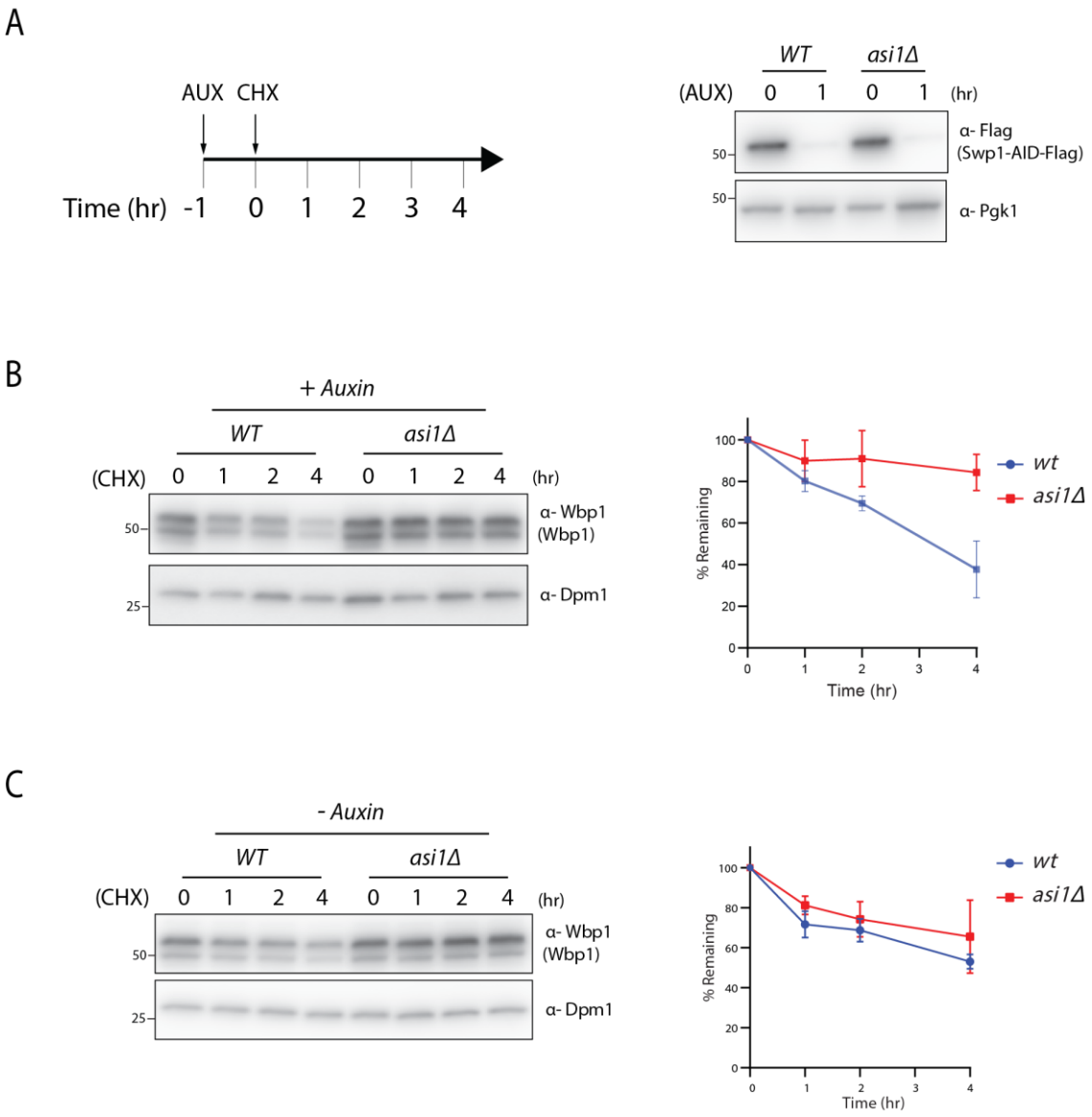


Figure 4.3 – Asi complex degrades Wbp1 under acute depletion of the binding partner Swp1

(A) Depletion of Swp1-AID was monitored in the indicated genotypes upon auxin treatment for 60 min. Whole-cell lysates were analysed by SDS-PAGE followed by immunoblotting for Swp1-AID-FLAG with anti-FLAG antibody. Pgk1 detected with anti- Pgk1 antibody was used as a loading control.

(B) Followed by the auxin-dependent depletion of Swp1, Wbp1 degradation was monitored in the indicated genotypes by the addition of cycloheximide (CHX). Whole-cell lysates

were prepared and analysed by SDS-PAGE followed by immunoblotting for Wbp1 with anti-Wbp1 antibody. Arrowheads indicate hypoglycosylated forms of Wbp1. Dpm1 detected with anti- Dpm1 antibody was used as a loading control.

(C) Here, auxin was replaced with DMSO which served as a control. Wbp1 degradation was monitored in the indicated genotypes by the addition of cycloheximide (CHX) and analysed as in (B).

Next, we wondered if unassembled/orphan subunits degraded by the Asi complex mutants cells would be competent to form functional complexes. To test this, we used the temperature-sensitive alleles and performed a growth assay. In this case, if the orphan subunits would be assembly competent, we would expect that preventing their degradation, such as in Asi complex mutants, will increase the chance of their assembly and have a growth rescue. We performed growth assays in cells expressing *wbp1-2* ts alleles. Intriguingly, in *wbp1-2* ts alleles, deletion of Asi complex components was able to rescue growth defects at the restrictive temperature of 33˚C (Figure- 4.4). Moreover, the growth defect was specific to Asi complex subunits and not to the other E3 ligases such as Hrd1 and Doa10. Hence, the orphan subunits degraded by the Asi complex at the INM are competent for assembly into functional complexes.

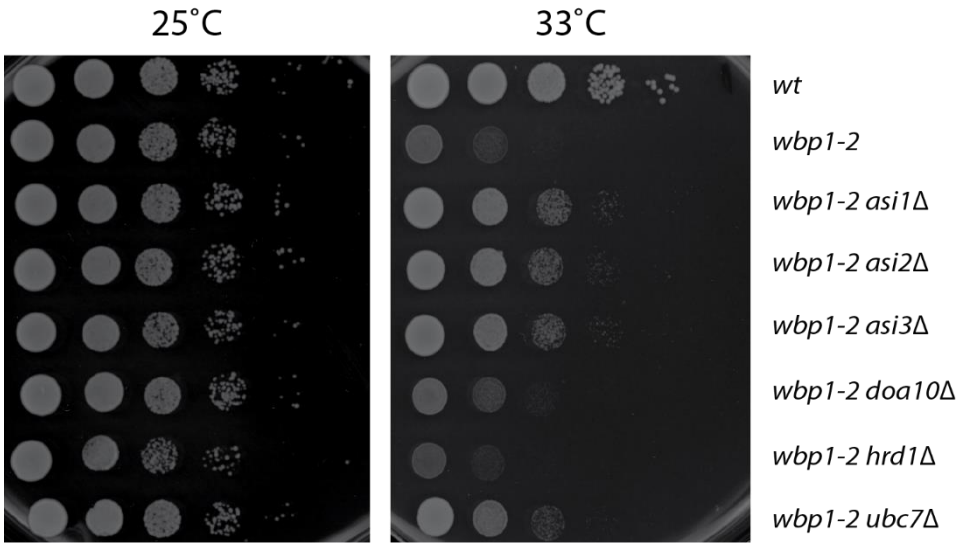


Figure 4.4 – Asi complex rescues growth defect in *wbp1-2* ts **alleles**

Yeast cells were grown to stationary phase and serial dilutions were prepared. Dilutions were spotted on YPD plates and incubated at the respective temperatures for 2-3 days and finally, plates were scanned.

4.3 Asi complex recognizes Vph1 as an orphan subunit for degradation

To test if there were other orphan subunits degraded by Asi complex, we investigated V-ATPase another well-characterized complex. V-ATPase is a 13 subunit complex that undergoes assembly in the ER before its delivery to the vacuole (Graham et al., 2003). Vph1 is a polytopic membrane protein subunit of the yeast V-ATPase complex. Previously, it was shown that Vph1p was an ERAD substrate only when it failed to assemble with its binding partners. Further, its degradation was dependent on ubiquitination and proteasome. However, the canonical Hrd1 and Doa10 ERAD ligases were not involved (Hill and Cooper, 2000). Based on this, we hypothesized that Vph1 could be a potential substrate of the Asi complex because its degradation was dependent on its assembly state. To test this hypothesis, I examined the turnover of GFP tagged Vph1 by a CHX shut-off experiment in the absence of its binding partners Vma3 and Vma16. Vph1 was quickly turned over in cells lacking either Vma3 or Vma16, as previously shown (Hill and Cooper, 2000). In contrast, Vph1 degradation was delayed in Asi complex mutant cells (Figure- 4.5). This result suggests that under improper complex assembly, Vph1 is targeted by the Asi complex for degradation.

Altogether, our data on the OST and V-ATPase complexes indicate that the Asi complex has a general role in the degradation of unassembled subunits.

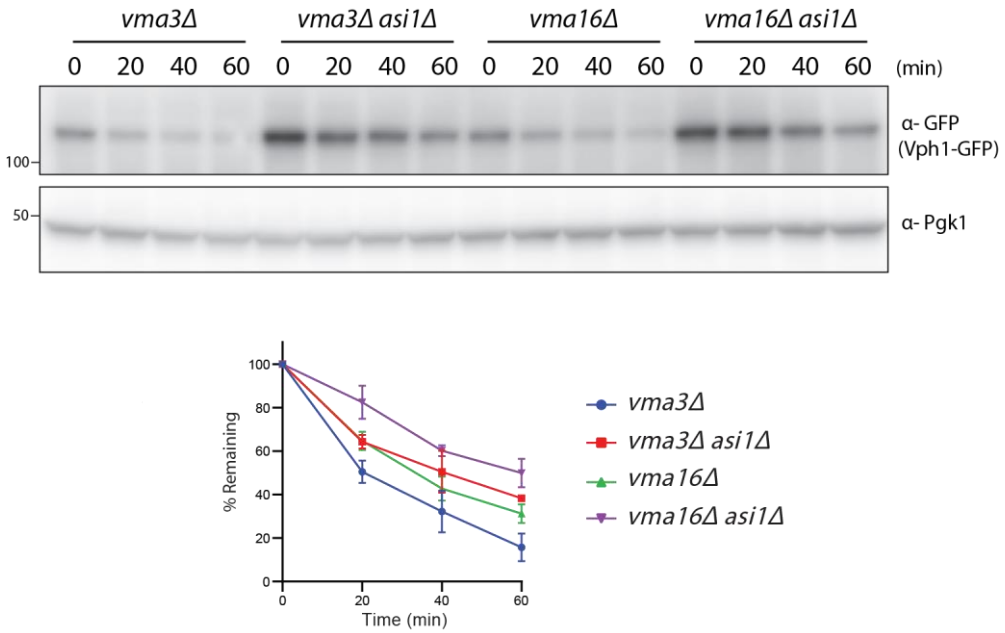


Figure 4.5 – Asi complex recognizes the Vph1 as an orphan substrate

Degradation of Vph1-GFP was analysed in the specified genotypes. Turnover rates were monitored upon addition of cycloheximide (CHX) to exponentially growing cells. Cell lysates were prepared and analysed for Vph1 with anti-GFP antibody. Pgk1 detected with anti- Pgk1 antibody and was used as a loading control.

4.4 Asi complex recognizes the transmembrane domain of Erg11

To understand the molecular mechanism by which the Asi complex recognizes its substrates, we took advantage of the constitutive substrate Erg11 (lanosterol demethylase)(Foresti et al., 2014). Previously, a yeast quantitative proteomics study showed that Erg11 levels were high in Asi deletion mutants when compared to the WT cells. Additional experiments proved that Erg11 is a very robust Asi

substrate and its degradation required all Asi complex subunits- Asi1, Asi2 and Asi3 (Foresti et al., 2014).

To understand how Asi recognizes its substrates we searched for the minimal Erg11 region necessary for its degradation. Towards this goal, we used *in vivo* truncation analysis. The crystal structure of Erg11 identified that the N-terminus of Erg11 contains an amphipathic helix (amino acid residues 6-23) followed by a single TMD (27-51) (Monk et al., 2014). The C-terminus of Erg11 encompasses a cytochrome p450 catalytic domain necessary for its activity (Figure- 4.6A). To evaluate if the TMD was sufficient to be recognized by the Asi complex, we constructed two truncated versions of Erg11, TM56- containing the first 56 amino acids and TM68 with the first 68 amino acids (Figure- 4.6A). To validate correct localization to the ER membrane, yeast cells expressing these constructs were subjected to fractionation experiment. We identified that both the truncated forms TM56 and TM68 were present in the total membrane fractions, suggesting that they were associated with the ER membranes (Figure- 4.6B). Using microscopy, we confirmed that the truncations were localized to the ER (data not shown).

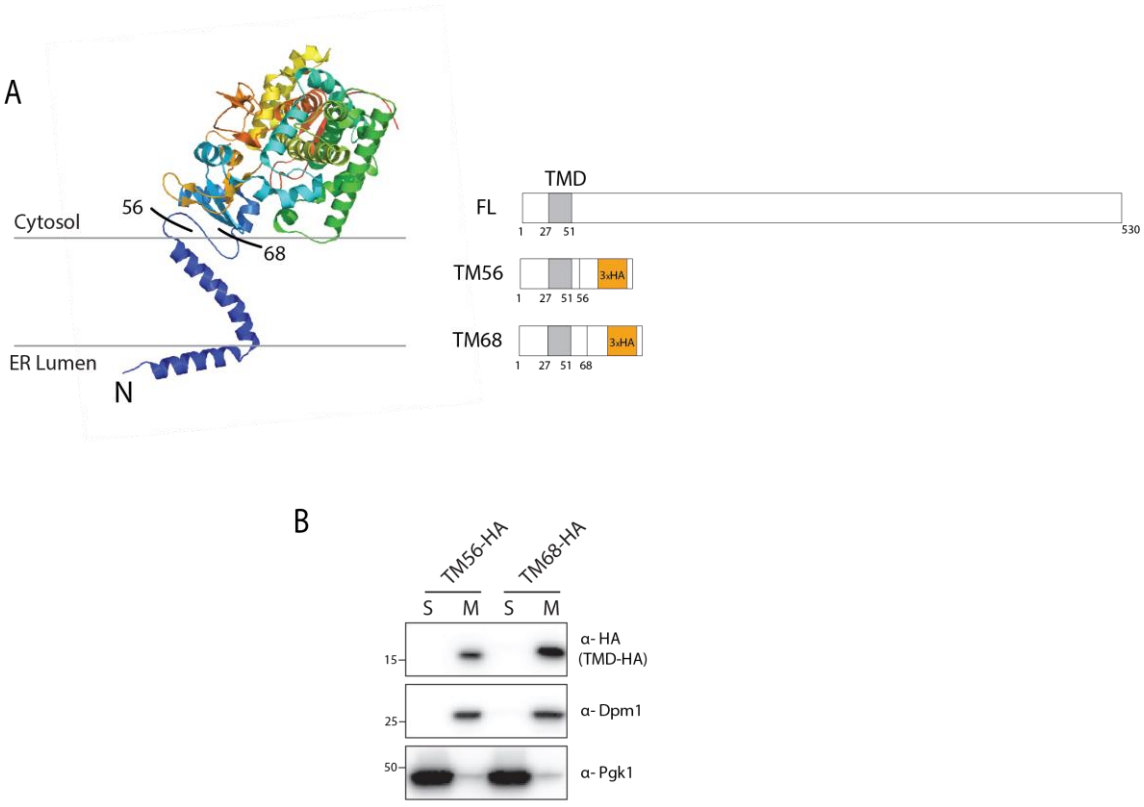


Figure 4.6 – Truncations on Erg11

(A) Resolved structure of Erg11 (Monk et al., 2014) and linear representation of full length (FL) Erg11, TM56 and TM68 represent the truncations consisting of the first 56 and 68 amino acids.

(B) Membrane pellet (M) and cytosolic soluble fraction (S) were isolated from WT cells expressing TM56 and TM68 on plasmids. They were analysed by SDS-PAGE followed by immunoblotting for endogenous TM56 and TM86 with an anti-HA antibody. Dpm1 was detected with anti-Dpm1 antibody as a control for membrane protein and Pgk1 was detected with anti-Pgk1 antibody as a control for soluble protein.

To determine the ability of Asi complex to degrade the TM56 and TM68, cycloheximide(CHX) shut off experiments were performed. In WT cells, both

constructs were degraded. Strikingly, in cells lacking Asi complex subunits Asi1, Asi2 or Asi3, degradation of both TM56 and TM68 were prevented. Consistent with the previous study, Hrd1 and Doa10 deletion mutants did not affect the degradation of the truncated forms (Figure- 4.7A-B). Altogether, these results suggest that just the TMD of Erg11 is sufficient for Asi-mediated degradation.

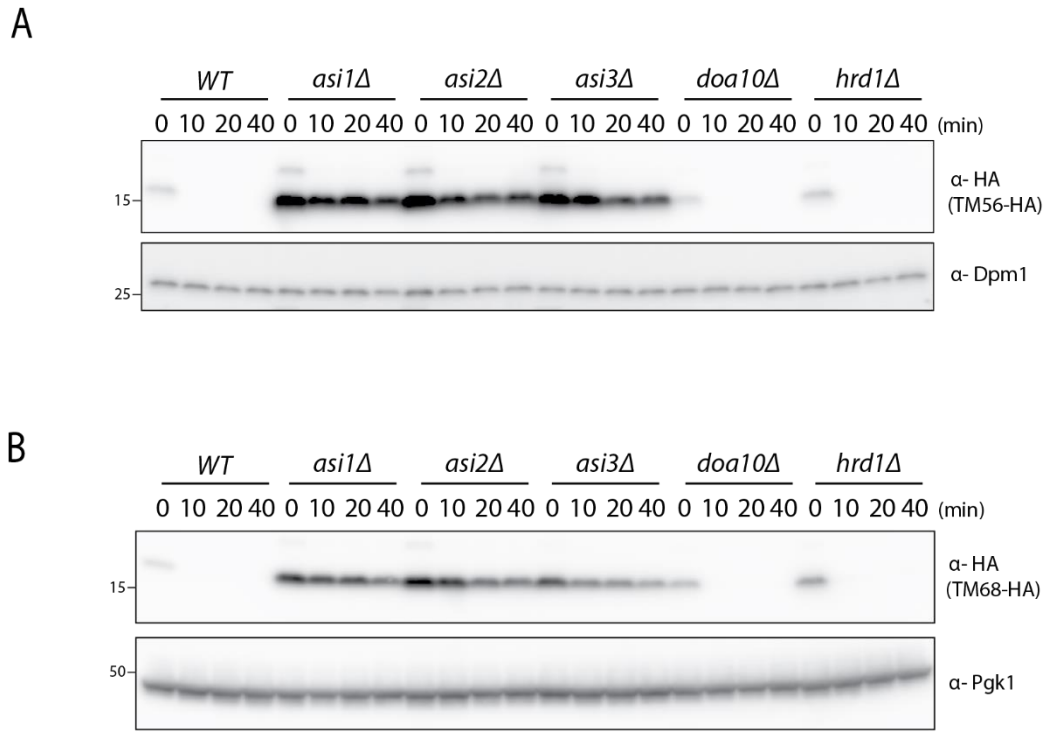


Figure 4.7 – Asi complex recognized the TMD of Erg11

(A) Degradation of TM56-HA was analysed in the specified genotypes. Turnover rates were monitored upon addition of cycloheximide (CHX) to exponentially growing cells. Cell lysates were prepared and analysed for TM56 with anti-HA antibody. Dpm1 detected with anti- Dpm1 antibody and was used as a loading control.

(B) Degradation of TM68-HA was analysed as in (A) but Pgk1 detected by anti- Pgk1 antibody was used as a loading control.

Previous findings from our lab showed that Asi complex-mediated substrate degradation is co-ordinated with E2 enzymes Ubc4 and Ubc7 (Foresti et al., 2014). Thus, we wondered if the TM56 and TM68 also required these E2 enzymes. CHX chase experiment with single deletion mutants of Ubc4 and Ubc7 indicated that TM68 degradation was partially impaired. However, in a double mutant lacking both Ubc4 and Ubc7, degradation of TM68 was inhibited (Figure 4.8). These results indicated that the truncated versions of Erg11 containing just the TMD had the same requirements as its full-length counterpart requiring Ubc4 and Ubc7 for efficient degradation. Altogether, these experiments show that the TMD of Erg11 is the minimal region recognized by Asi complex.

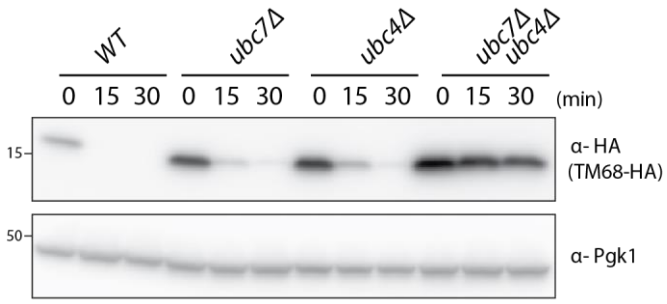


Figure 4.8 – TMD degradation requires Ubc4 and Ubc7

Degradation of TM68-HA was analysed in the specified genotypes. Turnover rates were monitored pon addition of cycloheximide (CHX) to exponentially growing cells. Cell lysates were analysed by immunoblotting for TM68 with anti-HA antibody. Pgk1 detected with anti- Pgk1 antibody and was used as a loading control.

4.5 Voa1 is a substrate of Asi complex

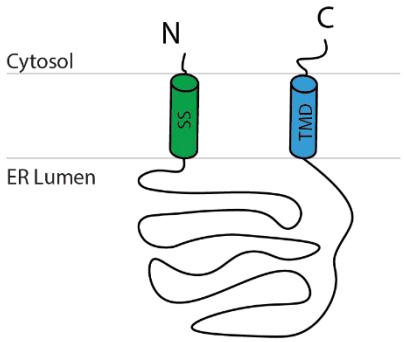
Quantitative proteomics experiments in SILAC-labelled cells identified Voa1 as a potential substrate for the Asi complex. Voa1 is an integral membrane protein initially shown to localize to the ER and functions as an assembly factor for V-ATPase complex (Ryan et al., 2008). However, it was recently shown to be an integral component of the V-ATPase complex (Roh et al., 2018). The N-terminus of Voa1 contains a signal sequence that is required for ER targeting which is followed by a bulky luminal domain and a single TMD at the C-terminal end (Figure- 4.9A). To directly determine the Asi-mediated degradation of Voa1, we performed CHX shut off experiment on yeast cells expressing a 3xHA tagged version of Voa1. In WT cells, Voa1 had a half-life of about 2 hr and its degradation was inhibited in Asi complex deleted mutants. However, in Hrd1 or Doa10 deleted mutants its degradation kinetics was similar to WT cells, confirming that Voa1 is degraded specifically by the Asi complex (Figure- 4.9B).

Next, we sought out to determine the E2 requirements for Voa1 degradation by performing CHX shut-off experiment in cells lacking the individual Ubc4, Ubc6 and Ubc7 and combinations of double mutants. (Figure- 4.9C). The turnover rate of Voa1 in WT cells and Ubc6 deletion mutant were similar. However, in Ubc4 and Ubc7 single deletions and double deletion mutants, we observed that the turnover of Voa1 was markedly impaired. While degradation Erg11 required both E2s (Ubc4 and Ubc7) for complete stabilization, Voa1 required only one for degradation. It suggests that in cells, there are redundancies in E2 requirements

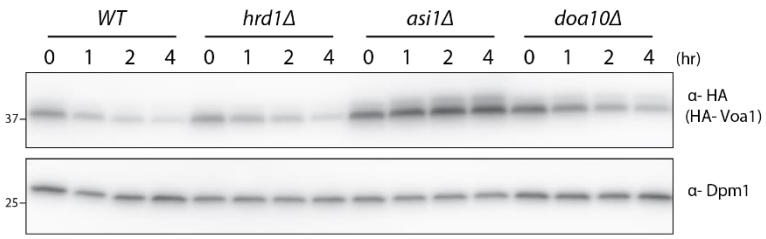
where multiple E2s might play a role for certain substrates. The reason for this might be to ensure continued degradation of a substrate even if one of the enzymes fails to function. Overall, these results indicated that Voa1 required Ubc4 and Ubc7 E2 conjugating enzymes for its degradation by the Asi complex.

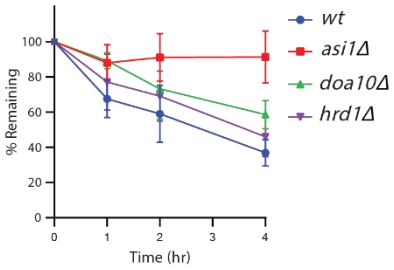
Next, we wondered if the Asi complex also recognized the TMD of Voa1 as it was the case for Erg11. To this end, I generated a Voa1 construct in which the large luminal domain was truncated but retained just the TMD (amino acid residues 217-265) and performed a CHX shut-off experiment. In WT cells, degradation kinetics of the TMD was similar to the full-length and was degraded with a half-life of about 2 hr. However, consistent with our hypothesis, its degradation was delayed in Asi deletion mutants (Figure- 4.9D). Altogether, data from Erg11 and Voa1 suggest that TMDs could behave as a degradation signal for Asi-mediated ERAD.

A

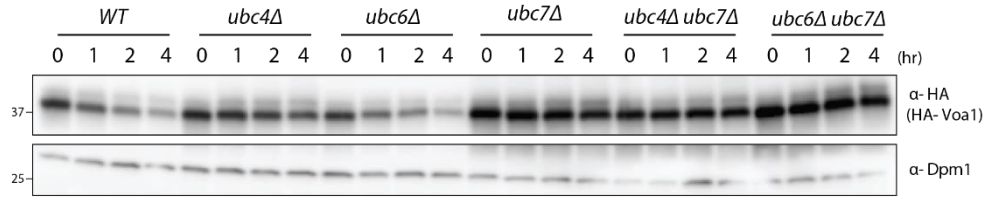

N
C
Cytosol
SS
TMD
ER Lumen

B

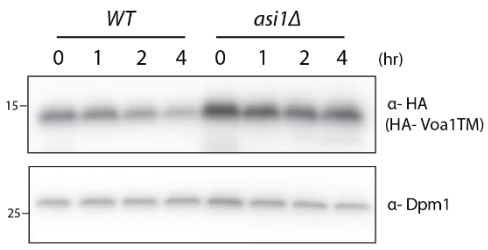

WT
hrd1Δ
asi1Δ
doa10Δ
0 1 2 4 0 1 2 4 0 1 2 4 0 1 2 4 (hr)
37
25
α- HA
(HA- Voa1)
α- Dpm1


% Remaining
Time (hr)
wt
asi1Δ
doa10Δ
hrd1Δ

C


WT
ubc4Δ
ubc6Δ
ubc7Δ
ubc4Δ ubc7Δ
ubc6Δ ubc7Δ
0 1 2 4 0 1 2 4 0 1 2 4 0 1 2 4 0 1 2 4 0 1 2 4 (hr)
37
25
α- HA
(HA- Voa1)
α- Dpm1

D


WT
asi1Δ
0 1 2 4 0 1 2 4 (hr)
15
25
α- HA
(HA- Voa1TM)
α- Dpm1

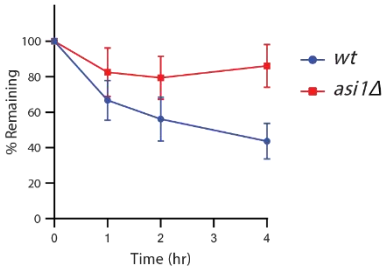

% Remaining
Time (hr)
wt
asi1Δ

Figure 4.9 – Degradation of Voa1 requires Asi complex

(A) Schematic representation of Voa1 full-length protein as per (Ryan et al., 2008). SS- represents a signal sequence that will be cleaved, TMD- Transmembrane domain

(B) Degradation of HA-Voa1 was analysed in the indicated genotypes. Turnover rates were monitored upon addition of cycloheximide (CHX) to exponentially growing cells. SDS-PAGE and immunoblotting were used to analyze whole-cell lysates for Voa1 with anti-HA antibody. Dpm1 was detected with anti- Dpm1 antibody was used as a loading control. Quantification of at least three independent replicates is represented in the graph on the right panel.

(C) Degradation of HA-Voa1 in the indicated genotypes was analysed as in (B)

(D) Degradation of HA-Voa1TM in the indicated genotypes was analysed as in (B). Quantification of at least three independent replicates is represented in the graph on the right panel.

4.6 TMDs are the degradation signal for Asi-mediated ERAD

To further investigate the hypothesis that Asi complex recognizes TMDs, its ability to degrade just TMDs of other ER membrane proteins were tested. We generated plasmids containing TMDs from Wbp1, Gpi8, and Gpi16 preceded by ER targeting sequence followed by a 3xHA tag (Figure- 4.5A). To evaluate the turnover of the TMDs, CHX shut-off experiments were performed. We found that the constructs were quickly degraded with different half-lives in the WT cells. However, their turnover was impaired in Asi mutants, confirming that TMD segments are recognized by the Asi complex (Figure- 4.10B-D).

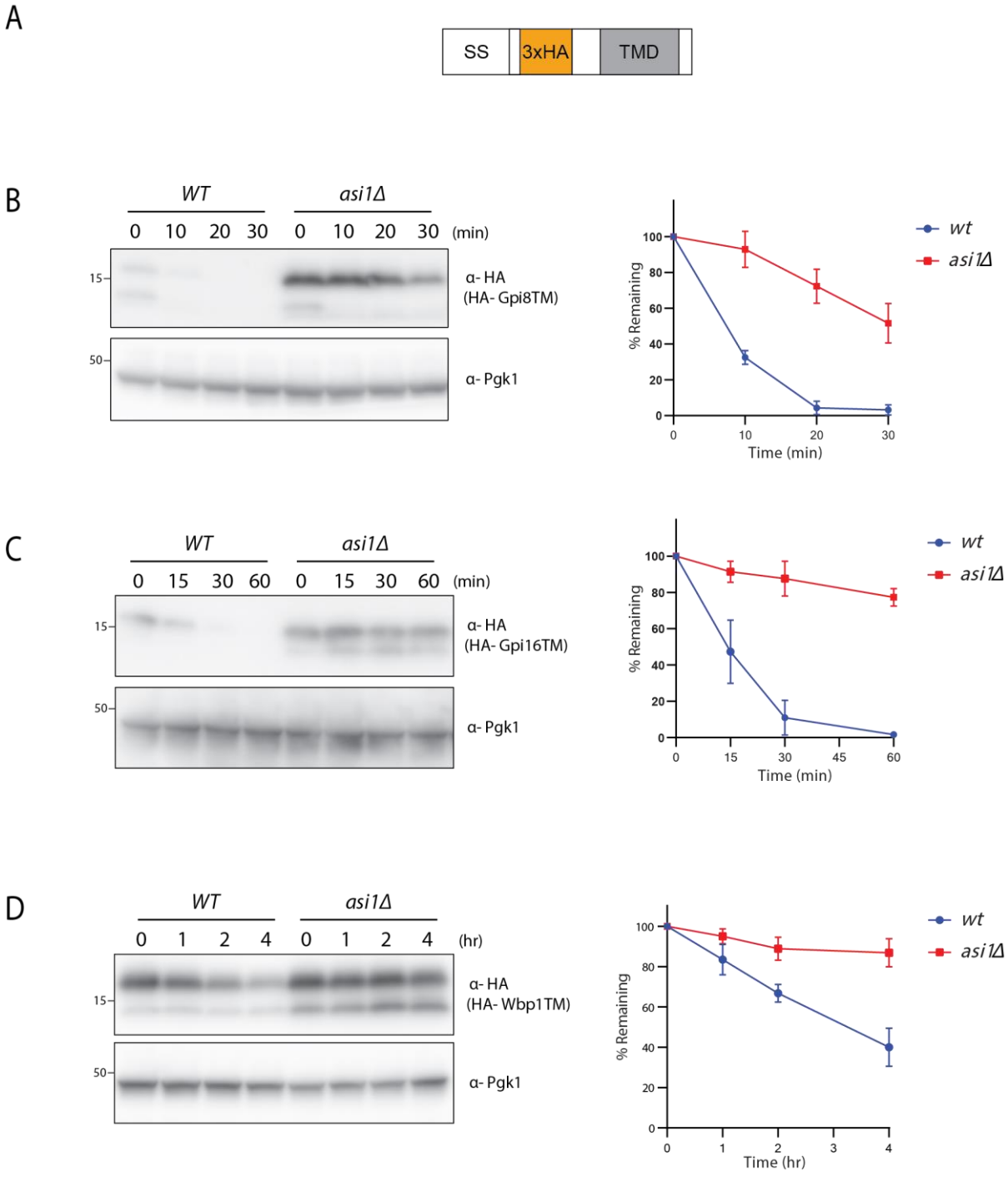


Figure 4.10 –Asi complex recognizes TMDs for degradation

(A) Schematic representation constructs containing TMDs. SS- represents signal sequence followed by a 3xHA tag and the different TMDs

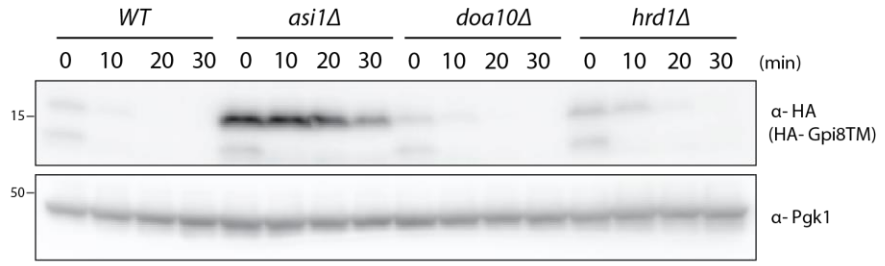
(B) Degradation of HA-Gpi8TM was analysed in the indicated genotypes. Turnover rates were monitored upon addition of cycloheximide (CHX) to exponentially growing cells. Whole-cell lysates were analysed by immunoblotting for Gpi8TM with anti-HA antibody. Pgk1 was detected with anti- Pgk1 antibody and was used as a loading control. Quantification of at least three independent replicates is represented in the graph on the right panel.

(C) Degradation of HA-Gpi16TM in the indicated genotypes was analysed as in (B)

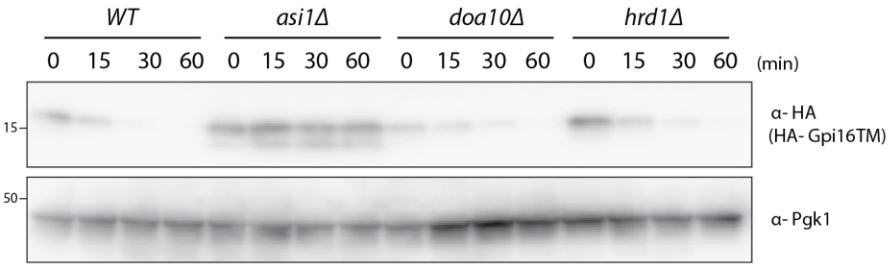
(D) Degradation of HA-Wbp1TM in the indicated genotypes was analysed as in (B).

Additionally, we also explored the degradation kinetics of these constructs in Hrd1 and Doa10 deleted mutants. While Gpi8 and Gpi16 TMDs degradation were not affected in these deletion mutants, Wbp1 was partially stabilised in Hrd1 mutant but not in Doa10 deleted mutant (Figure- 4.11A-C). Furthermore, we wondered if there was a particular feature or property of these TMDs for their recognition by the Asi complex. To this end, we bioinformatically explored various biophysical properties of these TMDs (Figure- 4.11D). We did not observe any direct correlation of these properties to their propensity to be substrates of Asi complex. Due to the wide range of values that we obtained, made it difficult to pinpoint a precise characteristic feature on the substrate that is important for it being explicitly targeted by Asi complex for degradation.

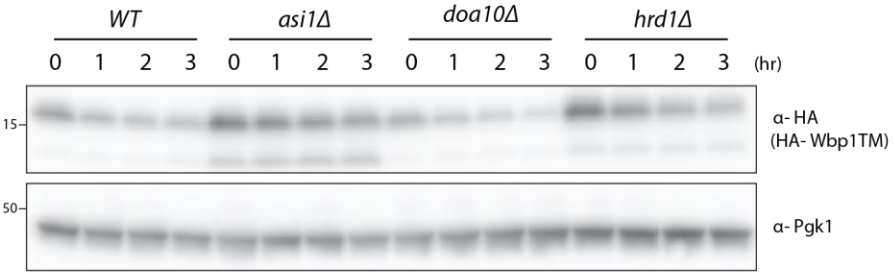
A



B



C



D

TM	Sequence	Length	ΔG (kcal/mol)	Hydrophobicity
Erg11	LAQRISLIIIIPFIYNIVWQLLYSL	25	-0.281	18.85
Gpi8	FKQSATIILALIVTILWFML	20	-1.393	17.80
Gpi16	YNVIILTSTIMGLIFGMLYNL	21	+0.419	17.59
Wbp1	WVYISAICGVIVAWIFFVVSFVT	23	-1.760	25.00
Voa1	GLLMCLIVSALLLFILIVALSWI	23	-4.617	29.48

Figure 4.11 – Asi complex specifically recognizes TMDs for degradation

(A) Degradation of HA-Gpi8TM was analysed in the indicated genotypes. Turnover rates were monitored upon addition of cycloheximide (CHX) to exponentially growing cells. Whole cell lysates were by immunoblotting for Gpi8TM with anti-HA antibody. Pgk1 was used as a loading control and detected with anti- Pgk1 antibody.

(B) Degradation of HA-Gpi16TM in the indicated genotypes was analysed as in (A)

(C) Degradation of HA-Wbp1TM in the indicated genotypes was analysed as in (A).

(D) The sequence of Erg11 TMD was obtained from the structure solved by (Monk et al., 2014). For the TMDs of Gpi8, Gpi16, Wbp1 (http://topcons.cbr.su.se/pred/) prediction program was used. Voa1 TMD was determined by (Ryan et al., 2008). (ΔG) was calculated using the online program http://dgpred.cbr.su.se/index.php?p=home (Hessa et al., 2005, 2007). Hydrophobicity was calculated based on (Zhao and London, 2006).

4.7 TM56 directly crosslinks to Asi complex components

Previously we showed that Asi complex components interact with the substrate Erg11 (Foresti et al., 2014). To further explore the possibility of direct interaction between substrate and the Asi complex, we decided to use *in vivo* photocrosslinking strategy. This method relies on site-specific incorporation of benzoyl-L-phenylalanine (BPA), which contains a photoreactive group. Upon UV irradiation, the protein with BPA can cross-link to its potential interactors in close proximity (Chin et al., 2003). Similar cross-linking approach has been utilized previously in dissecting interactions between E3 membrane ligases and their substrates (Carvalho et al., 2010; Mehnert et al., 2014; Stanley et al., 2011).

To this end, we decided to use the truncated version of Erg11- TM56 and examine its ability to form crosslink with the Asi complex. Amber codon (TAG) was incorporated into the TMD of TM56 by site-directed mutagenesis. With the help of plasmids encoding for an amber codon suppressor tRNA and a modified tRNA synthetase, BPA was incorporated in place of amber codon (TAG). BPA probe was incorporated in various positions on the TMD (L22- I53). Cells were grown in the presence of BPA for 4-5 hr, followed by irradiation with UV light for an hour. Total membrane extracts from these cells were prepared, solubilised under denaturing conditions, followed by immunoprecipitation of TM56 via the HA tag and analysed by immunoblotting. We observed the formation of various high molecular weight species of TM56 in UV-treatment dependent manner, suggesting of crosslinked products (Figure- 4.12). Some of the crosslinked products likely correspond to TM56 oligomers. The remaining crosslinked products could indicate an interaction between TM56 and any other proteins in close proximity.

To determine if subunits of the Asi complex components were crosslinked to TM56, the immunoprecipitated samples were immunoblotted for Asi1 and Asi2. Strikingly, we were able to observe Asi components crosslinked to various positions on the TMD. Further experiments in the lab showed that an intact Asi complex consisting of Asi1, Asi2 and Asi3 was required to obtain these crosslinks. Overall these data indicate that TMD of the substrates directly interacts with the Asi complex.

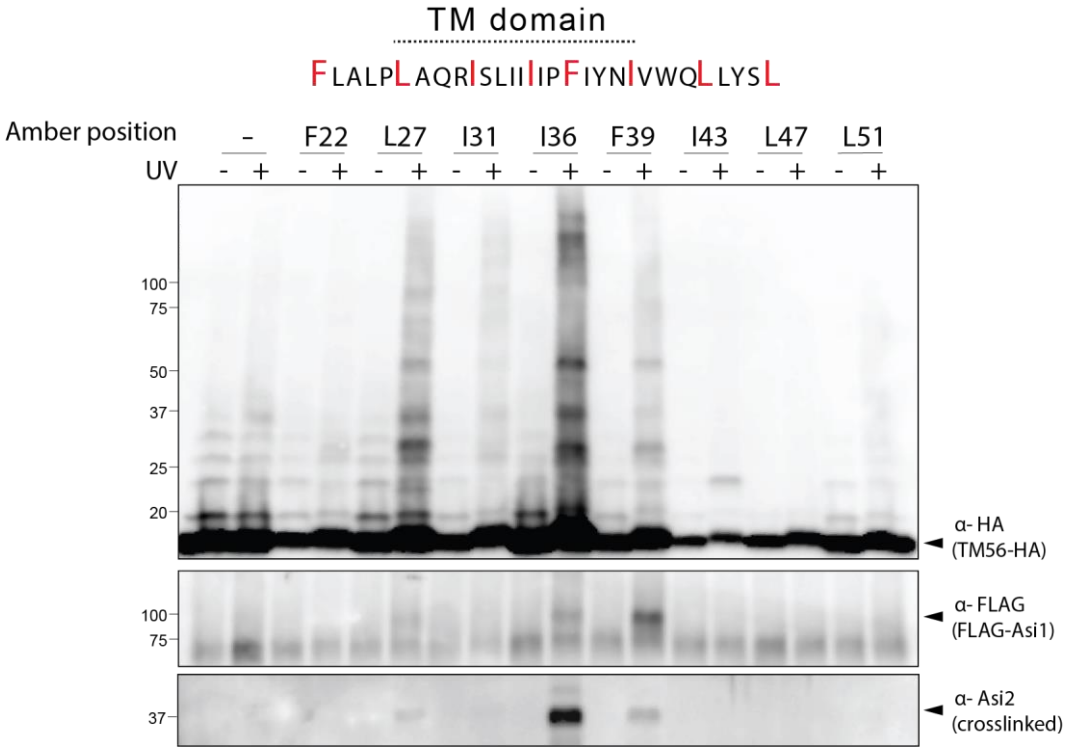


Figure 4.12 – Asi complex directly interacts with TM56

Benzoyl phenylalanine (BPA) was replaced in residues indicated in red on Erg11-TM. *ubc7Δ* cells containing TM56 on a plasmid with the photoreactive analog BPA at indicated positions were subjected to UV irradiation and non-irradiated cells were used as controls. This was followed by extraction of membranes, subsequent solubilization and immunoprecipitation with anti-HA beads. Proteins bound to the beads were eluted and analysed by SDS-PAGE followed by immunoblotting with anti-HA antibody to detect TM56. Anti-FLAG was used to detect Asi1 and anti-Asi2 antibody was used to detect endogenous Asi2. This particular experiment shown here was performed by Dr. Ombretta Foresti.

4.8 Discussion

In this chapter, we found a connection between protein complex assembly in the ER and mislocalized protein degradation at the INM by the Asi complex. Taking various results in this chapter into consideration, the below working model is proposed (Figure 4.12).

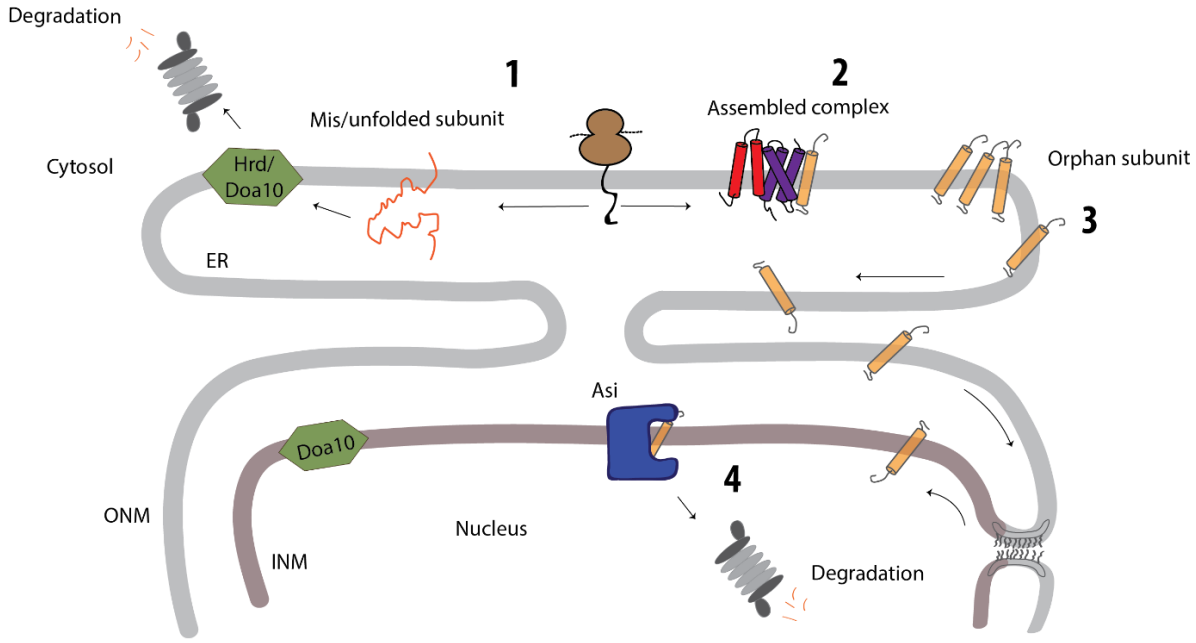


Figure 4.12 – Working Model

As the newly synthesized proteins enter the ER lumen, they are assisted with the help of chaperones to obtain their native conformation and assemble into complexes (1). However, proteins that misfold are targeted for degradation by Hrd1 or Doa10 ERAD complexes. Folded but unassembled subunits diffuse through the ER membrane and eventually assemble into functional complexes (2). Assembled complexes have a higher number of TMDs and at times large cytoplasmic domains that preclude their efficient diffusion into the INM. If folded

but unassembled subunits diffusing through the ER eventually reach the INM (3). At the INM, Asi complex recognizes these unassembled subunits through their TMD and promotes their degradation, a process that maintains INM homeostasis (4). Thus, based on the data we speculate that protein complex assembly in the ER is facilitated by spatially restricting quality control of orphan subunits to the INM thereby contributing to maintaining the INM proteome identity in yeast.

Degradation of orphan proteins has been in the limelight for a while and it is not exclusive to the Asi complex (Juszkiewicz and Hegde, 2018). Doa10 another E3 ligase that localizes to both ER and the INM in yeast has been implicated in the degradation of orphan translocon subunit Sbh2 (Habeck et al., 2015). However, further studies are required to understand if Doa10 degrades misfolded pool of Sbh2 in the ER or it exclusively targets the INM pool is yet to be known.

In the future, it would be essential to study if a parallel pathway exists in mammalian cells as they undergo open mitosis where the nuclear envelope breaks down and reforms at the end of mitosis. Such mechanisms might be essential to clear mislocalized proteins from the INM.

Further, we have tried to understand the mechanism by which Asi complex recognizes its substrates at the INM. With the help of Erg11 and a novel substrate Voa1, we show that TMDs of substrates are the degradation signal for Asi mediated ERAD. Moreover, we also show that the TMD directly interacts with the Asi complex components and is necessary for recognition and subsequent

degradation. *In vivo* crosslinking data shows very strong cross-links in the center of the helix from positions I35 to F39. When mapped into the structure of Erg11, these residues appear to be on the same side of the helical turn, which seems to be necessary for interaction with the Asi complex. Future experiments such as TMD mutagenesis, bioinformatical modeling and measurement of other biophysical properties can aid to identify the specific features on the TMDs that makes them a substrate of the Asi complex. However, most of the proteins recognized by Asi complex are ER residents. Until now, we have tested orphan subunits from – OST complex, GPI-T and V-ATPase complex that depend on Asi complex for degradation at the INM. However, we have not identified any orphan subunits that are Asi-independent. We hypothesize that it could be a general mechanism for all ER orphan subunits to be degraded at the INM. As by restricting quality control of orphan subunits to the INM, a relatively small region of the ER that is not involved in protein biogenesis, allows more time for subunits to find their partners favouring complex assembly in bulk ER membranes. Our data suggest the spatial segregation of the two processes, assembly in the ER and quality control at the INM, contributes for efficient complex assembly.

Interestingly, until now, there are no INM proteins that are degraded by the Asi complex. Hence, an essential question persists as to how INM proteins are not recognized for degradation and what features distinguish them. Future experiments might be able to answer some of these questions.

Chapter 5

Purification and *in vitro* reconstitution of the Asi complex

5 Purification and in vitro reconstitution of the Asi complex

5.1 Introduction

Aberrant proteins in the membrane and lumen of the endoplasmic reticulum (ER) are eliminated by a quality control system called ER-associated protein degradation (ERAD). ERAD is a multi-step process and starts with the recognition of a substrate to be degraded. Once selected, the substrate is transported across the ER membrane (retrotranslocation) and ubiquitinated on the cytoplasmic side of the ER membrane.

The key players in this process are the E3 ligases that recognize the specific substrate for ubiquitination and also co-ordinate with the E2 enzymes. In the earlier chapters, I concentrated on characterizing the E3 ligase- Asi complex and its substrate recognition mechanisms at the inner nuclear membrane. In this chapter, we focused on developing an *in vitro* system for Asi complex with purified components in order to understand if Asi complex defined the minimal unit required for recognition, ubiquitination and retrotranslocation of substrates.

In the case of Hrd1 and Doa10 ERAD pathways, bottom-up *in vitro* approaches using recombinant proteins have been instrumental in illuminating critical steps. (Baldridge and Rapoport, 2016; Stein et al., 2014). *In vitro* approaches defined the role of Hrd1 transmembrane segments in retrotranslocation of certain ERAD substrates (Baldridge and Rapoport, 2016), the diverse role of E2s in substrate

processing (Weber et al., 2016) and the mechanism of Cdc48-mediated substrate processing (Bodnar and Rapoport, 2017a; Stein et al., 2014).

Using an analogous *in vitro* system, I will evaluate the roles of individual Asi complex subunits in substrate recognition and contributions of E2 conjugating enzymes Ubc4 and Ubc7.

5.2 Construct design and small scale expression

To establish an *in vitro* ubiquitination assay for Asi complex-mediated ubiquitination it required the purification of the following proteins: the Asi complex consisting of Asi1, Asi2 and Asi3, a substrate that is recognized by the Asi complex, E1 activating enzyme and E2 conjugating enzymes. Below is the optimization to purify the Asi complex.

Previous attempts in the lab to recombinantly express subunits of the Asi complex in *E. coli* expression system have not been successful. Hence, we decided to use the budding yeast *S. cerevisiae* expression system to express and purify subunits of the Asi complex as an intact complex. The open reading frames of Asi1, Asi2 and Asi3 subunits were cloned individually into high copy shuttle vectors for expression under the galactose-inducible promoter. To determine the most appropriate tag for affinity purification, each subunit of the Asi complex was tagged with various affinity tags such as His14 tag, SBP (streptavidin binding peptide) tag and protease cleavage sites at either the N-terminus or C-terminus (Table 5.1)

Protein	N-terminal tags	Vector backbone
Asi1	His14-TEV-Asi1	pRS426 (2µ, URA, AmpR)
	His14-NEDD8-Asi1	pRS426 (2µ, URA, AmpR)
	SBP-TEV-Asi1	pRS426 (2µ, URA, AmpR)
Asi2	His-TEV-Asi2	pRS426 (2µ, URA, AmpR)
	SBP-TEV-Asi2	pRS426 (2µ, URA, AmpR)
Asi3	SBP-NEDD8-Asi3	pRS423 (2µ, HIS, AmpR)
	SBP-TEV-Asi3	pRS426 (2µ, URA, AmpR)
Protein	**C-terminal tags**	**Vector backbone**
Asi1	Asi1-TEV-SBP	pRS426 (2µ, URA, AmpR)
Asi2	Asi1-TEV-SBP	pRS426 (2µ, URA, AmpR)
Asi3	Asi1-TEV-SBP	pRS426 (2µ, URA, AmpR)

Table 5.1- List of constructs with N-terminal and C-terminal tags on each Asi complex subunit

Next, these constructs were utilised to determine the best expression conditions. To this end, starter culture was inoculated in 3ml of SD (synthetic drop out media) and grown for 24 hr. Expression of the protein was induced by the addition of YP media supplemented with 8% (w/v) galactose and 1ml of the sample was collected at 4hr, 8hr, 12 hr and 24 hr post-induction. In each case, the protein level was determined by SDS-PAGE and immunoblotting of the whole cell lysates. We observed robust induction of expression of Asi1, Asi2 and Asi3 subunits at 4 hours post-induction. Protein expression was observed to increase with time up to 24hr, upon which there was a reduction of expression of Asi1. A similar expression pattern was observed for all the constructs. Subsequent experiments used a 12hr induction period (Figure- 5.1).

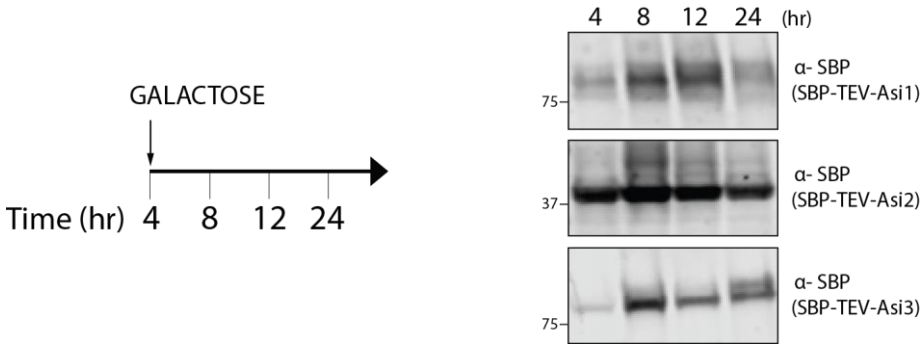


Figure 5.1 – Galactose induced expression of Asi complex subunits

Protein expression was induced by the addition of galactose. Yeast cells were collected at time points as shown and whole-cell lysates were prepared. They were analysed by SDS-PAGE followed by immunoblotting for SBP (Streptavidin binding peptide) tagged Asi1, Asi2 and Asi3 with anti- SBP antibody.

Purification of membrane protein complex requires their extraction from the lipid bilayer through detergent solubilisation. This is a critical step because we need to find the conditions in which the maximum amount of protein is solubilised while maintaining the integrity of the Asi complex during the process. To this end, I performed a FLAG immunoprecipitation under endogenous expression levels in cells that expressed FLAG-Asi1. Total membranes were extracted from whole cell lysates and were treated with 1% of various detergents (Figure- 5.2A). While most detergents tested resulted in immunoprecipitation of all three subunits of the Asi complex, solubilisation with DDM prevented the purification of an intact complex. We also noticed that certain detergents like digitonin, tend to precipitate in cold temperature which is needed for purification steps. From these

experiments, we decided to utilise the detergent decyl maltose neopentyl glycol (DMNG) for all our future experiments because it allows efficient solubilisation while preserving the integrity of the Asi complex.

Further, we tested the solubility of Asi1, Asi2 and Asi3 with various N and C-terminal tags with 1% DMNG. For most of the constructs, only a minor fraction of the total membrane extract was soluble (Figure- 5.2B-G).

Based on our finding that Asi1 is crucial to mediate the interaction between Asi2 and Asi3 proteins (discussed in Chapter 3), we decided to use Asi1 affinity-tagged constructs to purify the intact complex. The most soluble construct for Asi1 was N-terminally tagged SBP-TEV-Asi1 which seemed to be better than the other tags. Thus we chose SBP-TEV-Asi1, untagged-Asi2, FLAG-Asi3 constructs and performed large scale purification of the Asi complex.

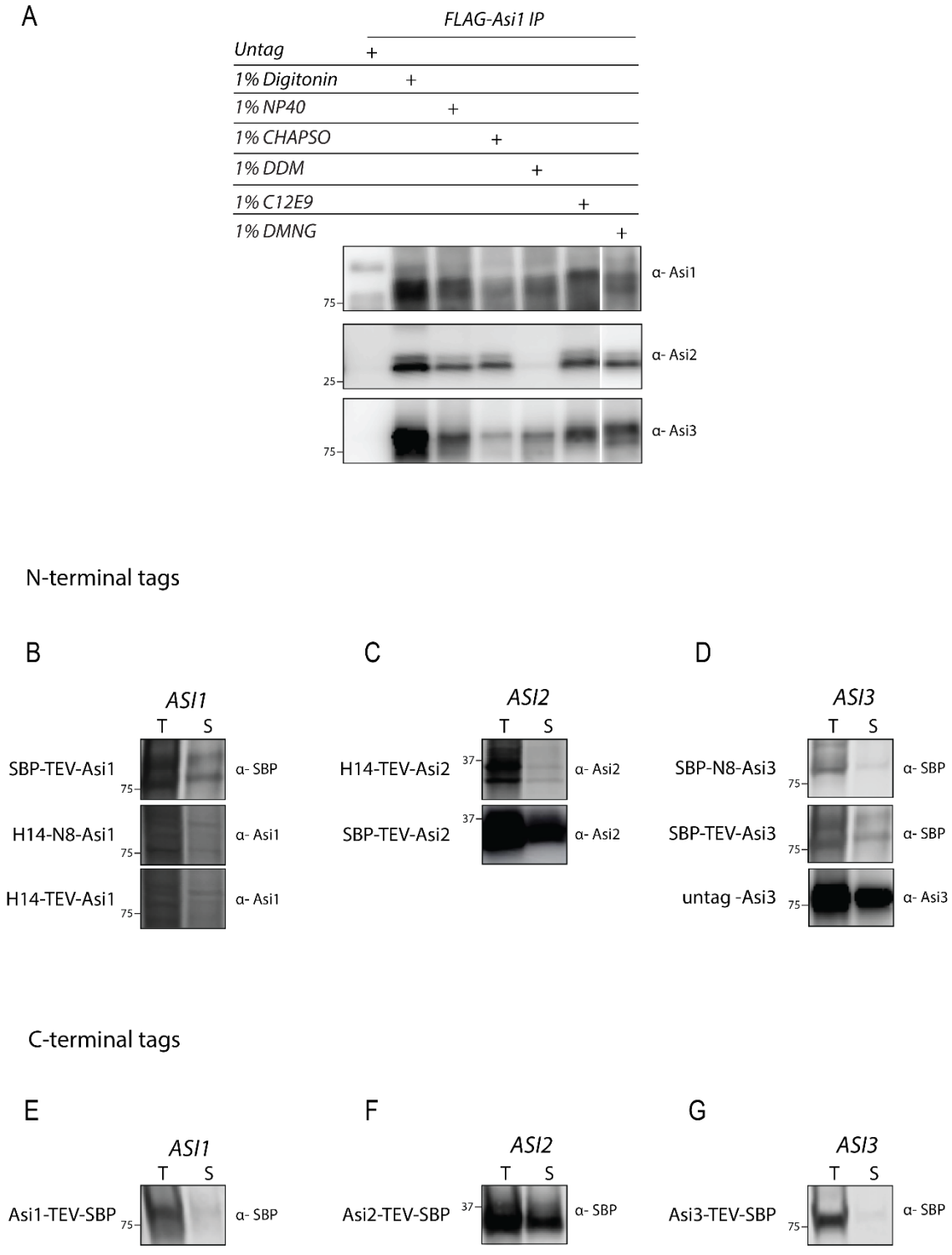


Figure 5.2 – Comparison of different detergents on interactions between Asi complex subunits and their solubility with various tags

(A) Immunoprecipitation with anti- FLAG antibody. Membrane fractions were prepared from WT(untag) and FLAG-Asi1 cells. Membrane pellets were solubilised with 1% digitonin, 1% NP40 (Nonidet P-40), 1% CHAPS (3-([3-Cholamidopropyl]dimethylammonio)-2-hydroxy-1-propane sulfonate), 1% DDM (n-Dodecyl-β-D-Maltopyranoside), 1% C12E9 ((n-Dodecyl)-nonaethyleneglycol), 1% DMNG (Decyl Maltose Neopentyl Glycol) and incubated with FLAG magnetic beads overnight. Bound proteins to the beads were eluted using SDS buffer and analysed by SDS-PAGE followed by immunoblotting for Asi1, Asi2 and Asi3 with anti- Asi1, anti-Asi2 and anti-Asi3 antibodies respectively

(B-D) Membrane fractions were isolated from cells with various N-terminal tags on Asi1, Asi2 and Asi3. Membranes were solubilised with 1% DMNG for 1.5 hr at 4˚C and analysed by SDS-PAGE followed by immunoblotting. T- represents total membrane extract, S- represents detergent-solubilised fraction

(E-G) Membrane fractions were isolated from cells with C-terminal tags on Asi1, Asi2 and Asi3. Membranes were solubilised with 1% DMNG for 1.5 hr at 4˚C and analysed by SDS-PAGE followed by immunoblotting with anti-SBP. T- represents total membrane extract, S- represents detergent-solubilised fraction

5.3 Large scale purification of the Asi complex on SBP-TEV-Asi1

Preculture was inoculated in 150ml synthetic drop out media. It was further diluted in 6L of fresh medium and grown for another 24 hr. Expression of Asi proteins was induced by the addition of 8% (w/v) galactose. After 12 hours, cell pellet was harvested, washed and lysed as described in chapter 2. After removing non-lysed cells by a low-speed spin, membranes were pelleted and solubilised

with 1% DMNG. A detergent extract was incubated overnight with streptavidin agarose resin. Bound proteins were eluted from the beads with buffer supplemented with Biotin and analysed by SDS-PAGE and Coomassie stain. Further, elutions were subjected to immunoblotting to confirm the co-elution of Asi2 and Asi3 (Figure- 5.3A).

To estimate the size of the intact Asi complex and to remove impurities and aggregates, biotin-eluted proteins were subjected to size exclusion chromatography. Biotin elutions were concentrated and loaded on a Superose 6 column. Peak (10-15 fractions) of the Asi complex was just after the void volume and was estimated to be around 600kDa when compared to the molecular weight standards (Figure- 5.3B). The peak elutions (10-15) from the column were pooled, concentrated and used in the future *in vitro* assays. In many experiments, Asi complex eluted right after streptavidin affinity purification was used.

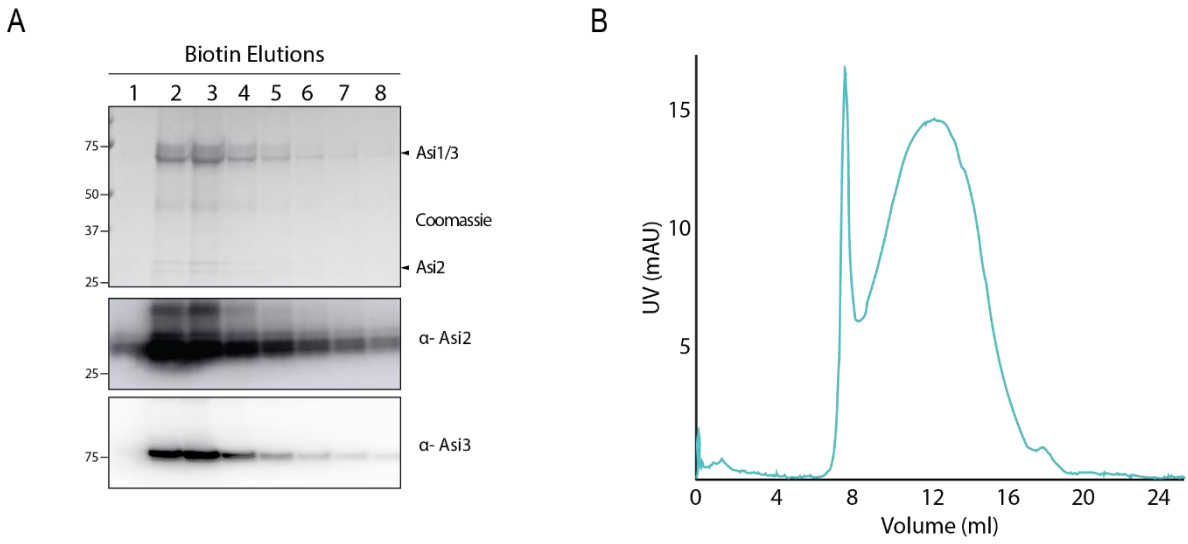


Figure 5.3 – SBP-TEV-Asi1 large scale affinity purification of the Asi complex

(D) Large scale affinity purification of the Asi complex with SBP beads. Membrane pellets were solubilised with 1% DMNG and incubated with SBP beads overnight. Bound proteins to the beads were eluted using buffer supplemented with biotin and analysed by SDS-PAGE followed by coomassie stain (top panel) and immunoblotting for Asi2 and Asi3 with anti- Asi2 and anti-Asi3 antibodies respectively.

(E) Fractions 2-5 from affinity purification were pooled, concentrated and applied on a Superose 6 column for size exclusion chromatography. Peak fractions 10-16 were again pooled, concentrated and used for *in vitro* assays.

5.4 Purification of the substrate for Asi complex

TM68 fragment of Erg11, which was described as a substrate in the previous chapter, was used as a substrate for *in vitro* ubiquitination. We engineered the TM68 construct to have a His14 affinity tag followed by a sumo protease cleavage at the N-terminus and an MBP (maltose binding peptide) tag and a sortase recognition site for labelling at the C-terminus (Figure- 5.4A). His14-Sumo-TM68-MBP construct was recombinantly expressed in *E. coli* and subsequently purified with Ni-NTA affinity beads, followed by elution from Ni-NTA beads with the digestion of the Sumo tag with Ulp1 (sumo protease) (Figure- 5.4B). Next, eluted TM68-MBP fragment was subjected to size exclusion chromatography using a Superdex 200 column (Figure- 5.4C). We obtained a single peak elution from the size exclusion which corresponds to pure TM68-MBP fusion protein as assessed

by SDS-PAGE (Figure- 5.4B). Peak fractions were collected, concentrated and labelled with Dy800 using sortase labelling technique (Stein et al., 2014).

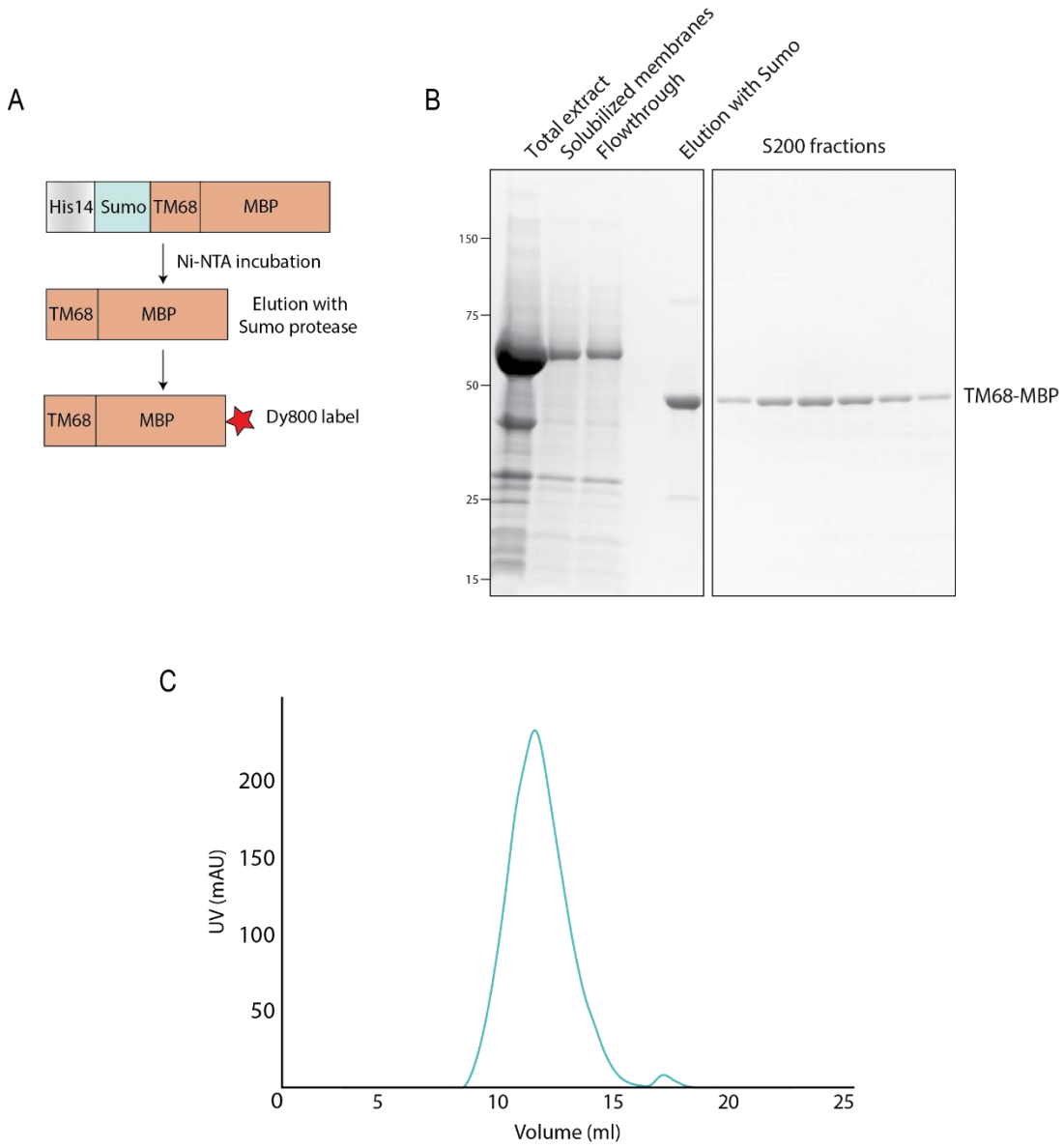


Figure 5.4 –Ni-NTA affinity purification of TM68-MBP

(A) Schematic representation of the construct purification procedure of TM68-MBP that was used for expression and purification from *E. coli*

(B) Purification of His14-Sumo-TM68-MBP. Membrane pellets were solubilised with 1% DDM and incubated with NiNTA beads. Bound proteins to the beads were eluted using

buffer supplemented with Ulp1 protease and analysed by SDS-PAGE followed coomassie stain.

(C) Elution from affinity purification concentrated and applied on a Superdex 200 column for size exclusion chromatography. Peak fractions 10-14 were pooled, concentrated and used for *in vitro* assays.

5.5 *In vitro* ubiquitination assay

To examine if the purified Asi complex was able to ubiquitinate the substrate, we performed a ubiquitination reaction assay in detergent. E1- Uba1, E2s - Ubc4, Ubc7 and its activator Cue1 (kindly provided by Alexander Stein's lab) were recombinantly purified from *E. Coli.* They were all added along with Asi complex, TM68-MBP and incubated for 1 hr at 30˚C. We did not observe any ubiquitination chain built on the substrate.

In chapter 4, we showed that Asi complex requires direct interaction with the TMD of the substrate. Hence we hypothesised that detergent micelles might be interfering with the interactions between Asi complex and TM68-MBP. Thus, we decided to reconstitute them into proteoliposomes, which better mimics the environment of the phospholipid layer and may recapitulate interactions between Asi complex and TM68-MBP in a better way.

To this end, we reconstituted Asi complex and TM68-MBP into liposomes. Proteoliposomes containing affinity-purified Asi complex and TM68-MBP were

incubated with the ubiquitination mix containing Uba1, Ubc4, Ubc7, Cue1, ubiquitin and ATP.

From preliminary experiments, we observed that ubiquitination modification on TM68-MBP was very minimal and inconsistent between replicates (Figure- 5.5A). In the past, we have noticed that some tags on Asi1 rendered it non-functional *in vivo* (Foresti et al., 2014). We hypothesised that the complex affinity purified on SBP-Asi1 was not very active. Hence, we decided to add the SBP affinity tag on Asi2 and purify the complex by affinity purification on SBP-Asi2, a fusion protein which was functional *in vivo* (Figure- 5.5B).

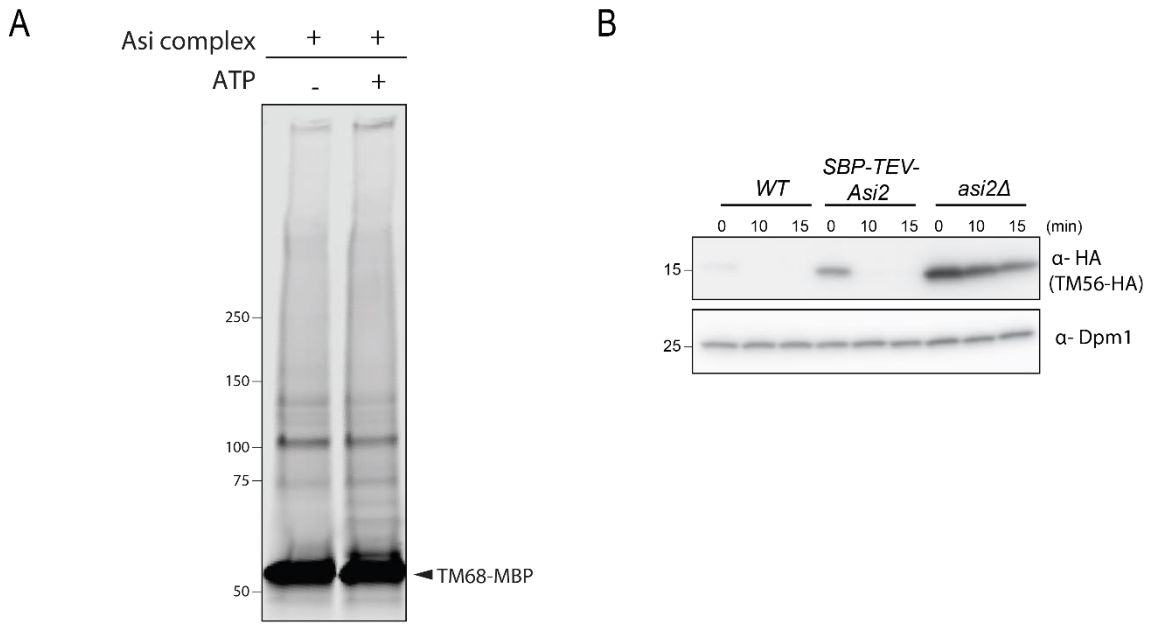


Figure 5.5 – *In vitro* Ubiquitination on proteoliposomes

(A) Asi complex affinity purified with SBP-Asi1 and TM68-MBP were reconstituted into proteoliposomes and were incubated with soluble ubiquitination machinery (Uba1,

Ubc4, Ubc7, Cue1, ubiquitin) for 1 hr at 30˚C. Reactions were stopped by addition of SDS buffer and analysed by direct fluorescence scanning for TM68-MBP.

(B) The degradation TM56-HA was followed after inhibition of protein synthesis by cycloheximide in cells with the indicated genotype. SDS–PAGE and immunoblotting was performed to analyse whole-cell extracts. TM56 and Dpm1 were detected with anti-HA and anti-Dpm1 antibodies, respectively.

5.6 Large scale purification of the Asi complex using SBP-Asi2 and reconstitution into proteoliposomes

Large scale purification of SBP-Asi2, untagged Asi1 and Asi3 was performed as previously described in section 5.2. Elutions were analysed by SDS-PAGE followed by immunoblot and Coomassie stain (Figure- 5.6A).

Asi complex affinity purified with SBP-Asi2 and TM68-MBP were reconstituted into liposomes by passing the mixture through spin columns designed to remove the detergent. Liposomes were composed of the following lipids -1-palmitoyl-2-oleoyl-sn-glycero-3-phosphocholine (POPC), 1,2-dioleoyl-sn-glycero-3-phosphoethanolamine (DOPE), 1,2-dioleoyl-sn-glycero-3-phospho-L-serine (DOPS), cholesterol and 1,2-dioleoyl-sn-glycero-3-phosphoethanolamine-N-(lissamine rhodamine B sulfonyl) ammonium salt (18:1 Liss Rhod PE) mixed at a percentage of (64.5:20:10:5:0.5).

To examine the efficiency of protein reconstitution into liposomes, we used a floatation assay with a glycerol gradient. Proteoliposomes were transferred in the

bottom of the tube and layered with a step gradient of glycerol (0-40%). It was subjected to centrifugation; fractions were collected from the top layer and analysed by immunoblotting. We observed that the majority of the Asi complex and TM68-MBP were present in fractions 2 and 3 with the liposomes confirming efficient reconstitution of the Asi complex into proteoliposomes (Figure- 5.6B).

To examine the orientation of the Asi complex on the proteoliposomes, we performed protease protection assay. The SBP affinity tag at the N-terminus of Asi2 was followed by a TEV protease site. Thus, to test whether Asi2 N-terminus was exposed to the outside, proteoliposomes were treated with TEV protease. Consistent with this possibility we noticed a reduction in the signal of SBP-Asi2 (Figure- 5.6C). Permeabilization of liposomes with the detergent DMNG lead to a reduction of similar magnitude indicating that the majority of Asi2 of molecules in proteoliposomes contains the N-terminus exposed to the outside. Considering the topology Asi1 and Asi3; this result suggests that their RING domains also faced the outside of liposomes. Although, the assay as presented contains few limitations, with regard to the use of DMNG that does not permeabilize the liposomes entirely. This assay could be repeated in the future with a stronger detergent like triton and also immunoblotting with anti-Asi2 would help to clearly observe the shift in bands followed by TEV protease cleavage.

The data presented in Figure 5.6B shows that both the Asi complex and TM68-MBP are reconstituted into proteoliposomes. However, it would be possible that

these proteins would be inserted in different proteoliposomes. To determine if TM68-MBP and the Asi complex were co-reconstituted into the same proteoliposome, we performed SBP-Asi2 pulldown and tested for the co-precipitation of TM68-MBP. To this end, TM68-MBP and Asi complex were reconstituted together in the same liposome (P1) and individually in different liposomes (P2 and P3) (Figure- 5.6D). *In vitro* SBP pull-down was performed in liposomes containing both TM68-MBP and Asi complex (P1) and by mixing individual liposomes (P2+P3). Immunoblotting confirmed that TM68-MBP was affinity-purified only in P1 condition confirming co-reconstitution of TM86-MBP and Asi complex (Figure- 5.6D). Altogether these experiments show that TM86-MBP and Asi complex were indeed reconstituted into the same proteoliposome.

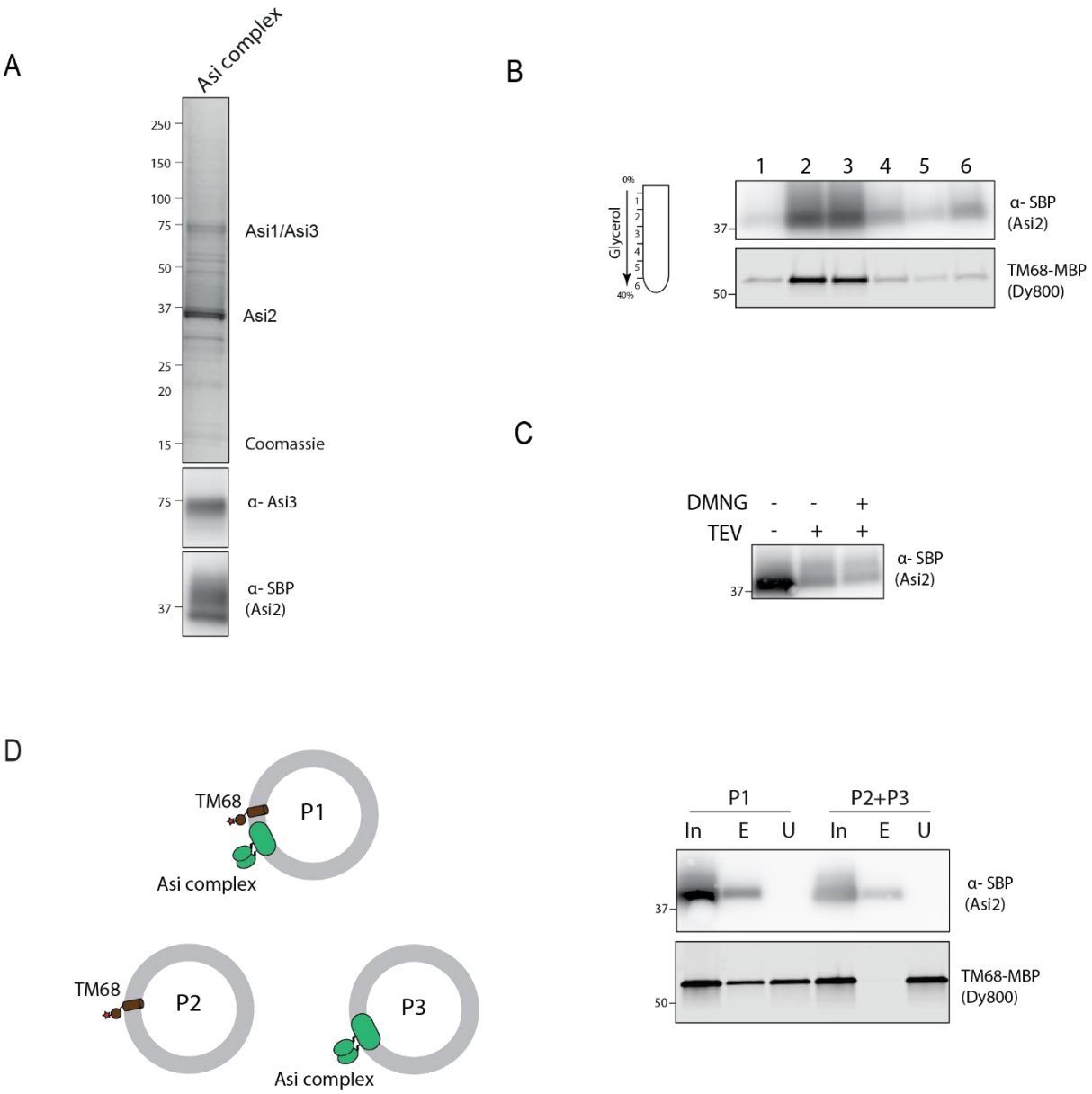


Figure 5.6 –Large scale affinity purification of the Asi complex with SBP-Asi2 and its reconstitution into proteoliposomes

(A) Membrane pellets from cells expressing SBP-Asi2, untagged Asi1 and Asi3 were solubilised with 1% DMNG and incubated with SBP beads overnight. Bound proteins to the beads were eluted using buffer supplemented with biotin and analysed by SDS-PAGE followed by coomassie stain (top panel) and immunoblotting for Asi2 and Asi3 with anti-SBP and anti-Asi3 antibodies, respectively.

(B) Proteoliposomes with both Asi complex and TM68-MBP were subjected to 0-40% glycerol gradient centrifugation. Fractions were collected from the top layer, followed by SDS-PAGE, immunoblotting for Asi2 with anti-SBP antibody and direct fluorescence scanning for TM68-MBP.

(C) Proteoliposomes with Asi complex contained a TEV cleavage site at the N-terminus of Asi2. They were treated with TEV protease (0.5µg) with and without DMNG (2mM) for 1 hr at RT. SDS-PAGE and immunoblotting were used to analyze Asi2 with an anti-SBP antibody.

(D) Schematic representation of the different proteoliposomes. P1- consists of both Asi complex and TM68-MBP. P2 consists of just the substrate TM68-MBP and P3 just the Asi complex. Proteoliposomes were immobilized on streptavidin beads for 1.5 hr at RT. Beads were subjected to washes and proteins bound to the beads were eluted using SDS buffer supplemented with 4mM biotin. They were analysed by SDS-PAGE followed by either immunoblotting for Asi2 with anti-SBP antibody and direct fluorescence scanning for TM68-MBP.

5.7 *In vitro* ubiquitination of TM68-MBP with SBP-Asi2 affinity-purified Asi complex

Proteoliposomes containing SBP-Asi2 affinity-purified Asi complex and TM68-MBP were incubated with ubiquitination mix containing Uba1, Ubc4, Ubc7, Cue1, ubiquitin and ATP. Upon SDS-PAGE analysis and fluorescent imaging, we observed the formation of higher molecular weights products of TM-68, which

were dependent on ATP and Asi complex (Figure- 5.7A). To confirm that the high molecular weight bands were ubiquitin-modified TM68-MBP, we repeated the ubiquitination experiment utilising His-tagged ubiquitin molecules and performed a Ni-NTA pull-down under denaturing conditions. Consistent with the initial ubiquitination experiment, we observed that poly-ubiquitinated TM68-MBP accumulated over time. (Figure- 5.7B).

To confirm that the activity observed was indeed dependent on the Asi complex and not form a contaminant protein similar experiments were performed with ubiquitin-ligase deficient Asi complex. RING domains of Asi1 and Asi3 confer the ligase activity and are essential for the degradation of substrates in vivo. To explore the requirement of the RING domains, we performed *in vitro* ubiquitination assay with purified Asi1/3 RING domain-deficient mutants (Figure-5.7C). We observed that the formation of ubiquitin chains were reduced in 1RΔ/3RΔ when compared to the WT Asi complex. However, there appears to be residual ubiquitination activity in the 1RΔ/3RΔ and negative control which could be a result of an unknown ligase present in the Asi complex purification. The observed residual ubiquitination is very minimal when compared to the WT condition. Hence, these data confirm that *in vitro* ubiquitination was dependent on the RING domains of Asi1 and Asi3 (Figure- 5.7D). Altogether, these results show that the Asi complex was sufficient to recognize and ubiquitinate an integral membrane substrate *in vitro*.

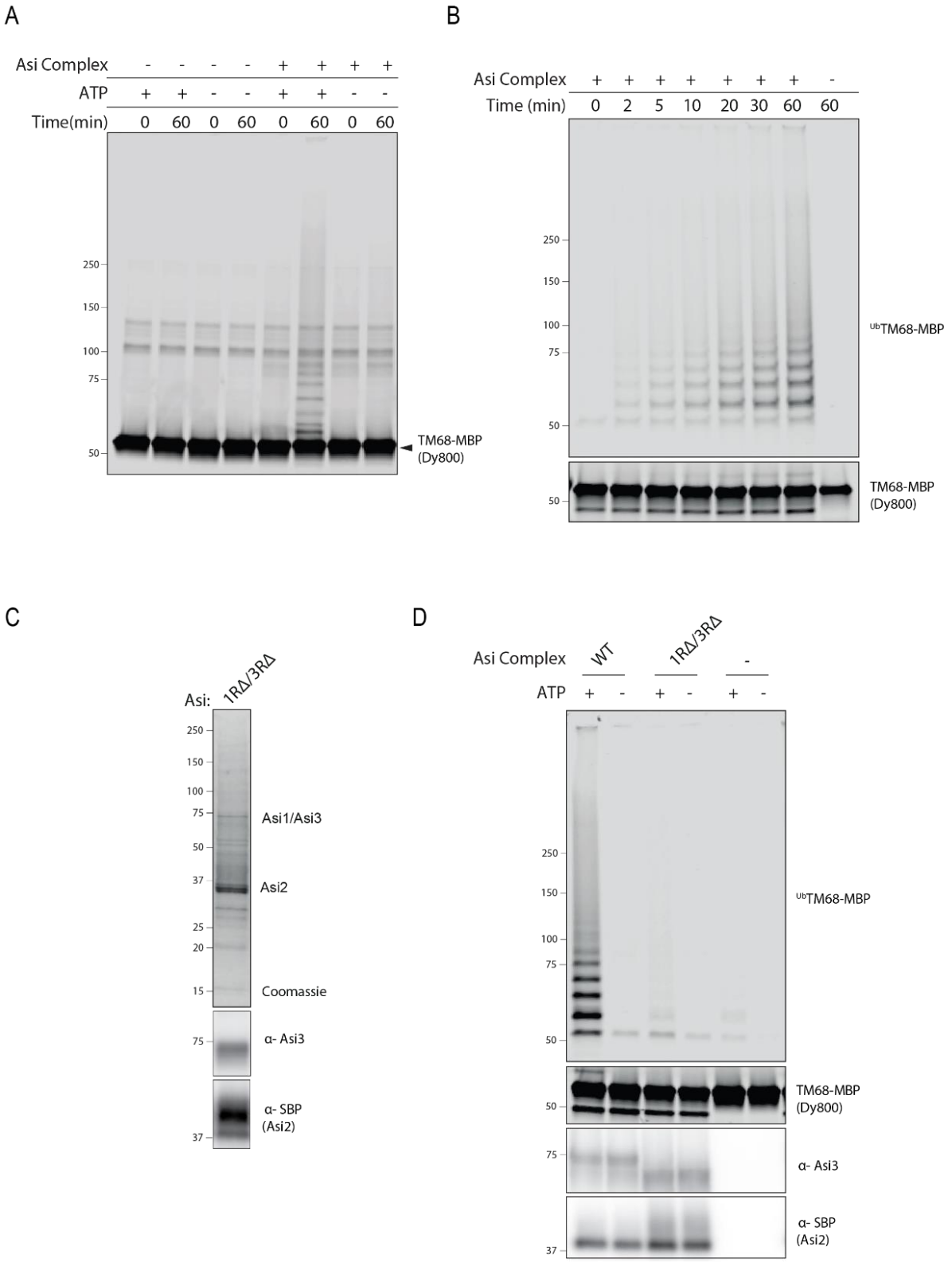

A
Asi Complex - - - - + + + +
ATP + + - - + + - -
Time(min) 0 60 0 60 0 60 0 60
250
150
100
75
50
TM68-MBP
(Dy800)
B
Asi Complex + + + + + + + -
Time (min) 0 2 5 10 20 30 60 60
250
150
100
75
50
UbTM68-MBP
50
TM68-MBP
(Dy800)
C
Asi: 1RΔ/3RΔ
250
150
100
75
50
37
25
20
15
Asi1/Asi3
Asi2
Coomassie
75
α- Asi3
α- SBP
(Asi2)
37
D
Asi Complex WT 1RΔ/3RΔ -
ATP + - + - + -
250
150
100
75
50
UbTM68-MBP
50
TM68-MBP
(Dy800)
75
α- Asi3
37
α- SBP
(Asi2)

Figure 5.7 – *In vitro* ubiquitination of TM68-MBP with Asi complex affinity-purified from SBP-Asi2

(A) Proteoliposomes with TM68-MBP and in the presence or absence of Asi complex were incubated with soluble ubiquitination machinery (Uba1, Ubc4, Ubc7, Cue1, ubiquitin) and ATP for 1 hr at 30˚C. Reactions were stopped by addition of SDS buffer and analysed by SDS-PAGE followed by direct fluorescence scanning for TM68-MBP.

(B) Proteoliposomes with TM68-MBP and Asi complex were incubated with soluble ubiquitination machinery (Uba1, Ubc4, Ubc7, Cue1, His-ubiquitin) and ATP for 1 hr at 30˚C. Reactions were split into two, a part of it analysed directly by fluorescence scanning for TM68-MBP (bottom panel). The second part was further solubilised with 1% triton and incubated with NiNTA beads under denaturing conditions for His-ubiquitin affinity purification. Bound proteins were eluted from the beads using SDS buffer supplemented with imidazole and analysed by SDS-PAGE followed by fluorescence scanning.

(C) RING deficient Asi complex was purified by extracting membranes. Membrane pellets were solubilised with 1% DMNG and incubated with SBP beads overnight. Bound proteins to the beads were eluted using buffer supplemented with biotin and analysed by SDS-PAGE followed by coomassie stain (top panel) and immunoblotting for Asi2 and Asi3 with anti- SBP and anti-Asi3 antibodies, respectively.

(D) Proteoliposomes containing WT Asi complex and RING deficient Asi complex were incubated with soluble ubiquitination machinery (Uba1, Ubc4, Ubc7, Cue1, ubiquitin) and ATP for 1 hr at 30˚C. Reaction mixture was solubilised with 1% triton and incubated with NiNTA beads under denaturing conditions for His-ubiquitin affinity purification. Proteins bound to the be were eluted from the beads using SDS buffer supplemented with imidazole and analysed by SDS-PAGE followed by fluorescence scanning for TM68-

MBP. Immunoblotting was performed to analyze Asi2 and Asi3 with anti- SBP and anti-Asi3 antibodies, respectively. Kim Wendrich performed experiments in panels (B-D).

5.8 Role of ubiquitin-conjugating enzymes

With the help of the developed *in vitro* functional system, I wanted to explore various aspects of Asi mediated ERAD pathway. Now, I focused on the roles of the E2 ubiquitin-conjugating enzymes that work along with the Asi complex for the degradation of substrates. Previous *in vivo* studies showed that degradation of Asi-dependent substrates required the ubiquitin-conjugating enzymes Ubc4 and Ubc7 (Foresti et al., 2014). To explore if the E2 requirements would be similar *in vitro,* we used the developed system to examine their contributions for substrate ubiquitination. Thus, we performed ubiquitination reactions with supplementing either Ubc4 or Ubc7 individually. When the ubiquitination reaction was performed with Ubc4 alone, we observed a slight increase in monoubiquitinated conjugates on TM68-MBP and reduced polyubiquitinated species in comparison to the reaction containing both Ubc4 and Ubc7. Interestingly, when the ubiquitination reaction contains Ubc7 alone, ubiquitination modification on TM68-MBP was absent. These results suggest that Ubc4 was required for the initiation of ubiquitination on substrates of Asi complex and that Ubc7 extends the initial ubiquitin chains to make polyubiquitinated TM68-MBP. Asi3 was also ubiquitinated *in vitro*, a modification mostly dependent on Ubc4 (Figure- 5.8).

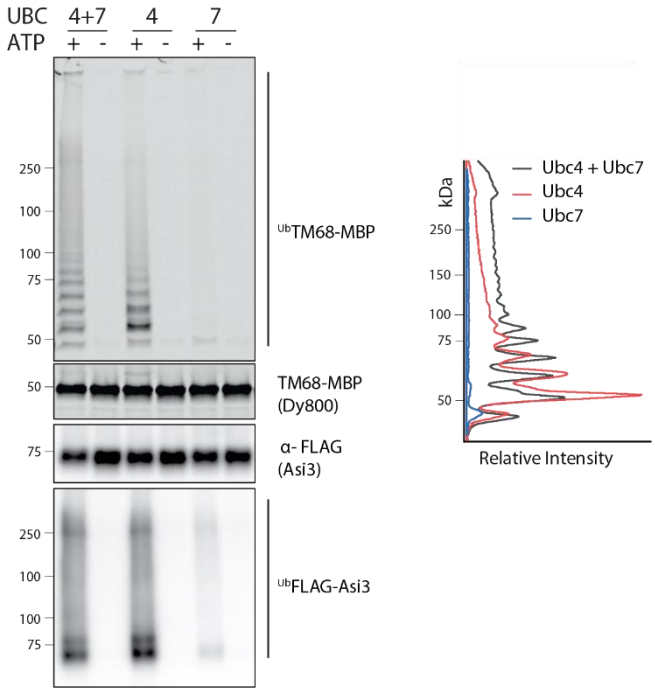


Figure 5.8 – Ubc4 initiates ubiquitin chains on the substrates

Proteoliposomes with TM68-MBP and Asi complex were incubated with Uba1 (ubiquitin-activating enzyme) and the indicated ubiquitin-conjugating enzymes (Ubc4 or Ubc7 or both). Ubiquitination was initiated by the addition of ATP and incubated for 1 hr at 30˚C. Reaction mixture was solubilised with 1% triton and incubated with NiNTA beads under denaturing conditions for His-ubiquitin affinity purification. Bound proteins were eluted from the beads using SDS buffer supplemented with imidazole and analysed by SDS-PAGE followed by fluorescence scanning for TM68-MBP. Immunoblotting was performed to analyze Asi2 and Asi3 with anti- SBP and anti-FLAG antibodies, respectively. Kim Wendrich performed this experiment.

5.9 Asi2 recognizes transmembrane segment on substrates

Using *in vivo* cross-linking experiments the Asi complex interacts directly with substrates through their membrane region. Here, we took advantage of our *in*

vitro system to investigate whether membrane interaction was required for recognition and ubiquitination of the substrates *in vitro*.

To this end, TM68-MBP and Asi complex were reconstituted together in the same liposome or individually in different liposomes (Figure- 5.9A). Ubiquitination reactions were performed in liposomes containing both TM68-MBP and Asi complex (P1) and by mixing liposomes containing exclusively TM68-MBP or the Asi complex (P2+P3). We observed that TM68-MBP could be ubiquitinated only when Asi complex and TM68-MBP were present on the same proteoliposomes (Figure- 5.9B). These data indicate that a direct interaction between the Asi complex subunits and TM68-MBP is required prior ubiquitination.

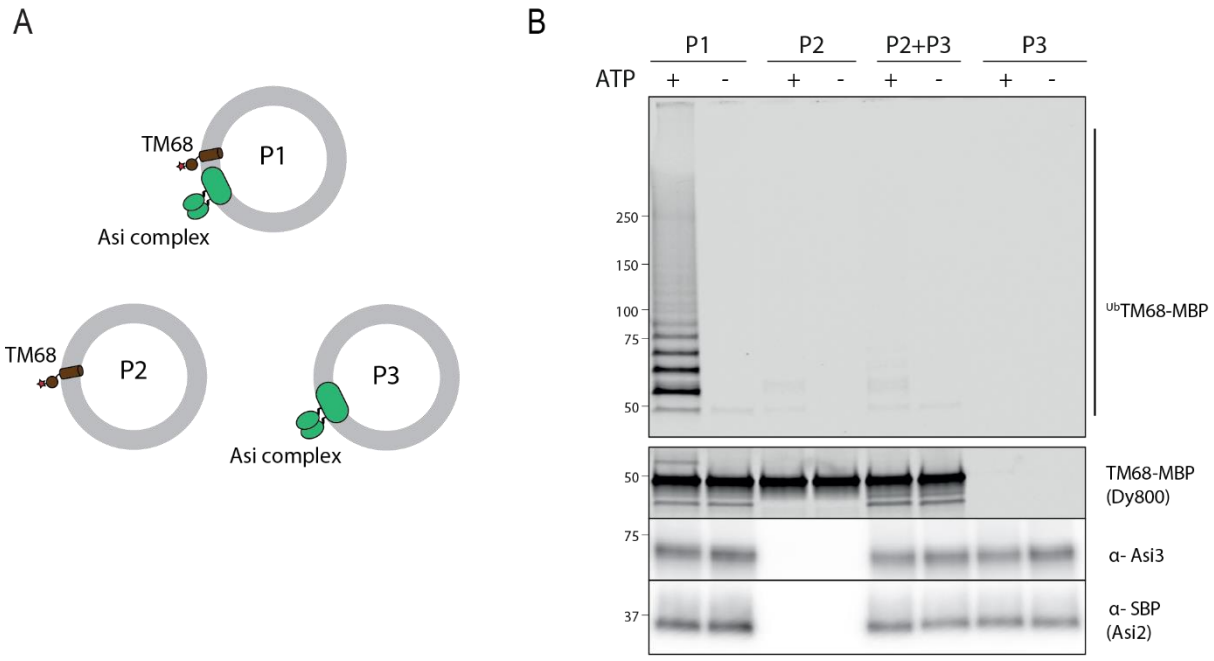


Figure 5.9 – Asi complex recognizes transmembrane domains of the substrate

(A) Schematic representation of the different proteoliposomes used in (B). P1- consists of both Asi complex and TM68-MBP. P2 consists of just the substrate TM68-MBP and P3 just the Asi complex.

(B) Different proteoliposomes as indicated were incubated with soluble ubiquitination machinery (Uba1, Ubc4, Ubc7, Cue1, His-ubiquitin) and ATP for 1 hr at 30˚C. Reactions were split into two, a part of it analysed directly SDS-PAGE and fluorescence scanning for TM68-MBP (bottom panel). The second part was further solubilised with 1% triton and incubated with NiNTA beads under denaturing conditions for His-ubiquitin affinity purification. Bound proteins were eluted from the beads using SDS buffer supplemented with imidazole and analysed by SDS-PAGE followed by fluorescence scanning

To identify the Asi complex subunit(s) that directly bind substrate, we used an *in vitro* cysteine cross-linking strategy. The substrate TM68-MBP did not contain any cysteine residue in the entire fusion protein. To this end, we purified a mutant version of the substrate- TM68(I36C)-MBP, in which a single cysteine substitution was made within the TMD of TM68. The construct was recombinantly expressed and purified from *E. coli* and subsequently reconstituted into liposomes together with Asi complex. To ensure proper insertion of the mutant substrate into the liposome and interaction with Asi complex, we performed a control ubiquitination assay. We observed that the mutant TM68(I36C)-MBP was ubiquitinated similarly to the WT TM68-MBP (Figure- 5.10A).

Proteoliposomes containing the Asi complex and TM68(I36C)-MBP were treated (or incubated) with the bifunctional crosslinker bismaleimidobutane (BMB). BMB forms irreversible covalent crosslinks between sulfhydryl groups in proteins. As a control, proteoliposomes with only TM68(I36C)-MBP or without Asi complex were included in the crosslinking assay. Upon SDS-PAGE and immunoblotting for TM68 with anti-MBP antibody, we observed that the TM68(I36C)-MBP forms a dimer. Additionally, we also observed a band around 75kDa, only when the proteoliposomes contains Asi complex. Based on the theoretical molecular weight of the subunits of Asi complex, a 75kDa species could correspond to a crosslink between SBP-Asi2 (37kDa) and the TM68(I36C)-MBP. Also, Asi2 contains only one cysteine residue at the 264^{th} position in the TMD when compared to 19 in Asi1 and 15 in Asi3 supporting that Asi2 could be crosslinked to the substrates. To unambiguously determine the identity of the crosslinked product, we immunoblotted the same crosslinked samples with an anti-Asi2 antibody. Strikingly, we observed a strong band present at around 75kDa, confirming the crosslink between Asi2 and TM68(I36C)-MBP (Figure- 5.10B).

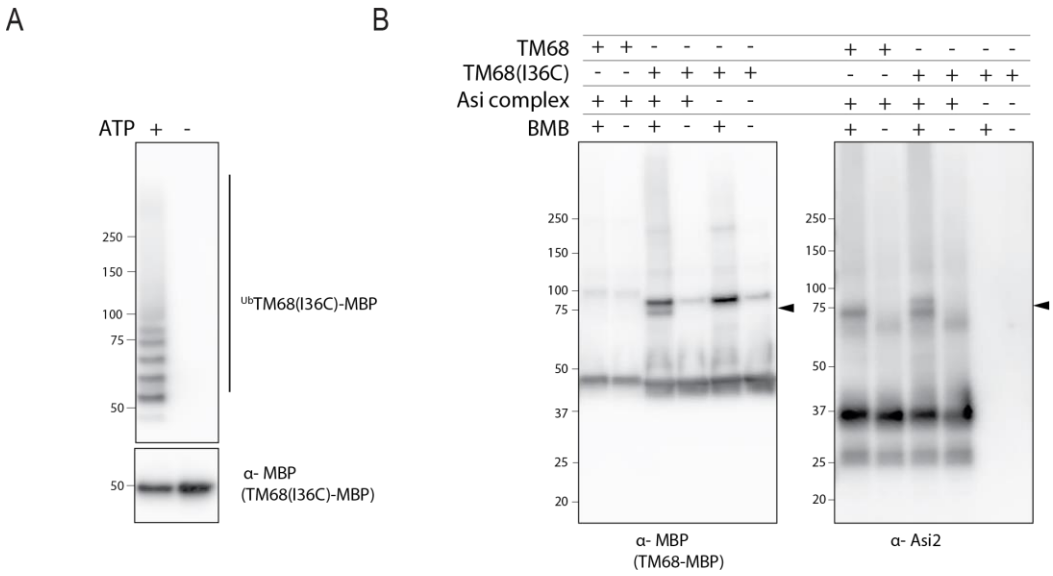


Figure 5.10 – Asi complex recognizes transmembrane domains of the substrate

(A) Mutant version of the substrate TM68(I36C)-MBP was reconstituted along with Asi complex into proteoliposomes and incubated with soluble ubiquitination machinery (Uba1, Ubc4, Ubc7, Cue1, His-ubiquitin) and ATP for 1 hr at 30˚C. It was further solubilised with 1% triton and incubated with NiNTA beads under denaturing conditions for His-ubiquitin affinity purification. Bound proteins were eluted from the beads using SDS buffer supplemented with imidazole and analysed by SDS-PAGE followed by immunoblotting with anti-MBP antibody.

(B) Proteoliposomes reconstituted with either TM68-MBP or mutant version TM68(I36C)-MBP were incubated with the bifunctional cysteine-reactive crosslinker BMB for 1 hr at RT. It was analysed by SDS-PAGE followed by immunoblotting for TM68-MBP and Asi2 with anti-MBP and anti-Asi2 antibodies, respectively. Arrowheads indicate crosslinked product of TM68-MBP and Asi2.

These data suggested that C-terminal TMD of Asi2 is in proximity to the substrate. To explore if this Asi2 TMD was important for substrate recognition and degradation, we generated a mutant Asi2Δ4, in which the TMD was shortened by four amino acids, including the cysteine residue (Figure- 5.11A). Asi2D4 allele was generated directly at ASI2 locus and gave rise to almost normal protein levels. To examine if Asi2Δ4 still interacted with Asi1 and Asi3 to form the Asi complex *in vivo*, we performed immunoprecipitation with antibodies against endogenous Asi1 and Asi2. We observed that Asi2Δ4 still assembled into a complex with Asi1 and Asi3 (Figure- 5.11B). Thus, the mutations on Asi2 do not dramatically affect the protein structure.

Next, we asked if Asi2Δ4 would affect substrate degradation. We used the Erg11-FL as a substrate *in vivo* and performed a CHX shut-off experiment under endogenous and overexpression levels of Asi2Δ4. In *WT* cells, Erg11-FL had a half-life of about 60 min and its degradation rate was decreased in Asi2Δ4 under both endogenous as well as overexpression conditions (Figure- 5.11C). To the addition of Asi2Δ4, we also generated single point mutations of the cysteine residue by replacing it with leucine and tryptophan on a plasmid. These mutants did not affect the degradation of the substrate (data not shown).

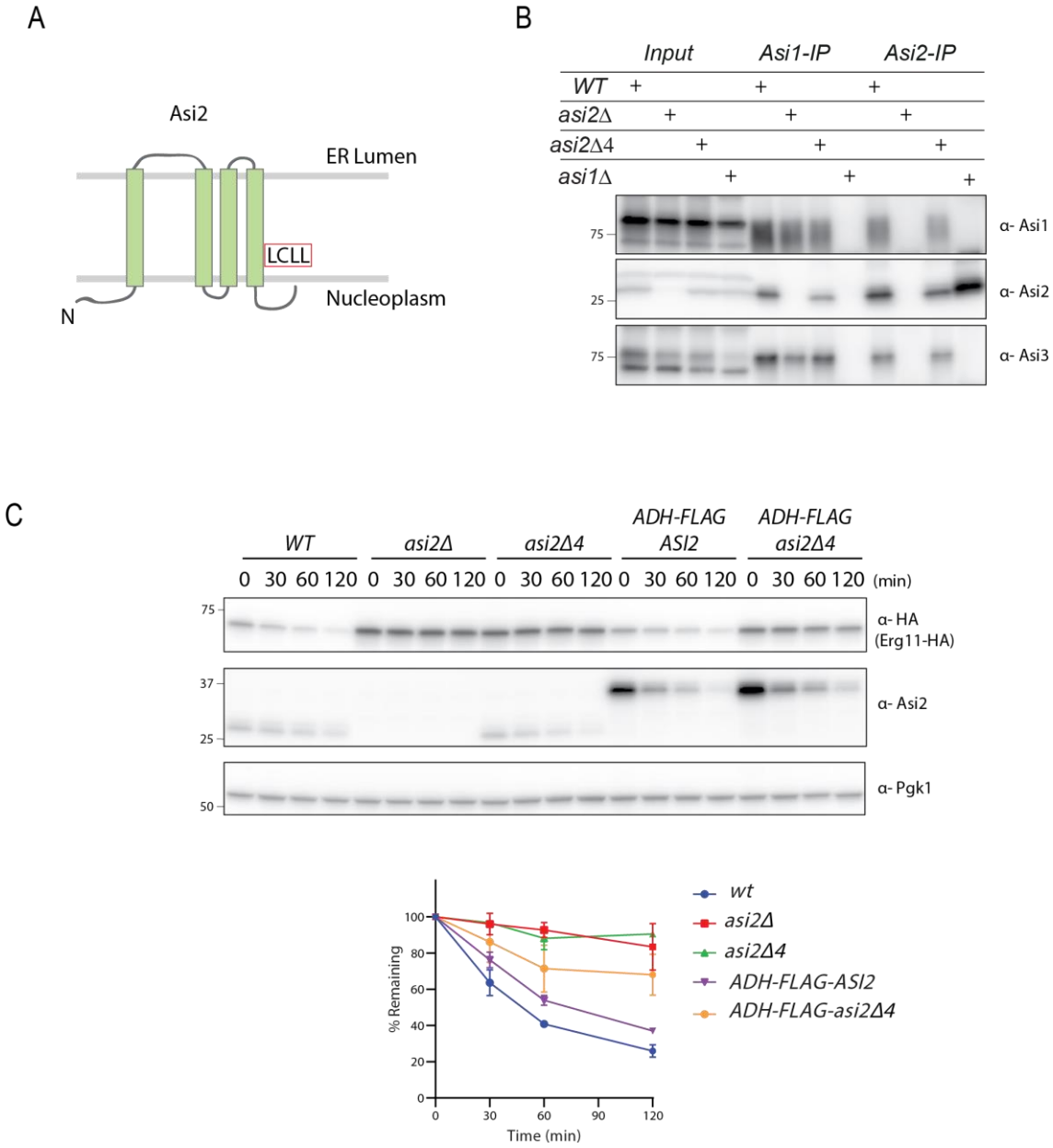


Figure 5.11 – Asi2 recognizes transmembrane domains of the substrate

(A) Schematic representation of Asi2 indicating the cysteine residue on the C-terminal TMD.

(B) Immunoprecipitation with anti- Asi1 and anti-Asi2 antibodies. Membrane fractions were prepared from cells with the indicated genotypes. Membrane pellets were solubilised with 1% DMNG and incubated with respective antibodies conjugated protein-A magnetic beads overnight. Bound proteins were eluted from the beads using SDS buffer

and analysed by SDS-PAGE followed by immunoblot for Asi1, Asi2 and Asi3 with anti-Asi1, anti-Asi2 and anti-Asi3 antibodies, respectively.

(C) Degradation of Erg11-FL was analysed in the specified genotypes. Turnover rates were monitored upon addition of cycloheximide (CHX) to exponentially growing cells. Cell lysates were prepared and analysed for Erg11 and Asi2 with anti-HA and anti-Asi2 antibodies, respectively. Pgk1 detected with anti- Pgk1 antibody and was used as a loading control.

Altogether, these results indicate that membrane interactions between Asi2 and substrates are crucial for recognition and degradation of substrates. Altogether, these data indicate the potential role for Asi2 as a receptor for recognizing the TMD on the substrates within the Asi complex.

5.10 Discussion

In this chapter, we present an *in vitro* biochemical approach to dissect mechanistic details on the functions of the Asi complex in INM quality control. To systematically express and purify active subunits of Asi E3 ligase complex, we screened several detergents, different tags, optimized the expression and purification conditions. We successfully expressed and purified a functional Asi complex. As per the superpose 6 gel filtration data, Asi complex seemed to be about 600kDa. Future experiments should be directed towards optimization of the purification protocol to obtain better yield and perform structural characterization of the complex.

Our *in vitro* reconstitution and ubiquitination system demonstrates that the Asi complex formed a minimal system sufficient to recognize and ubiquitinate the substrates. Furthermore, we recapitulated the TMD recognition of the substrate by the Asi complex before ubiquitination. We also showed that among the Asi complex subunits, Asi2 recognizes and binds directly to the TMD of the substrates. Using Asi2Δ4 allele we showed that the C-terminal TMD of Asi2 is necessary for efficient degradation of substrates. In order to test if there are any adverse implication of Asi2Δ4 on the other Asi complex substrates, it would be important to check if there is any change in dependency of Asi2 independent substrates. In the future, Asi2 independent substrates should also be tested to confirm that their degradation dependency remains the same in Asi2Δ4

mutation. While we focused on single TMD substrates, it would be interesting to analyse if the TMDs of the multipass membrane substrates are also recognized similarly. Future studies by analysing a large number of membrane and soluble substrates should be able to identify structural features on substrates that are recognized by Asi2.

Interestingly, some of the substrates do not require Asi2 for degradation (Foresti et al., 2014). Whether Asi1/Asi3 or any other unknown factor is involved in recognition of these Asi2-independent substrates needs further investigation.

Previously, it was shown that Ubc4 and Ubc7 E2 conjugating enzymes are involved in the degradation of Asi complex substrates. Here, using the *in vitro* system, we showed that Ubc4 is required to initiate ubiquitin chains that are further extended by Ubc7. Strikingly, Ubc7 is unable to add the initial ubiquitins on the substrate. These results are in accordance with the published data where they observed a similar role of Ubc7 for Doa10 substrates (Weber et al., 2016). In this case, Ubc6 initiated the ubiquitin chain formation that was extended by Ubc7. Studies in our lab were also able to recapitulate Cdc48-dependent extraction of ubiquitinated species in the *in vitro* system. Previously, it was shown that Hrd1 ubiquitin ligase facilitates the retrotranslocation and membrane extraction of its substrates (Baldridge and Rapoport, 2016; Carvalho et al., 2010) but whether Asi complex would also form a retrotranslocation channel for the

substrates to be extracted from the lipid bilayer should be the focus of future studies using the *in vitro* system.

Another intriguing feature of the Asi complex is the presence of two non-redundant RING domain-containing proteins Asi1 and Asi3. While the other membrane-bound ligases Hrd1 and Doa10 complexes can function with a single RING domain ligase, it would be interesting to understand the reason for the requirement of two RING domain-containing subunits in the Asi complex. The developed functional *in vitro* assay could be helpful in the future to elucidate if each RING domain generates a distinct mode of ubiquitination or whether they have a preference to generate specific types of linkages and how they interact with the E2s.

Chapter 6

Conclusions and Future Directions

6 Conclusions and future directions

6.1 Characterization of the Asi complex

The Asi complex with its subunits Asi1, Asi2 and Asi3, was initially shown to be a negative regulator of the Ssy1-Ptr3-Ssy5 (SPS) amino acid sensing pathway (Forsberg et al., 2001; Ljungdahl and Daignan-Fornier, 2012). Later it was shown to play an essential role in the protein quality control at the INM by degrading mislocalized and misfolded proteins thereby important for INM and ER homeostasis (Foresti et al., 2014; Khmelinskii et al., 2014)

In this study, I aimed to biochemically characterize the Asi complex and dissect the molecular mechanism of substrate recognition by the Asi complex at the INM. I showed that the Asi complex subunits Asi2 and Asi3 have short half-lives, consistent with published observations (Boban et al., 2014; Pantazopoulou et al., 2016). We further demonstrate that Asi1 plays essential roles in maintaining the integrity of the complex – in the absence of Asi1, Asi2 cannot interact with Asi3 and Asi3 gets degraded very quickly. By performing sucrose gradient centrifugation, I also found that the Asi complex forms a high molecular weight complex. We speculate that Asi complex components form oligomers. In the future, structural characterization of the Asi complex would be important to determine the stoichiometry of the complex and to understand how Asi1 regulates the stability of Asi3 and bridges the interaction between Asi2 and Asi3.

6.2 Role of Asi complex in the quality control of unassembled subunits of ER membrane complexes

To characterize the molecular mechanism of Asi mediated ERAD, we used genetic, biochemical and *in vitro* reconstitution approaches. We observed an unexpected connection between the quality control of protein complex assembly in the ER and INM homeostasis.

By studying the well-characterized OST complex, we show that Wbp1 in the absence of its partners Ost2 or Swp1 undergoes degradation by the Asi complex. Our data is consistent with prior research on OST complex assembly in yeast (Mueller et al., 2015). The study showed that under overexpression conditions, there was a minor contribution of Hrd1 and Doa10 ERAD branches in the degradation of unassembled subunits (Mueller et al., 2015).

Many studies have reported the degradation of unassembled subunits via ERAD. For example, in mammalian cells TCR-α chain is degraded in the absence of its binding partner TCR-β chain (Bonifacino et al., 1989). Sbh2 the translocon subunit in yeast when not bound by its binding partner is degraded in a Doa10-dependent manner (Habeck et al., 2015). Also, Vph1 a subunit of the V-ATPase complex was shown to be degraded by an unknown pathway in the absence of its binding partner Vma22 (Hill and Cooper, 2000). We now show that Vph1 is recognized by the Asi complex for degradation at the INM.

Based on experimental results, we propose the following step-by-step model for quality control of protein complex assembly by the Asi complex at the INM.

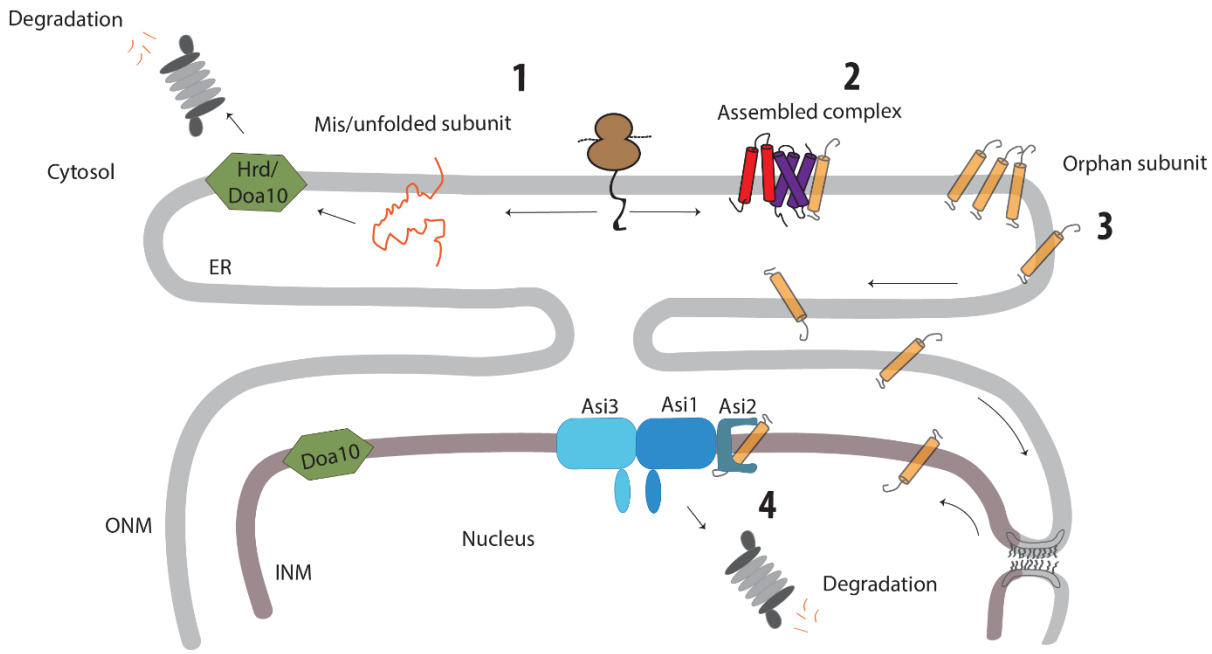


Figure 6.1- Proposed model for the Asi-mediated protein degradation at the INM

As the newly synthesized polypeptide enters the ER, it is folded to attain its native conformation and assemble into complexes. When a protein subunit misfolds, it is being targeted by the Hrd/Doa10 complex for degradation (1). There is a possibility that subunits fold but do not immediately assemble into complexes and diffuse through the ER (2). When compared to unassembled protein subunits, assembled complexes have a higher number of TMDs that impede their passage into the INM (Ungricht and Kutay, 2015). Subunits in over-stoichiometric amounts or those that remain unassembled, continuously diffuse through the ER and ultimately reach the INM (3). At the INM, Asi2 recognizes the TMD of the

mislocalized subunit and promotes its degradation through Asi1/3 (4). Thus, we hypothesize that restricting the degradation of unassembled subunits to the INM favors complex assembly in the bulk ER membranes. Supporting the biochemical data, genetic suppression of temperature-sensitive alleles in Asi complex mutants strongly argues for an important role of this ERAD branch in the degradation of unassembled/orphan subunits at the INM.

The model proposed is also comparable with recent proteomics studies on age-dependent protein degradation. Many subunits of protein complexes display biphasic degradation kinetics, where they are short-lived immediately after synthesis, prior assembly. Eventually, they become more stable as they mature and after successful assembly with their partners (McShane et al., 2016).

It will be interesting to examine whether similar spatial segregation between complex assembly and quality control also occurs in mammalian cells. In these cells, degradation of proteins directly from the INM by an ERAD-like process was described for a mutant version of the lamin-B receptor (Tsai et al., 2016), but the components involved in the degradation have not been identified. Furthermore, as mammalian cells undergo open mitosis during which the NE in metazoan cells breaks down, NPCs and lamins disassemble and transmembrane proteins distribute into the ER. After chromosome segregation, the NE envelope re-forms around the chromosomes in the daughter cells and the INM proteome has to re-establish (Wandke and Kutay, 2013). Under these conditions, quality control

mechanisms at the INM might play an important role in maintaining the proteome identity of INM, a topic that merits further investigation in the future.

The delivery of unassembled subunits to the Asi complex at the INM could imply that there is more burden on the nuclear proteasomes for degradation and might affect other nuclear activities that require the proteasome. We think that this is not the case, as in exponentially growing yeast cells majority (≈80%) of proteasomes are localized in the nucleus (Russell et al., 1999). As per my knowledge, there is no data suggesting that an increase in responsibility of ERAD substrates for nuclear proteasomes affects its other nuclear activities.

6.3 Role of Asi2 in recognition of orphan substrates

With the help of various substrates, I was able to show that Asi complex recognizes the TMD on the substrate to be degraded. Using *in vivo* and *in vitro* cross-linking strategies, I demonstrate that among the Asi complex subunits, Asi2 directly binds and recognizes the TMDs of the orphan/unassembled substrate at the INM. Although all substrates analysed in this study comprise a single TMD, Asi2 is also required for the degradation of some multispanning membrane proteins (Foresti et al., 2014; Khmelinskii et al., 2014). Future structural studies are required to gain a mechanistic understanding of the substrate recognition process. It also requires a more detailed analysis of a large number of substrates to identify any unique structural features that is recognized by Asi2 on the orphan

substrates. Moreover, among the Asi substrates recognized so far, no INM resident proteins were identified. This suggests that additional regulatory mechanisms exist that spare these proteins from Asi-dependent degradation (Foresti et al., 2014; Khmelinskii et al., 2014; Smoyer et al., 2019). How this is achieved remains to be addressed. Intriguingly, degradation of some Asi substrates does not require Asi2 (Foresti et al., 2014; Khmelinskii et al., 2014). Further experiments are required to understand whether these Asi2-independent substrates are directly recognized by Asi1 and Asi3 or involve any other additional unknown factors. Asi complex is also indicated to degrade soluble transcription factors Stp1 (Omnus and Ljungdahl, 2014). Hence, it would be intriguing to study the mechanism of recognition and processing of soluble proteins.

6.4 Role of E2 conjugating enzymes Ubc4 and Ubc7

Our *in vitro* reconstitution approach revealed that Ubc4 and Ubc7 conjugating enzymes are necessary for distinct, non-redundant functions in substrate ubiquitination. Ubc4 is required to initiate the process of ubiquitination on the substrate, which is then extended into polyubiquitin chains by Ubc7. Importantly, Ubc7 was unable to initiate substrate ubiquitination. A similar process of priming followed by Ubc7-dependent extension of the ubiquitin chain was also observed for the substrates of Doa10 complex. However, in this case, the initial priming

step was carried on by the conjugating enzyme Ubc6. Ubc6-priming was required for ubiquitination of lysine-less substrates, as Ubc6 facilitates ubiquitin conjugation to lysine as well as hydroxylated residues (Weber et al., 2016). Interestingly, Ubc7 is also required for Hrd1 substrates and in this case, Ubc7 alone is sufficient to perform ubiquitination of ER luminal and membrane substrates (Bazirgan et al., 2006; Hirsch et al., 2009). Strikingly, RING domains of Doa10 and Hrd1 differentially stimulate the ubiquitin chain elongation by Ubc7 and propose that RING domain of Hrd1 stabilises the closed conformation of Ubc7-ubiquitin conjugate better that Doa10 RING domain (Cohen et al., 2015). It will be interesting to investigate further as to how Asi1/3 RING domains interact with Ubc7 or if each RING domains interact with a specific E2 conjugating enzyme needs further investigation.

It would be also essential to elucidate if the sequential action of Ubc4 and Ubc7 generate distinct modes of ubiquitination such as multi-monoubiquitination or poly-ubiquitination and whether they have a preference to generate a specific type of linkages. Thus, the established *in vitro* functional assay has the potential to illuminate critical aspects of this pathway of INM quality control.

Further studies in the lab were also able to recapitulate Cdc48-dependent extraction of ubiquitinated species in the *in vitro* system. Previously, it was shown that Hrd1 ubiquitin ligase facilitates the retrotranslocation and membrane extraction of its substrates (Baldridge and Rapoport, 2016; Carvalho et al., 2010)

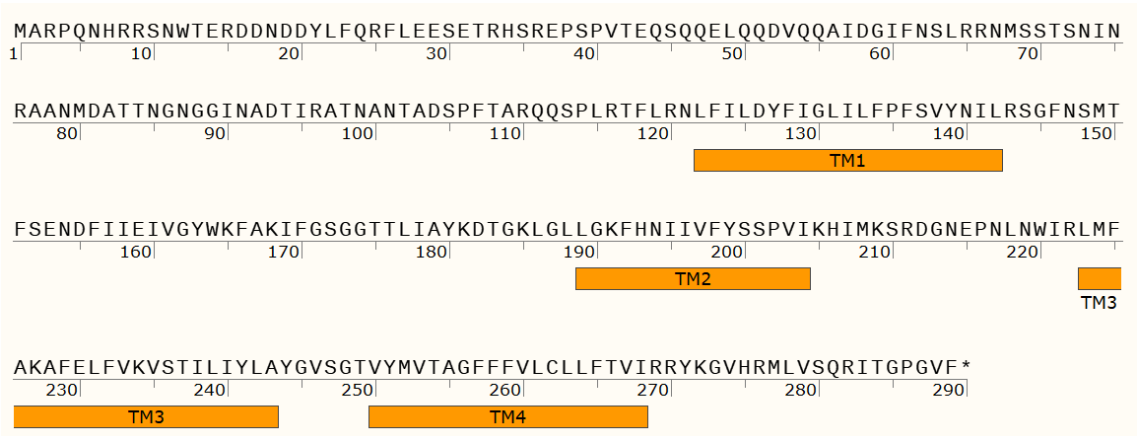
but whether Asi complex would work in a similar fashion should also be the focus of future studies.

Appendix

Protein sequence of Asi1 and transmembrane (TM) domains represented by orange bars.



Protein sequence of Asi2 and transmembrane (TM) domains represented by orange bars.



Protein sequence of Asi3 and transmembrane (TM) domains represented by orange bars.



References

Antonin, W., Ungricht, R., and Kutay, U. (2011). Traversing the NPC along the pore membrane: targeting of membrane proteins to the INM. Nucleus *2*, 87–91.

Baldridge, R.D., and Rapoport, T.A. (2016). Autoubiquitination of the hrd1 ligase triggers protein retrotranslocation in ERAD. Cell *166*, 394–407.

Bays, N.W., Gardner, R.G., Seelig, L.P., Joazeiro, C.A., and Hampton, R.Y. (2001). Hrd1p/Der3p is a membrane-anchored ubiquitin ligase required for ER-associated degradation. Nat. Cell Biol. *3*, 24–29.

Bazirgan, O.A., Garza, R.M., and Hampton, R.Y. (2006). Determinants of RING-E2 fidelity for Hrd1p, a membrane-anchored ubiquitin ligase. J. Biol. Chem. *281*, 38989–39001.

Beilharz, T., Egan, B., Silver, P.A., Hofmann, K., and Lithgow, T. (2003). Bipartite signals mediate subcellular targeting of tail-anchored membrane proteins in Saccharomyces cerevisiae. J. Biol. Chem. *278*, 8219–8223.

Benyair, R., Ron, E., and Lederkremer, G.Z. (2011). Protein quality control, retention, and degradation at the endoplasmic reticulum. Int. Rev. Cell Mol. Biol. *292*, 197–280.

Benyair, R., Ogen-Shtern, N., and Lederkremer, G.Z. (2015). Glycan regulation of ER-associated degradation through compartmentalization. Semin. Cell Dev. Biol. *41*, 99–109.

Berndsen, C.E., and Wolberger, C. (2014). New insights into ubiquitin E3 ligase mechanism. Nat. Struct. Mol. Biol. *21*, 301–307.

Biederer, T., Volkwein, C., and Sommer, T. (1997). Role of Cue1p in ubiquitination and degradation at the ER surface. Science *278*, 1806–1809.

Boban, M., Zargari, A., Andréasson, C., Heessen, S., Thyberg, J., and Ljungdahl, P.O. (2006). Asi1 is an inner nuclear membrane protein that restricts promoter access of two latent transcription factors. J. Cell Biol. *173*, 695–707.

Boban, M., Pantazopoulou, M., Schick, A., Ljungdahl, P.O., and Foisner, R. (2014). A nuclear ubiquitin-proteasome pathway targets the inner nuclear membrane protein Asi2 for degradation. J. Cell Sci. *127*, 3603–3613.

Bodnar, N., and Rapoport, T. (2017a). Toward an understanding of the Cdc48/p97 ATPase. [version 1; peer review: 4 approved]. F1000Res. *6*, 1318.

Bodnar, N.O., and Rapoport, T.A. (2017b). Molecular mechanism of substrate processing by the cdc48 atpase complex. Cell *169*, 722–735.e9.

Boettcher, B., and Barral, Y. (2013). The cell biology of open and closed mitosis. Nucleus *4*, 160–165.

Boni, A., Politi, A.Z., Strnad, P., Xiang, W., Hossain, M.J., and Ellenberg, J. (2015). Live imaging and modeling of inner nuclear membrane targeting reveals its molecular requirements in mammalian cells. J. Cell Biol. *209*, 705–720.

Bonifacino, J.S., and Lippincott-Schwartz, J. (1991). Degradation of proteins within the endoplasmic reticulum. Curr. Opin. Cell Biol. *3*, 592–600.

Bonifacino, J.S., Suzuki, C.K., Lippincott-Schwartz, J., Weissman, A.M., and Klausner, R.D. (1989). Pre-Golgi degradation of newly synthesized T-cell antigen receptor chains: intrinsic sensitivity and the role of subunit assembly. J. Cell Biol. *109*, 73–83.

Bonifacino, J.S., Cosson, P., Shah, N., and Klausner, R.D. (1991). Role of potentially charged transmembrane residues in targeting proteins for retention and degradation within the endoplasmic reticulum. EMBO J. *10*, 2783–2793.

Bordallo, J., Plemper, R.K., Finger, A., and Wolf, D.H. (1998). Der3p/Hrd1p Is Required for Endoplasmic Reticulum-associated Degradation of Misfolded Lumenal and Integral Membrane Proteins. Mol. Biol. Cell *9*, 209–222.

Braakman, I., and Bulleid, N.J. (2011). Protein folding and modification in the mammalian endoplasmic reticulum. Annu. Rev. Biochem. *80*, 71–99.

Braakman, I., and Hebert, D.N. (2013). Protein folding in the endoplasmic reticulum. Cold Spring Harb. Perspect. Biol. *5*, a013201.

Brown, M.S., and Goldstein, J.L. (2009). Cholesterol feedback: from Schoenheimer's bottle to Scap's MELADL. J. Lipid Res. *50 Suppl*, S15–27.

Buchwalter, A., Kaneshiro, J.M., and Hetzer, M.W. (2019). Coaching from the sidelines: the nuclear periphery in genome regulation. Nat. Rev. Genet. *20*, 39–50.

Budhidarmo, R., Nakatani, Y., and Day, C.L. (2012). RINGs hold the key to ubiquitin transfer. Trends Biochem. Sci. *37*, 58–65.

Bupp, J.M., Martin, A.E., Stensrud, E.S., and Jaspersen, S.L. (2007). Telomere anchoring at the nuclear periphery requires the budding yeast Sad1-UNC-84 domain protein Mps3. J. Cell Biol. *179*, 845–854.

Burke, B., and Stewart, C.L. (2014). Functional architecture of the cell's nucleus in development, aging, and disease. Curr Top Dev Biol *109*, 1–52.

Callis, J. (2014). The ubiquitination machinery of the ubiquitin system. Arabidopsis Book *12*, e0174.

Carvalho, P., Goder, V., and Rapoport, T.A. (2006). Distinct ubiquitin-ligase complexes define convergent pathways for the degradation of ER proteins. Cell *126*, 361–373.

Carvalho, P., Stanley, A.M., and Rapoport, T.A. (2010). Retrotranslocation of a misfolded luminal ER protein by the ubiquitin-ligase Hrd1p. Cell *143*, 579–591.

Chen, Z., and Pickart, C.M. (1990). A 25-kilodalton ubiquitin carrier protein (E2) catalyzes multi-ubiquitin chain synthesis via lysine 48 of ubiquitin. J. Biol. Chem. *265*, 21835–21842.

Chen, C.-Y., Chi, Y.-H., Mutalif, R.A., Starost, M.F., Myers, T.G., Anderson, S.A., Stewart, C.L., and Jeang, K.-T. (2012). Accumulation of the inner nuclear envelope protein Sun1 is pathogenic in progeric and dystrophic laminopathies. Cell *149*, 565–577.

Chen, J., Gardner, J.M., Yu, Z., Smith, S.E., McKinney, S., Slaughter, B.D., Unruh, J.R., and Jaspersen, S.L. (2019). Yeast centrosome components form a noncanonical LINC complex at the nuclear envelope insertion site. J. Cell Biol. *218*, 1478–1490.

Chen, P., Johnson, P., Sommer, T., Jentsch, S., and Hochstrasser, M. (1993a). Multiple ubiquitin-conjugating enzymes participate in the in vivo degradation of the yeast MAT alpha 2 repressor. Cell *74*, 357–369.

Chen, P., Johnson, P., Sommer, T., Jentsch, S., and Hochstrasser, M. (1993b). Multiple ubiquitin-conjugating enzymes participate in the in vivo degradation of the yeast MATα2 repressor. Cell *74*, 357–369.

Chen, Y., Zhang, Y., Yin, Y., Gao, G., Li, S., Jiang, Y., Gu, X., and Luo, J. (2005). SPD--a web-based secreted protein database. Nucleic Acids Res. *33*, D169–73.

Chin, J.W., Cropp, T.A., Anderson, J.C., Mukherji, M., Zhang, Z., and Schultz, P.G. (2003). An expanded eukaryotic genetic code. Science *301*, 964–967.

Christianson, J.C., and Ye, Y. (2014). Cleaning up in the endoplasmic reticulum: ubiquitin in charge. Nat. Struct. Mol. Biol. *21*, 325–335.

Clerc, S., Hirsch, C., Oggier, D.M., Deprez, P., Jakob, C., Sommer, T., and Aebi, M. (2009). Htm1 protein generates the N-glycan signal for glycoprotein degradation in the endoplasmic reticulum. J. Cell Biol. *184*, 159–172.

Cohen, I., Wiener, R., Reiss, Y., and Ravid, T. (2015). Distinct activation of an E2 ubiquitin-conjugating enzyme by its cognate E3 ligases. Proc. Natl. Acad. Sci. USA *112*, E625–32.

Cohen, M., Lee, K.K., Wilson, K.L., and Gruenbaum, Y. (2001). Transcriptional repression, apoptosis, human disease and the functional evolution of the nuclear lamina. Trends Biochem. Sci. *26*, 41–47.

Conrad, M.N., Lee, C.-Y., Chao, G., Shinohara, M., Kosaka, H., Shinohara, A., Conchello, J.A., and Dresser, M.E. (2008). Rapid telomere movement in meiotic prophase is promoted by NDJ1, MPS3, and CSM4 and is modulated by recombination. Cell *133*, 1175–1187.

de Godoy, L.M.F., Olsen, J.V., Cox, J., Nielsen, M.L., Hubner, N.C., Fröhlich, F., Walther, T.C., and Mann, M. (2008). Comprehensive mass-spectrometry-based proteome quantification of haploid versus diploid yeast. Nature *455*, 1251–1254.

Debose-Boyd, R.A. (2007). A helping hand for cytochrome p450 enzymes. Cell Metab. *5*, 81–83.

Deng, M., and Hochstrasser, M. (2006). Spatially regulated ubiquitin ligation by an ER/nuclear membrane ligase. Nature *443*, 827–831.

Dikic, I., Wakatsuki, S., and Walters, K.J. (2009). Ubiquitin-binding domains - from structures to functions. Nat. Rev. Mol. Cell Biol. *10*, 659–671.

Dittmer, T.A., and Misteli, T. (2011). The lamin protein family. Genome Biol. *12*, 222.

Doblas, V.G., Amorim-Silva, V., Posé, D., Rosado, A., Esteban, A., Arró, M., Azevedo, H., Bombarely, A., Borsani, O., Valpuesta, V., et al. (2013). The SUD1 gene encodes a putative E3 ubiquitin ligase and is a positive regulator of 3-hydroxy-3-methylglutaryl coenzyme a reductase activity in Arabidopsis. Plant Cell *25*, 728–743.

Feige, M.J., and Hendershot, L.M. (2013). Quality control of integral membrane proteins by assembly-dependent membrane integration. Mol. Cell *51*, 297–309.

Foresti, O., Ruggiano, A., Hannibal-Bach, H.K., Ejsing, C.S., and Carvalho, P. (2013). Sterol homeostasis requires regulated degradation of squalene monooxygenase by the ubiquitin ligase Doa10/Teb4. Elife *2*, e00953.

Foresti, O., Rodriguez-Vaello, V., Funaya, C., and Carvalho, P. (2014). Quality control of inner nuclear membrane proteins by the Asi complex. Science *346*, 751–755.

Forsberg, H., Hammar, M., Andréasson, C., Molinér, A., and Ljungdahl, P.O. (2001). Suppressors of ssy1 and ptr3 null mutations define novel amino acid sensor-independent genes in Saccharomyces cerevisiae. Genetics *158*, 973–988.

Foster, L.J., de Hoog, C.L., Zhang, Y., Zhang, Y., Xie, X., Mootha, V.K., and Mann, M. (2006). A mammalian organelle map by protein correlation profiling. Cell *125*, 187–199.

Frey, S., and Görlich, D. (2014). A new set of highly efficient, tag-cleaving proteases for purifying recombinant proteins. J. Chromatogr. A *1337*, 95–105.

Gardner, B.M., Pincus, D., Gotthardt, K., Gallagher, C.M., and Walter, P. (2013). Endoplasmic reticulum stress sensing in the unfolded protein response. Cold Spring Harb. Perspect. Biol. *5*, a013169.

Gardner, R.G., Shearer, A.G., and Hampton, R.Y. (2001). In vivo action of the HRD ubiquitin ligase complex: mechanisms of endoplasmic reticulum quality control and sterol regulation. Mol. Cell. Biol. *21*, 4276–4291.

Gauss, R., Kanehara, K., Carvalho, P., Ng, D.T.W., and Aebi, M. (2011). A complex of Pdi1p and the mannosidase Htm1p initiates clearance of unfolded glycoproteins from the endoplasmic reticulum. Mol. Cell *42*, 782–793.

Gibson, D.G., Young, L., Chuang, R.-Y., Venter, J.C., Hutchison, C.A., and Smith, H.O. (2009). Enzymatic assembly of DNA molecules up to several hundred kilobases. Nat. Methods *6*, 343–345.

Goldstein, J.L., and Brown, M.S. (1990). Regulation of the mevalonate pathway. Nature *343*, 425–430.

Graham, L.A., Flannery, A.R., and Stevens, T.H. (2003). Structure and assembly of the yeast V-ATPase. J Bioenerg Biomembr *35*, 301–312.

Gruenbaum, Y., Margalit, A., Goldman, R.D., Shumaker, D.K., and Wilson, K.L. (2005). The nuclear lamina comes of age. Nat. Rev. Mol. Cell Biol. *6*, 21–31.

Habeck, G., Ebner, F.A., Shimada-Kreft, H., and Kreft, S.G. (2015). The yeast ERAD-C ubiquitin ligase Doa10 recognizes an intramembrane degron. J. Cell Biol. *209*, 621.

Hampton, R.Y., Gardner, R.G., and Rine, J. (1996). Role of 26S proteasome and HRD genes in the degradation of 3-hydroxy-3-methylglutaryl-CoA reductase, an integral endoplasmic reticulum membrane protein. Mol. Biol. Cell *7*, 2029–2044.

Haraguchi, T., Kojidani, T., Koujin, T., Shimi, T., Osakada, H., Mori, C., Yamamoto, A., and Hiraoka, Y. (2008). Live cell imaging and electron microscopy reveal dynamic processes of BAF-directed nuclear envelope assembly. J. Cell Sci. *121*, 2540–2554.

Hartl, F.U., and Hayer-Hartl, M. (2009). Converging concepts of protein folding in vitro and in vivo. Nat. Struct. Mol. Biol. *16*, 574–581.

Hassink, G., Kikkert, M., van Voorden, S., Lee, S.-J., Spaapen, R., van Laar, T., Coleman, C.S., Bartee, E., Früh, K., Chau, V., et al. (2005). TEB4 is a C4HC3 RING finger-containing ubiquitin ligase of the endoplasmic reticulum. Biochem. J. *388*, 647–655.

Hebert, D.N., Garman, S.C., and Molinari, M. (2005). The glycan code of the endoplasmic reticulum: asparagine-linked carbohydrates as protein maturation and quality-control tags. Trends Cell Biol. *15*, 364–370.

Te Heesen, S., Knauer, R., Lehle, L., and Aebi, M. (1993). Yeast Wbp1p and Swp1p form a protein complex essential for oligosaccharyl transferase activity. EMBO J. *12*, 279–284.

Hessa, T., Kim, H., Bihlmaier, K., Lundin, C., Boekel, J., Andersson, H., Nilsson, I., White, S.H., and von Heijne, G. (2005). Recognition of transmembrane helices by the endoplasmic reticulum translocon. Nature *433*, 377–381.

Hessa, T., Meindl-Beinker, N.M., Bernsel, A., Kim, H., Sato, Y., Lerch-Bader, M., Nilsson, I., White, S.H., and von Heijne, G. (2007). Molecular code for transmembrane-helix recognition by the Sec61 translocon. Nature *450*, 1026–1030.

Hetzer, M.W. (2010). The nuclear envelope. Cold Spring Harb. Perspect. Biol. *2*, a000539.

Hicke, L., Schubert, H.L., and Hill, C.P. (2005). Ubiquitin-binding domains. Nat. Rev. Mol. Cell Biol. *6*, 610–621.

Hill, K., and Cooper, A.A. (2000). Degradation of unassembled Vph1p reveals novel aspects of the yeast ER quality control system. EMBO J. *19*, 550–561.

Hiller, M.M., Finger, A., Schweiger, M., and Wolf, D.H. (1996). ER degradation of a misfolded luminal protein by the cytosolic ubiquitin-proteasome pathway. Science *273*, 1725–1728.

Hirsch, C., Gauss, R., Horn, S.C., Neuber, O., and Sommer, T. (2009). The ubiquitylation machinery of the endoplasmic reticulum. Nature *458*, 453–460.

Hughes, A.L., Powell, D.W., Bard, M., Eckstein, J., Barbuch, R., Link, A.J., and Espenshade, P.J. (2007). Dap1/PGRMC1 binds and regulates cytochrome P450 enzymes. Cell Metab. *5*, 143–149.

Huyer, G., Piluek, W.F., Fansler, Z., Kreft, S.G., Hochstrasser, M., Brodsky, J.L., and Michaelis, S. (2004). Distinct machinery is required in Saccharomyces cerevisiae for the endoplasmic reticulum-associated degradation of a multispanning membrane protein and a soluble luminal protein. J. Biol. Chem. *279*, 38369–38378.

Jan, C.H., Williams, C.C., and Weissman, J.S. (2014). Principles of ER cotranslational translocation revealed by proximity-specific ribosome profiling. Science *346*, 1257521.

Janke, C., Magiera, M.M., Rathfelder, N., Taxis, C., Reber, S., Maekawa, H., Moreno-Borchart, A., Doenges, G., Schwob, E., Schiebel, E., et al. (2004). A versatile toolbox for PCR-based tagging of yeast genes: new fluorescent proteins, more markers and promoter substitution cassettes. Yeast *21*, 947–962.

Jaspersen, S.L., Martin, A.E., Glazko, G., Giddings, T.H., Morgan, G., Mushegian, A., and Winey, M. (2006). The Sad1-UNC-84 homology domain in Mps3 interacts with Mps2 to connect the spindle pole body with the nuclear envelope. J. Cell Biol. *174*, 665–675.

Jensen, T.J., Loo, M.A., Pind, S., Williams, D.B., Goldberg, A.L., and Riordan, J.R. (1995). Multiple proteolytic systems, including the proteasome, contribute to CFTR processing. Cell *83*, 129–135.

Juszkiewicz, S., and Hegde, R.S. (2018). Quality control of orphaned proteins. Mol. Cell *71*, 443–457.

Katta, S.S., Smoyer, C.J., and Jaspersen, S.L. (2014). Destination: inner nuclear membrane. Trends Cell Biol. *24*, 221–229.

Kelleher, D.J., and Gilmore, R. (1994). The Saccharomyces cerevisiae oligosaccharyltransferase is a protein complex composed of Wbp1p, Swp1p, and four additional polypeptides. J. Biol. Chem. *269*, 12908–12917.

Khmelinskii, A., Blaszczak, E., Pantazopoulou, M., Fischer, B., Omnus, D.J., Le Dez, G., Brossard, A., Gunnarsson, A., Barry, J.D., Meurer, M., et al. (2014). Protein quality control at the inner nuclear membrane. Nature *516*, 410–413.

Kikkert, M., Doolman, R., Dai, M., Avner, R., Hassink, G., van Voorden, S., Thanedar, S., Roitelman, J., Chau, V., and Wiertz, E. (2004). Human HRD1 is an E3 ubiquitin ligase involved in degradation of proteins from the endoplasmic reticulum. J. Biol. Chem. *279*, 3525–3534.

King, M.C., Lusk, C.P., and Blobel, G. (2006). Karyopherin-mediated import of integral inner nuclear membrane proteins. Nature *442*, 1003–1007.

Knop, M., Finger, A., Braun, T., Hellmuth, K., and Wolf, D.H. (1996). Der1, a novel protein specifically required for endoplasmic reticulum degradation in yeast. EMBO J. *15*, 753–763.

Koegl, M., Hoppe, T., Schlenker, S., Ulrich, H.D., Mayer, T.U., and Jentsch, S. (1999). A novel ubiquitination factor, E4, is involved in multiubiquitin chain assembly. Cell *96*, 635–644.

Komander, D., and Rape, M. (2012). The ubiquitin code. Annu. Rev. Biochem. *81*, 203–229.

Kostova, Z., Tsai, Y.C., and Weissman, A.M. (2007). Ubiquitin ligases, critical mediators of endoplasmic reticulum-associated degradation. Semin. Cell Dev. Biol. *18*, 770–779.

Kreft, S.G., Wang, L., and Hochstrasser, M. (2006). Membrane topology of the yeast endoplasmic reticulum-localized ubiquitin ligase Doa10 and comparison with its human ortholog TEB4 (MARCH-VI). J. Biol. Chem. *281*, 4646–4653.

Kushnirov, V.V. (2000). Rapid and reliable protein extraction from yeast. Yeast *16*, 857–860.

Laughery, M.F., Hunter, T., Brown, A., Hoopes, J., Ostbye, T., Shumaker, T., and Wyrick, J.J. (2015). New vectors for simple and streamlined CRISPR-Cas9 genome editing in Saccharomyces cerevisiae. Yeast *32*, 711–720.

Lippincott-Schwartz, J., Bonifacino, J.S., Yuan, L.C., and Klausner, R.D. (1988). Degradation from the endoplasmic reticulum: disposing of newly synthesized proteins. Cell *54*, 209–220.

Ljungdahl, P.O., and Daignan-Fornier, B. (2012). Regulation of amino acid, nucleotide, and phosphate metabolism in Saccharomyces cerevisiae. Genetics *190*, 885–929.

Longtine, M.S., McKenzie, A., Demarini, D.J., Shah, N.G., Wach, A., Brachat, A., Philippsen, P., and Pringle, J.R. (1998). Additional modules for versatile and economical PCR-based gene deletion and modification in Saccharomyces cerevisiae. Yeast *14*, 953–961.

Lorick, K.L., Jensen, J.P., Fang, S., Ong, A.M., Hatakeyama, S., and Weissman, A.M. (1999). RING fingers mediate ubiquitin-conjugating enzyme (E2)-dependent ubiquitination. Proc. Natl. Acad. Sci. USA *96*, 11364–11369.

Lü, S., Zhao, H., Des Marais, D.L., Parsons, E.P., Wen, X., Xu, X., Bangarusamy, D.K., Wang, G., Rowland, O., Juenger, T., et al. (2012). Arabidopsis ECERIFERUM9 involvement in cuticle formation and maintenance of plant water status. Plant Physiol. *159*, 930–944.

De Magistris, P., and Antonin, W. (2018). The dynamic nature of the nuclear envelope. Curr. Biol. *28*, R487–R497.

Margalit, A., Brachner, A., Gotzmann, J., Foisner, R., and Gruenbaum, Y. (2007). Barrier-to-autointegration factor--a BAFfling little protein. Trends Cell Biol. *17*, 202–208.

Mehnert, M., Sommer, T., and Jarosch, E. (2014). Der1 promotes movement of misfolded proteins through the endoplasmic reticulum membrane. Nat. Cell Biol. *16*, 77–86.

Meinema, A.C., Laba, J.K., Hapsari, R.A., Otten, R., Mulder, F.A.A., Kralt, A., van den Bogaart, G., Lusk, C.P., Poolman, B., and Veenhoff, L.M. (2011). Long unfolded linkers facilitate membrane protein import through the nuclear pore complex. Science *333*, 90–93.

Mekhail, K., and Moazed, D. (2010). The nuclear envelope in genome organization, expression and stability. Nat. Rev. Mol. Cell Biol. *11*, 317–328.

Meseroll, R.A., and Cohen-Fix, O. (2016). The malleable nature of the budding yeast nuclear envelope: flares, fusion, and fenestrations. J. Cell Physiol. *231*, 2353–2360.

Metzger, M.B., Pruneda, J.N., Klevit, R.E., and Weissman, A.M. (2014). RING-type E3 ligases: master manipulators of E2 ubiquitin-conjugating enzymes and ubiquitination. Biochim. Biophys. Acta *1843*, 47–60.

Monk, B.C., Tomasiak, T.M., Keniya, M.V., Huschmann, F.U., Tyndall, J.D.A., O'Connell, J.D., Cannon, R.D., McDonald, J.G., Rodriguez, A., Finer-Moore, J.S., et al. (2014). Architecture of a single membrane spanning cytochrome P450 suggests constraints that orient the catalytic domain relative to a bilayer. Proc. Natl. Acad. Sci. USA *111*, 3865–3870.

Morawska, M., and Ulrich, H.D. (2013). An expanded tool kit for the auxin-inducible degron system in budding yeast. Yeast *30*, 341–351.

Mueller, S., Wahlander, A., Selevsek, N., Otto, C., Ngwa, E.M., Poljak, K., Frey, A.D., Aebi, M., and Gauss, R. (2015). Protein degradation corrects for imbalanced subunit stoichiometry in OST complex assembly. Mol. Biol. Cell *26*, 2596–2608.

Mumberg, D., Müller, R., and Funk, M. (1994). Regulatable promoters of Saccharomyces cerevisiae: comparison of transcriptional activity and their use for heterologous expression. Nucleic Acids Res. *22*, 5767–5768.

Nakatsukasa, K., and Brodsky, J.L. (2008). The recognition and retrotranslocation of misfolded proteins from the endoplasmic reticulum. Traffic *9*, 861–870.

Nishimura, K., Fukagawa, T., Takisawa, H., Kakimoto, T., and Kanemaki, M. (2009). An auxin-based degron system for the rapid depletion of proteins in nonplant cells. Nat. Methods *6*, 917–922.

Omnus, D.J., and Ljungdahl, P.O. (2014). Latency of transcription factor Stp1 depends on a modular regulatory motif that functions as cytoplasmic retention determinant and nuclear degron. Mol. Biol. Cell *25*, 3823–3833.

Pantazopoulou, M., Boban, M., Foisner, R., and Ljungdahl, P.O. (2016). Cdc48 and Ubx1 participate in a pathway associated with the inner nuclear membrane that governs Asi1 degradation. J. Cell Sci. *129*, 3770–3780.

Pickart, C.M. (2001). Mechanisms underlying ubiquitination. Annu. Rev. Biochem. *70*, 503–533.

Popken, P., Ghavami, A., Onck, P.R., Poolman, B., and Veenhoff, L.M. (2015). Size-dependent leak of soluble and membrane proteins through the yeast nuclear pore complex. Mol. Biol. Cell *26*, 1386–1394.

Quan, E.M., Kamiya, Y., Kamiya, D., Denic, V., Weibezahn, J., Kato, K., and Weissman, J.S. (2008). Defining the glycan destruction signal for endoplasmic reticulum-associated degradation. Mol. Cell *32*, 870–877.

Rape, M., Reddy, S.K., and Kirschner, M.W. (2006). The processivity of multiubiquitination by the APC determines the order of substrate degradation. Cell *124*, 89–103.

Ravid, T., Doolman, R., Avner, R., Harats, D., and Roitelman, J. (2000). The ubiquitin-proteasome pathway mediates the regulated degradation of mammalian 3-hydroxy-3-methylglutaryl-coenzyme A reductase. J. Biol. Chem. *275*, 35840–35847.

Roh, S.-H., Stam, N.J., Hryc, C.F., Couoh-Cardel, S., Pintilie, G., Chiu, W., and Wilkens, S. (2018). The 3.5-Å CryoEM Structure of Nanodisc-Reconstituted Yeast Vacuolar ATPase Vo Proton Channel. Mol. Cell *69*, 993–1004.e3.

Ron, D., and Walter, P. (2007). Signal integration in the endoplasmic reticulum unfolded protein response. Nat. Rev. Mol. Cell Biol. *8*, 519–529.

Rotin, D., and Kumar, S. (2009). Physiological functions of the HECT family of ubiquitin ligases. Nat. Rev. Mol. Cell Biol. *10*, 398–409.

Rout, M.P., Aitchison, J.D., Suprapto, A., Hjertaas, K., Zhao, Y., and Chait, B.T. (2000). The yeast nuclear pore complex: composition, architecture, and transport mechanism. J. Cell Biol. *148*, 635–651.

Ruggiano, A., Foresti, O., and Carvalho, P. (2014). ER-associated degradation: protein quality control and beyond. J. Cell Biol. *204*, 869–879.

Russell, S.J., Steger, K.A., and Johnston, S.A. (1999). Subcellular localization, stoichiometry, and protein levels of 26 S proteasome subunits in yeast. J. Biol. Chem. *274*, 21943–21952.

Ryan, M., Graham, L.A., and Stevens, T.H. (2008). Voa1p functions in V-ATPase assembly in the yeast endoplasmic reticulum. Mol. Biol. Cell *19*, 5131–5142.

Sano, R., and Reed, J.C. (2013). ER stress-induced cell death mechanisms. Biochimica et Biophysica Acta (BBA)-Molecular Cell ….

Schirmer, E.C., and Gerace, L. (2005). The nuclear membrane proteome: extending the envelope. Trends Biochem. Sci. *30*, 551–558.

Schirmer, E.C., Florens, L., Guan, T., Yates, J.R., and Gerace, L. (2003). Nuclear membrane proteins with potential disease links found by subtractive proteomics. Science *301*, 1380–1382.

Schoebel, S., Mi, W., Stein, A., Ovchinnikov, S., Pavlovicz, R., DiMaio, F., Baker, D., Chambers, M.G., Su, H., Li, D., et al. (2017). Cryo-EM structure of the protein-conducting ERAD channel Hrd1 in complex with Hrd3. Nature *548*, 352–355.

Schubert, U., Antón, L.C., Gibbs, J., Norbury, C.C., Yewdell, J.W., and Bennink, J.R. (2000). Rapid degradation of a large fraction of newly synthesized proteins by proteasomes. Nature *404*, 770–774.

Schulman, B.A., and Harper, J.W. (2009). Ubiquitin-like protein activation by E1 enzymes: the apex for downstream signalling pathways. Nat. Rev. Mol. Cell Biol. *10*, 319–331.

Schwartz, A.L., and Ciechanover, A. (2009). Targeting proteins for destruction by the ubiquitin system: implications for human pathobiology. Annu. Rev. Pharmacol. Toxicol. *49*, 73–96.

Smoyer, C.J., Katta, S.S., Gardner, J.M., Stoltz, L., McCroskey, S., Bradford, W.D., McClain, M., Smith, S.E., Slaughter, B.D., Unruh, J.R., et al. (2016). Analysis of membrane proteins localizing to the inner nuclear envelope in living cells. J. Cell Biol. *215*, 575–590.

Smoyer, C.J., Smith, S.E., Gardner, J.M., McCroskey, S., Unruh, J.R., and Jaspersen, S.L. (2019). Distribution of Proteins at the Inner Nuclear Membrane Is Regulated by the Asi1 E3 Ligase in Saccharomyces cerevisiae. Genetics *211*, 1269–1282.

Sommer, T., and Jentsch, S. (1993). A protein translocation defect linked to ubiquitin conjugation at the endoplasmic reticulum. Nature *365*, 176–179.

Sosa, B.A., Rothballer, A., Kutay, U., and Schwartz, T.U. (2012). LINC complexes form by binding of three KASH peptides to domain interfaces of trimeric SUN proteins. Cell *149*, 1035–1047.

Sosa, B.A., Kutay, U., and Schwartz, T.U. (2013). Structural insights into LINC complexes. Curr. Opin. Struct. Biol. *23*, 285–291.

Stanley, A.M., Carvalho, P., and Rapoport, T. (2011). Recognition of an ERAD-L substrate analyzed by site-specific in vivo photocrosslinking. FEBS Lett. *585*, 1281–1286.

Starr, D.A. (2012). Laminopathies: too much SUN is a bad thing. Curr. Biol. *22*, R678–80.

Starr, D.A., and Fischer, J.A. (2005). KASH' ' ’n Karry: the KASH domain family of cargo-specific cytoskeletal adaptor proteins. Bioessays *27*, 1136–1146.

Stein, A., Ruggiano, A., Carvalho, P., and Rapoport, T.A. (2014). Key steps in ERAD of luminal ER proteins reconstituted with purified components. Cell *158*, 1375–1388.

Swanson, R., Locher, M., and Hochstrasser, M. (2001). A conserved ubiquitin ligase of the nuclear envelope/endoplasmic reticulum that functions in both ER-associated and Matalpha2 repressor degradation. Genes Dev. *15*, 2660–2674.

Tabas, I., and Ron, D. (2011). Integrating the mechanisms of apoptosis induced by endoplasmic reticulum stress. Nat. Cell Biol. *13*, 184–190.

Tsai, P.-L., Zhao, C., Turner, E., and Schlieker, C. (2016). The Lamin B receptor is essential for cholesterol synthesis and perturbed by disease-causing mutations. Elife *5*.

Uhlén, M., Fagerberg, L., Hallström, B.M., Lindskog, C., Oksvold, P., Mardinoglu, A., Sivertsson, Å., Kampf, C., Sjöstedt, E., Asplund, A., et al. (2015). Proteomics. Tissue-based map of the human proteome. Science *347*, 1260419.

Ungricht, R., and Kutay, U. (2015). Establishment of NE asymmetry—targeting of membrane proteins to the inner nuclear membrane. Curr. Opin. Cell Biol. *34*, 135–141.

Ungricht, R., and Kutay, U. (2017). Mechanisms and functions of nuclear envelope remodelling. Nat. Rev. Mol. Cell Biol. *18*, 229–245.

Vashist, S., and Ng, D.T.W. (2004). Misfolded proteins are sorted by a sequential checkpoint mechanism of ER quality control. J. Cell Biol. *165*, 41–52.

Wandke, C., and Kutay, U. (2013). Enclosing chromatin: reassembly of the nucleus after open mitosis. Cell *152*, 1222–1225.

Ward, C.L., Omura, S., and Kopito, R.R. (1995). Degradation of CFTR by the ubiquitin-proteasome pathway. Cell *83*, 121–127.

Weber, A., Cohen, I., Popp, O., Dittmar, G., Reiss, Y., Sommer, T., Ravid, T., and Jarosch, E. (2016). Sequential Poly-ubiquitylation by Specialized Conjugating Enzymes Expands the Versatility of a Quality Control Ubiquitin Ligase. Mol. Cell *63*, 827–839.

Webster, B.M., Thaller, D.J., Jäger, J., Ochmann, S.E., Borah, S., and Lusk, C.P. (2016). Chm7 and Heh1 collaborate to link nuclear pore complex quality control with nuclear envelope sealing. EMBO J. *35*, 2447–2467.

Werner, E.D., Brodsky, J.L., and McCracken, A.A. (1996). Proteasome-dependent endoplasmic reticulum-associated protein degradation: an unconventional route to a familiar fate. Proc. Natl. Acad. Sci. USA *93*, 13797–13801.

Wild, R., Kowal, J., Eyring, J., Ngwa, E.M., Aebi, M., and Locher, K.P. (2018). Structure of the yeast oligosaccharyltransferase complex gives insight into eukaryotic N-glycosylation. Science *359*, 545–550.

Worman, H.J. (2016). Human diseases related to nuclear envelope proteins. The Functional Nucleus.

Woulfe, J. (2008). Nuclear bodies in neurodegenerative disease. Biochim. Biophys. Acta *1783*, 2195–2206.

Yang, L., Guan, T., and Gerace, L. (1997). Integral membrane proteins of the nuclear envelope are dispersed throughout the endoplasmic reticulum during mitosis. J. Cell Biol. *137*, 1199–1210.

Ye, Y., and Rape, M. (2009). Building ubiquitin chains: E2 enzymes at work. Nat. Rev. Mol. Cell Biol. *10*, 755–764.

Ye, Y., Meyer, H.H., and Rapoport, T.A. (2001). The AAA ATPase Cdc48/p97 and its partners transport proteins from the ER into the cytosol. Nature *414*, 652–656.

Ye, Y., Meyer, H.H., and Rapoport, T.A. (2003). Function of the p97-Ufd1-Npl4 complex in retrotranslocation from the ER to the cytosol: dual recognition of nonubiquitinated polypeptide segments and polyubiquitin chains. J. Cell Biol. *162*, 71–84.

Zargari, A., Boban, M., Heessen, S., Andréasson, C., Thyberg, J., and Ljungdahl, P.O. (2007). Inner nuclear membrane proteins Asi1, Asi2, and Asi3 function in concert to maintain the latent properties of transcription factors Stp1 and Stp2. J. Biol. Chem. *282*, 594–605.

Zattas, D., and Hochstrasser, M. (2015). Ubiquitin-dependent protein degradation at the yeast endoplasmic reticulum and nuclear envelope. Crit Rev Biochem Mol Biol *50*, 1–17.

Zelcer, N., Sharpe, L.J., Loregger, A., Kristiana, I., Cook, E.C.L., Phan, L., Stevenson, J., and Brown, A.J. (2014). The E3 ubiquitin ligase MARCH6 degrades squalene monooxygenase and affects 3-hydroxy-3-methyl-glutaryl coenzyme A reductase and the cholesterol synthesis pathway. Mol. Cell. Biol. *34*, 1262–1270.

Zhao, G., and London, E. (2006). An amino acid “transmembrane tendency” scale that approaches the theoretical limit to accuracy for prediction of transmembrane helices: relationship to biological hydrophobicity. Protein Sci. *15*, 1987–2001.